AD_____

Award Number: DAMD17-03-1-0501

TITLE: Brain's DNA Repair Response to Neurotoxicants

PRINCIPAL INVESTIGATOR: Juan Sanchez-Ramos, Ph.D., M.D.

CONTRACTING ORGANIZATION: University of South Florida
Tampa, Florida 33620

REPORT DATE: January 2007

TYPE OF REPORT: Final

PREPARED FOR: U.S. Army Medical Research and Materiel Command
Fort Detrick, Maryland 21702-5012

REPORT DOCUMENTATION PAGE

Form Approved
OMB No. 0704-0188

1. REPORT DATE *(DD-MM-YYYY)*	**2. REPORT TYPE**	**3. DATES COVERED** *(From - To)*
01-01-2007	Final	1 Jul 2003 – 31 Dec 2006

4. TITLE AND SUBTITLE

Brain's DNA Repair Response to Neurotoxicants

5a. CONTRACT NUMBER

5b. GRANT NUMBER
DAMD17-03-1-0501

5c. PROGRAM ELEMENT NUMBER

6. AUTHOR(S)

Juan Sanchez-Ramos, Ph.D., M.D.

E-Mail: jsramos@hsc.usf.edu

5d. PROJECT NUMBER

5e. TASK NUMBER

5f. WORK UNIT NUMBER

7. PERFORMING ORGANIZATION NAME(S) AND ADDRESS(ES)

University of South Florida
Tampa, Florida 33620

8. PERFORMING ORGANIZATION REPORT NUMBER

9. SPONSORING / MONITORING AGENCY NAME(S) AND ADDRESS(ES)
U.S. Army Medical Research and Materiel Command
Fort Detrick, Maryland 21702-5012

10. SPONSOR/MONITOR'S ACRONYM(S)

11. SPONSOR/MONITOR'S REPORT NUMBER(S)

12. DISTRIBUTION / AVAILABILITY STATEMENT
Approved for Public Release; Distribution Unlimited

13. SUPPLEMENTARY NOTES

14. ABSTRACT

Parkinson's Disease (PD) is associated with death of dopaminergic (DA) neurons in the substantia nigra (SN) of the brain. Military personnel abroad are at a greater risk of exposure to pesticides and toxins which may selectively damage DA neurons in the SN and increase the probability of development of Parkinson's disease (PD) later in life. The toxins of interest are mitochondrial poisons that create a bioenergetic crisis and generate toxic oxyradicals which damage macromolecules, including DNA. We hypothesized that regulation of the DNA repair response within certain neurons of the SN (the pars compacta) may be a critical determinant for their vulnerability to these neurotoxicants. We have measured regional differences in the brain's capacity to increase repair of oxidized DNA (indicated by oxyguanosine glycosylase (OGG1) activity) to three distinct chemical classes of neurotoxins (MPTP, two mycotoxins, and an organochloriine pesticide). We have found that the temporal and spatial profile of OGG1 activity across brain regions elicited by each class of neurotoxicant is distinct and unique. Even though all 3 toxicants caused various degrees of depletion of striatal dopamine, the temporal profile of DA depletion and OGG1 activity in striatum was distinct for each toxicant. DNA repair gene expression in response to OTA and dieldrin revealed differences in VTA and SN compartments that may relate to differential vulnerability to oxidative stressors.

15. SUBJECT TERMS
DNA Damage, DNA Repair, Brain, Neurotoxicants, Mycotoxins

16. SECURITY CLASSIFICATION OF:			**17. LIMITATION OF ABSTRACT**	**18. NUMBER OF PAGES**	**19a. NAME OF RESPONSIBLE PERSON**
a. REPORT	**b. ABSTRACT**	**c. THIS PAGE**			USAMRMC
U	U	U	UU	117	**19b. TELEPHONE NUMBER** *(include area code)*

Standard Form 298 (Rev. 8-98)
Prescribed by ANSI Std. Z39.18

Table of Contents

INTRODUCTION

Parkinson's Disease (PD) is associated with death of dopaminergic (DA) neurons in the substantia nigra (SN) of the brain (1-3). Military personnel abroad are at a greater risk of exposure to pesticides and toxins (4) some of which may selectively damage DA neurons in the SN and increase the probability of development of Parkinson's disease (PD) later in life. The toxins of interest are mitochondrial poisons that create a bioenergetic crisis and generate toxic oxyradicals which damage macromolecules, including DNA. We hypothesize that the DNA repair response within certain neurons of the SN (the pars compacta) may be a critical determinant for their vulnerability to these neurotoxicants. The technical objectives were to measure regional and cellular differences in the brain's DNA repair response to three neurotoxins known to interfere with mitochondrial function (the mycotoxin ochratoxin-A; the pesticide dieldrin, and the classic dopaminergic neurotoxin, MPTP). An improved understanding of the DNA repair response to neurotoxicants and development of methods to enhance DNA repair will form the basis for potential preventive measures against the effects of military threat agents and military operational hazards, and also lead to treatment interventions for Parkinson's disease

BODY

STATEMENT OF WORK: The Brain's DNA Repair Response to Neurotoxicants.

We propose to test the hypothesis that differences in DNA repair responses determine intrinsic neuronal susceptibility to exogenous or endogenous neurotoxicants. Corollaries of this hypothesis are:

a) The DNA repair response, in particular the ability to upregulate the activities of 8-oxoguanine glycosylase-1 (Ogg1) and redox factor-1 (Ref-1), will determine whether a neuron will survive exposure to neurotoxicological insults.
b) Overactivation of poly(ADP-ribose) polymerase-1 (PARP-1) in response to oxidative stress will exacerbate the toxicity of xenobiotics and lead to degeneration of neurons.
c) Agents that increase Ogg1 and Ref-1 activity and expression or inhibit PARP-1 will provide protection against neurotoxicants.

Task 1: **To determine the differences in oxidative DNA damage and DNA repair responses elicited by mycotoxins (ochratoxin-A; rubratoxin-B), an organochlorine pesticide (dieldrin), and the classical DA neurotoxicant, MPTP**

Task 2: **To measure the effects of chronic low dose administration of a mycotoxin and a pesticide on brain region oxidative DNA damage and DNA repair**

Task 3**: To determine whether exposure to agents that up-regulate Ogg1 and Ref-1 DNA repair or inhibit PARP-1 will protect against the neurotoxicity elicited by a mycotoxin and a pesticide**

Task 4: **To measure the effects of neurotoxicant exposure on the DNA repair response in DA neurons from two specific sub-populations of the midbrain, the SN-pars compacta and the ventral tegmental area (VTA)**

SUMMARY OF RESULTS FROM TASK 1

a) Acute Effects of Rubratoxin

Rubratoxin-B (RB) is a mycotoxin with potential neurotoxic effects that have not yet been characterized. Based on existing evidence that RB interferes with mitochondrial electron transport to produce oxidative stress in peripheral tissues, we hypothesized that RB would produce oxidative damage t o macromolecules in specific brain regions. Parameters of oxidative DNA damage and repair, lipid peroxidation and superoxide dismutase (SOD) activity were measured across 6 mouse brain regions 24 hrs after administration of a single dose of RB. Lipid peroxidation and oxidative DNA damage was either unchanged or decreased in all brain regions in RB-treated mice compared to vehicle-treated mice. Concomitant with these decreased indices of oxidative macromolecular damage, SOD activity was significantly increased in all brain regions. Oxyguanosine glycosylase activity (OGG1), a key enzyme in the repair of oxidized DNA, was significantly increased in three brain regions cerebellum (CB), caudate/putamen (CP), and cortex (CX) but not hippocampus(H), midbrain(MB), and pons/medulla(PM). The RB-enhanced OGG1 catalytic activity in these brain regions was not due to increased OGG1 protein expression, but was a result of enhanced catalytic activity of the enzyme. In conclusion, specific brain regions responded to an acute dose of RB by significantly altering SOD and OGG1 activities to maintain the degree of oxidative DNA damage equal to, or less than, that of normal steady-state levels. Details of this study have been published (5). The report can be found in the Appendix section.

b) Acute Effects of Ochratoxin-A

Ochratoxin-A (OTA) is a fungal metabolite with potential toxic effects on the central nervous system. OTA has complex mechanisms of action that include evocation of oxidative stress, bioenergetic compromise, inhibition of protein synthesis, production of DNA single-strand breaks and formation of OTA–DNA adducts. The time course of acute effects of OTA were investigated in the context of DNA damage, DNA repair and global oxidative stress across six brain regions. Oxidative DNA damage, as measured with the ‘‘comet assay’’, was significantly increased in the six brain regions at all time points up to 72 h, with peak effects noted at 24 h in midbrain (MB), CP (caudate/putamen) and HP (hippocampus). Oxidative DNA repair activity (oxyguanosine glycosylase or OGG1) was inhibited in all regions at 6 h, but recovered to control levels in cerebellum (CB) by 72 h, and showed a trend to recovery in other regions of brain. Other indices of oxidative stress were also elevated. Lipid peroxidation and superoxide dismutase (SOD) increased over time throughout the brain. In light of the known vulnerability of the nigro-striatal dopaminergic neurons to oxidative stress, levels of striatal dopamine (DA) and its metabolites were also measured. Administration of OTA (0–6 mg/kg i.p.) to mice resulted in a dose-dependent decrease in striatal DA content and turnover with an ED50 of 3.2 mg/kg. A single dose of 3.5 mg/kg decreased the intensity of tyrosine hydroxylase immunoreactivity (TH+) in fibers of striatum, TH+ cells in substantia nigra (SN) and TH+ cells of the locus ceruleus. TUNEL staining did not reveal apoptotic profiles in MB, CP or in other brain regions and did not alter DARPP32 immunoreactivity in striatum. In conclusion, OTA caused acute depletion of striatal DA on a background of globally increased oxidative stress and transient inhibition of oxidative DNA repair. Details of this study have been published and can be found in the Appendix (6).

c) Acute Effects of MPTP

The primary objective of this study was to map the normal distribution of the base excision enzyme oxyguanosine glycosylase (OGG1) across mouse-brain regions as a prelude to assessing the effects of various neurotoxicants, ranging from highly selective molecules like MPTP to more global toxic agents, including the mycotoxin OTA and the pesticide dieldrin. This research is based on the hypothesis that regional brain vulnerability to a toxicant is determined, in part, by variation in the intrinsic capacity of cellular populations to successfully repair oxidative DNA damage. After mapping the normal distributions of OGG1 and superoxide dismutase (SOD) across 44 loci dissected from mouse brain, MPTP, a mitochondrial toxicant with selective dopamine (DA) neuron cytotoxicity was used to elicit focal oxidative stress and DNA repair responses. A single dose of MPTP (20 mg/kg, i.p.) elicited time- and regiondependent changes in both SOD and OGG1, with early increases in DNA repair and anti-oxidant

activities throughout all regions of brain. In some sampled loci, notably the substantia nigra (SN) and hippocampus, the heightened DNA repair and antioxidant responses were not maintained beyond 48 h. Other loci from cerebellum, cerebral cortex and pons maintained high levels of activity up to 72 h. Levels of dopamine (DA) were decreased significantly at all time points and remained below control levels in nigro-striatal and mesolimbic systems (ventral tegmental area and nucleus accumbens). Assessment of apoptosis by TUNEL staining revealed a significant increase in number of apoptotic nuclei in the substantia nigra at 72 h and not in other loci. The marked degree of apoptosis that became evident in SN at 72 h was associated with large decreases in SOD and DNA repair activity at that locus. In conclusion, MPTP elicited global effects on DNA repair and antioxidant activity in all regions of brain, but the most vulnerable loci were unable to maintain elevated DNA repair and antioxidant responses. The full report has been published and can be found in the Appendix (7).

d) Acute Effects of Dieldrin

Dieldrin, an organochlorine pesticide, has several molecular characteristics that make it a potential etiological agent for Parkinson's Disease. The half life of dieldrin in soil is approximately 5 years. This persistence, combined with high lipid solubility, provides the necessary conditions for dieldrin to bioconcentrate and biomagnify in organisms. Dieldrin appears to be retained for life in lipid-rich tissue and has been measured in human brain. It was found at high concentrations in caudate nucleus from post-mortem brain of idiopathic Parkinson's Disease (IPD) cases. Dieldrin has toxic effects for dopaminergic (DA) and monoaminergic neurons in many species, both *in vitro* and *in vivo*. Like rotenone and the dopaminergic neurotoxin 1-methyl-4-phenyl-pyridinium (MPP+), dieldrin interferes with mitochondrial oxidative phosphorylation. Insights derived from studies of 1-methyl-4-phenyl-1,2,3,6-tetrahydropyridine (MPTP) led to the observation that mitochondrial function appears to be compromised in brain and peripheral tissues from PD patients.

The present study was designed to test the hypothesis that the DNA repair response to dieldrin is a determinant of the vulnerability of DA neurons of the nigro-striatal system. The activity of the mammalian base excision repair enzyme oxyguanosine glycosylase (Ogg1) was utilized as the index of DNA repair. Other measures of oxidative stress were also studied, including the regional distribution of lipid peroxidation and superoxide dismutase (SOD) activity. The primary objectives of this component of the study were to determine the effects of acute and slow infusion of dieldrin on a) DA and its metabolites in the striatum and b) to measure the regional distribution of the brain's DNA repair response and parameters of oxidative stress. Secondary objectives were to note observable changes in motor behavior and to measure whole body tremor elicited by dieldrin administration.

Effects of Dieldrin on Striatal DA and metabolites

Four groups (6-8 mice per group) of mice were injected with dieldrin i.p. (6 mg/kg or 30 mg/kg). Animals were euthanatized at 6, 24 and 72 hrs after injections. Brains were dissected and striatal tissue was harvested for assay of DA and metabolites. Striatal DA levels were transiently decreased at 6 hrs, but recovered to levels equal to or greater than baseline by 72 hrs (**Figs 1, 2**). In the group of mice that received the high dose of dieldrin (30 mg/kg) the levels at 72 hrs far exceeded baseline levels. Striatal DA turnover was initially increased but by 72 hrs was significantly diminished (**Fig 2**).

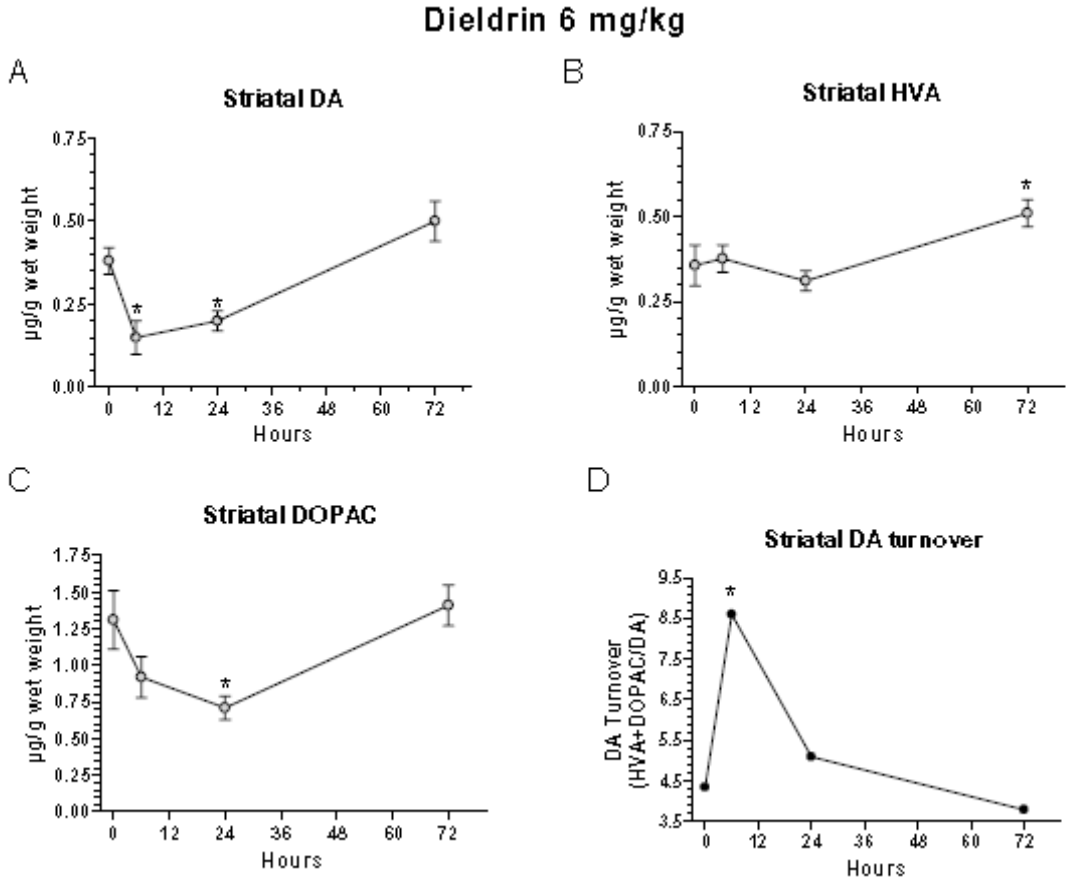

Fig 1. Acute effects of dieldrin (6 mg/kg i.p) on striatal dopamine and metabolites. A. Striatal DA was initially decreased at early time points and returned to levels above baseline at 72 hrs. B. Dieldrin had no effect on HVA at early time points and only was significantly increased at 72 hrs. C. Dieldrin decreased DOPAC levels significantly at 24 hrs but levels returned to baseline by 72 hours. D. DA turnover One-way ANOVA showed that the DA, DOPAC and DA turnover means were significantly different ($p < 0.05$) and Dunnett's multiple comparison test showed significant differences in striatal DA, DOPAC and DA turnover at times indicated by asterisks.

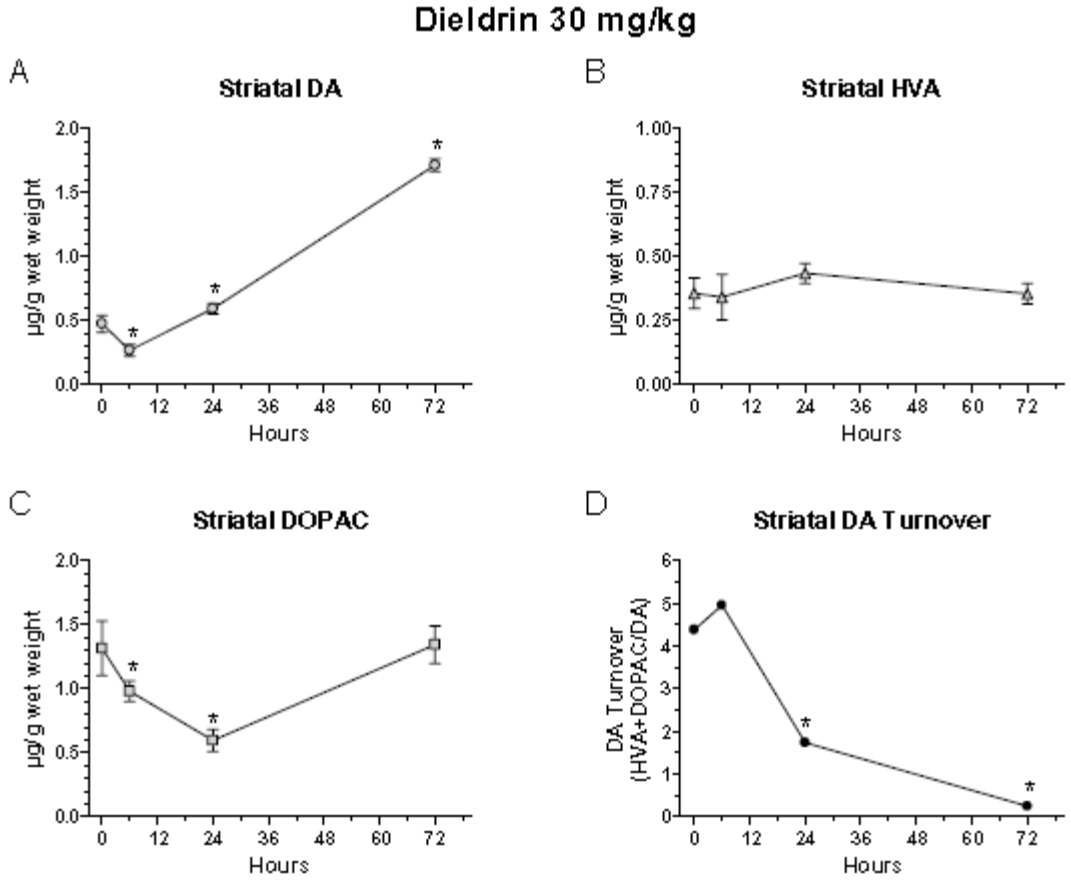

Fig 2. Acute effects of dieldrin (30 mg/kg i.p.). A. Striatal DA was initially decreased at 6 hrs to half the baseline levels and then was elevated significantly above baseline at 24 and 72 hrs. B. Dieldrin had no effect on HVA at all time points. C. Dieldrin decreased DOPAC levels significantly at 6 and 24 hours. D. DA turnover was decreased significantly at 24 and 72 hrs. One-way ANOVA showed that the DA, DOPAC and DA turnover means were significantly different ($p < 0.05$) and Dunnett's multiple comparison test showed significant differences in striatal DA, DOPAC and DA turnover at times indicated by asterisks.

Acute Effects of Dieldrin on Regional DNA Repair (OGG1 activity)

Four groups of mice (n=6 per group) were injected with 6 or 30 mg/kg of dieldrin i.p. or vehicle. Groups were euthanatized at 6, 24 and 72 hrs after injection. (Data from the low dose is not shown but was similar to the effects of the high dose in the time-course and brain regional pattern). Dieldrin elicited a significant time and brain-region dependent increase in OGG1 activity (**Fig 3**). The greatest extent of increased activity was measured in MB (5 fold), followed closely by PM (4.3 fold) and CP (4.2 fold). These three regions have high levels of monoaminergic neuronal activities. Notably all regions of brain exhibited at least a 2.5 fold increase in OGG1 activity at 72 hrs after dieldrin injection.

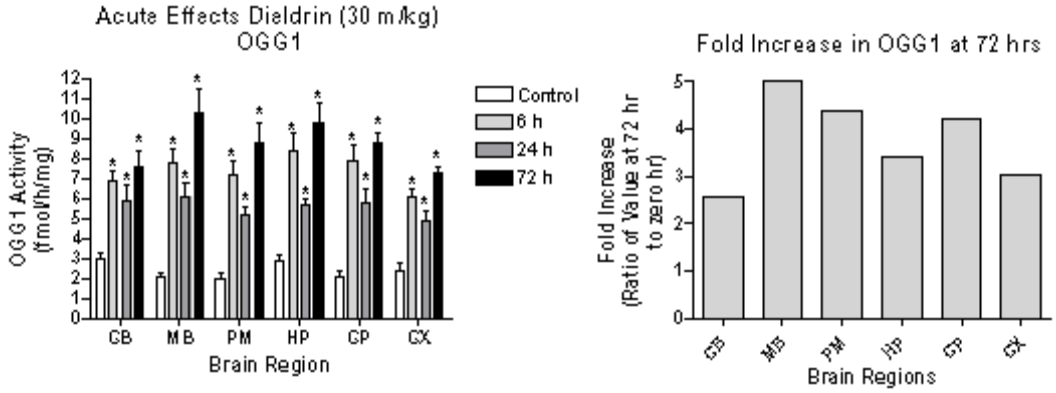

Fig 3 Acute effects of 30 mg/kg dieldrin on OGG1 activity. Left panel: OGG1 activity plotted against brain region reveals a brain and time-dependent increase in OGG1 activity. Two-way ANOVA showed that time contributed 72% of total variance ($p < 0.0001$); brain regions accounted for 4% of total variance ($p< 0.01$) and the interaction with brain region accounted for 3% of total variance. Asterisks indicate significant differences from control values based on post-hoc t-tests with Bonferroni corrections for multiple comparisons. Right panel: Fold Increase of OGG1 activity (ratio of values at 72 hrs to control values) plotted against brain regions. The MB showed the greatest increase in DNA repair activity, followed by PM and CP. CB=cerebellum; MB= midbrain; PONS=pons; MD=medulla; T/HT=thalamus/hypothalamus; HP=hippocampus; CP= caudate/putamen; CX= cerebral cortex.

SUMMARY OF RESULTS FROM TASK 2

a) Effects of slow infusion of OTA via osmotic minipump over two weeks

The effects of chronic low dose OTA exposure on regional brain oxidative stress and striatal DA metabolism was studied and a manuscript summarizing the results has been published (8). (A reprint of the manuscript is found in the Appendix). The continuous subcutaneous administration of OTA at low doses over a period of 2 weeks caused small, but significant depletion of striatal DA. OTA also caused pronounced global oxidative stress, evoking a strong antioxidative and DNA repair response across the entire brain. Even though the depletion of striatal DA did not cause overt parkinsonism in these mice, it is important to consider that the superimposition of normal age-related decline in striatal DA could ultimately result in signs of parkinsonism such as slowness of movement and rigidity in the mice. Without completing the understanding why DA terminals in striatum are especially vulnerable to OTA, it is likely that a toxic insult to the nigro-striatal system will increase the risk of developing Parkinson's Disease at an earlier age than normal. This hypothesis can be tested by studying the long term consequences of episodes of OTA exposure in mice during the aging process. In the real world, it will be important to monitor the neurological status of Gulf War veterans as they age.

b) Effects of slow infusion of dieldrin on striatal DA and metabolites

Slow sub-cutaneous infusion of dieldrin with an ALZET osmotic pump over 2 wks (50 mg/kg cumulative dose) resulted in significantly increased levels of striatal DA and HVA but not DOPAC (**Fig 4**). DA turnover was significantly decreased at 14 days (**Fig 4**).

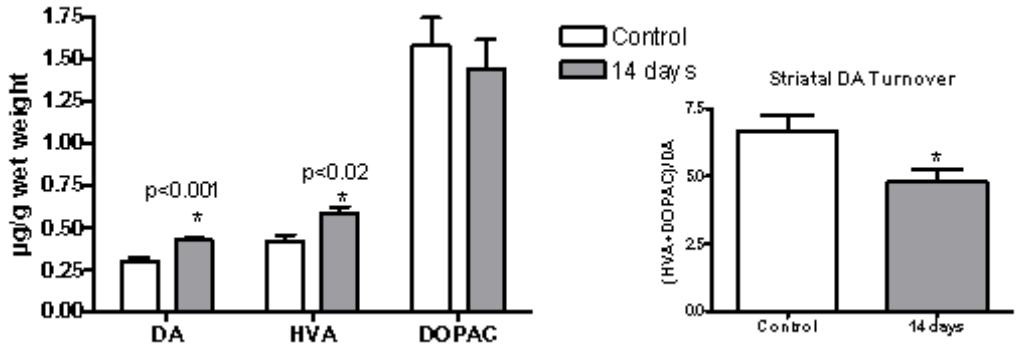

Fig 4 Effects of slow infusion of dieldrin on striatal DA and metabolites. Left panel: Striatal DA and metabolites following 2 wks of infusion of dieldrin by osmotic pump (cumulative dose 50 mg/kg). Right panel: Striatal DA turnover at 14 days compared to control turnover. Asterisks denote significant difference between values at baseline and 14 days (unpaired t-tests)

c) Effects of dieldrin infusion over 2 weeks on DNA Repair (OGG1)

Six groups of mice (n=8 per group) were implanted with osmotic pumps loaded with dieldrin and calibrated to deliver 3, 6, 12, 24 and 48 mg/kg over a period of 2 weeks. After euthanasia and rapid dissection of brain, OGG1 activities were determined. Dieldrin infusion elicited a dose dependent increase of OGG1 activities in all brain regions, with maximum effects reaching a plateau between 24 and 48 mg/kg (**Fig 5**). The distribution of OGG1 activity across brain regions was fairly homogenous. However, at the 24mg/kg cumulative dose, there was a more heterogeneous distribution of activity, with pons exhibiting significantly greater activity than striatum and cerebral cortex (**Fig 5**).

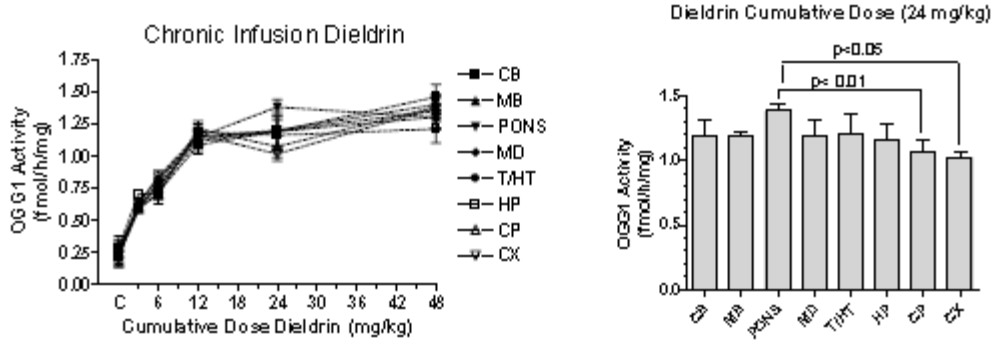

Fig 5 Effects of 2 wk infusion of dieldrin on DNA repair (OGG1 activity) Left panel depicts OGG1 activity as a function of the cumulative dose of dieldrin. The increase in OGG1 activity was significantly

dependent on the cumulative dose delivered but did not vary significantly as a function of brain region. Two-way ANOVA revealed that cumulative concentration of dieldrin accounted for 79% of total variance ($p < 0.0001$) and brain regions accounted for 1.84% of total variance ($p=0.61$). Post-hoc t-tests with Bonferroni corrections for multiple comparisons showed OGG1 activities in the pons were significantly higher than in the CP and CX following a cumulative dose of 24 mg/kg (right panel). CB=cerebellum; MB= midbrain; PONS=pons; MD=medulla; T/HT=thalamus/hypothalamus; HP=hippocampus; CP= caudate/putamen; CX= cerebral cortex.

d) Effects of slow infusion of dieldrin on lipid peroxidation:

Slow infusion of dieldrin resulted in a dose-dependent increase in oxidative stress across all brain regions as indicated by measurements of lipid peroxidation (**Fig 6**). This curve resembled the DNA repair response shown in **Fig 6**. The maximum effect was produced following infusion of 48 mg/kg over 2 weeks. The increase in lipid peroxidation was significantly dependent on dose and did not vary significantly with brain region similar to the effects on OGG1. However, post-hoc t-tests revealed that lipid peroxidation was significantly higher in CB than in MB following a dose of 12 mg/kg ($p<0.05$). Similarly, lipid peroxidation was greater in CB than in the PONS following 24 mg/kg.

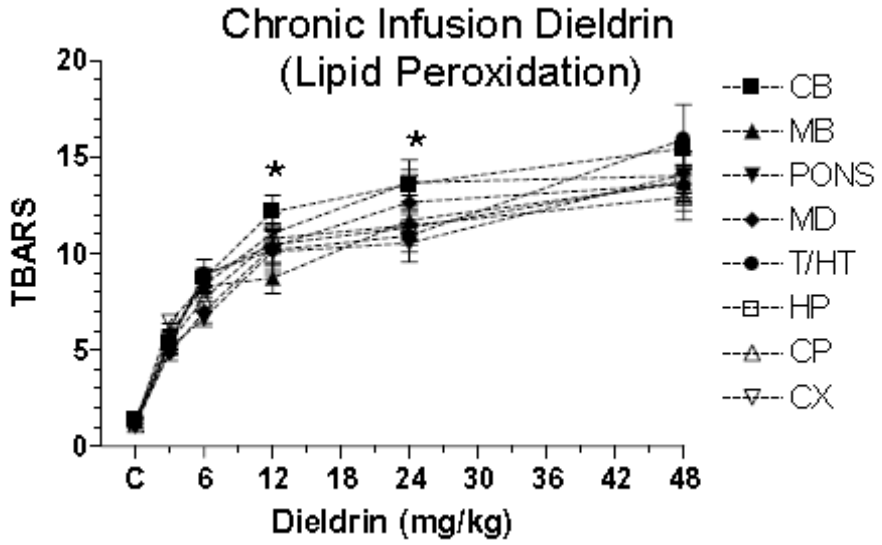

.

Fig 6 Effects of 2 wk infusion of dieldrin (with pump) on lipid peroxidation (TBARS units). The increase in TBARS was significantly dependent on the cumulative dose delivered but did not vary significantly as a function of brain region. Two-way ANOVA revealed that cumulative concentration of dieldrin accounted for 76% of total variance ($p < 0.0001$) and brain regions accounted for 0.9 4% of total variance ($p=0.36$). * Posthoc t-tests with Bonferroni corrections for multiple comparisons showed TBARS in the CB were significantly higher than in the MB ($p < 0.05$) following a cumulative dose of 12 mg/kg; TBARS in CB were also significantly higher than in the PONS ($p<0.05$) following 24 mg/kg.

SUMMARY OF RESULTS FROM TASK 3

***Task 3*: To determine whether exposure to agents that up-regulate Ogg1 and APEX DNA repair will protect against the neurotoxicity elicited by a mycotoxin and a pesticide**

Measurement of DNA Damage with a Modification of the PARP Assay.

Background

Poly(ADP-ribose) polymerase (PARP) is nuclear protein of 116 kDa present at approximately 1 x 10^6 copies in somatic cells. PARP undergoes a conformational change on binding to damaged DNA via a zinc finger domain. This activated PARP converts NAD to nicotinamide and polymers of ADP-ribose. The PARP assay allows determining PARP activity by measuring the incorporation of radiolabeled NAD in presence of activated DNA. Quantitative values are determined from scintillation counting. The assay may be also used for ***indirect quantitative measure of DNA damage*** in cell extracts without addition of exogenous activated DNA. Carrying out reaction in presence of exogenous PARP enzyme allows incorporation of radiolabeled NAD in extent that reflects the degree of DNA damage in cell extract.

Assay protocol

Approximately 50 mg of tissue was sonicated in 450 μL of Extraction buffer for about 10 s following centrifugation at 3,000 g for 5 min at 4 ˚C. Supernatant was transferred in pre-chilled test tube and concentration of protein was adjusted to 1 μg/μL. Core Reaction Mixture (CRM) was prepared by mixing together: 2·(n+1) μL of ^{32} P-NAD; 10·(n+1) μL of Histone H1 (1mg/ml); 10·(n+1) μL of NAD (1 mM) and 10·(n+1) μL of 10 x buffer (n - is a number of reactions). The following components were dispensed into test tubes contained 20 μL of tissue extract: 32 μL of CRM; 1 μL of PARP enzyme and 47 μL of distilled water. Additional set of test tubes using for measure of background contained 20 μL of tissue extract; 32 μL of CRM; 1 μL of PARP enzyme; 6 μL of aminobenzamide (an inhibitor of PARP) and 41 μL of distilled water. Tubes were incubated for 10 min at room temperature and were transferred on ice. 900 μL of ice cold 20% TCA was added followed by centrifugation at 12,000 g for 10 min at room temperature. Supernatant was removed and 1mL of liquid scintillation cocktail was added to each tube. Each tube was vortexed for about 1 min to solubilize the protein pellet. Tubes were placed in a standard scintillation vial and counted for ^{32}P. Background was subtracted from each measurement to calculate the degree of DNA damage.

Measurement of DNA Repair Activities (OGG1, PARP)

Measurement of OGG1 enzymatic activy was performed as previously described (6, 8). PARP enzymatic activity was measured with the Poly(ADP-Ribose) Polymerase Assay Kit (Trevigen, Gaithersburg, MD)

Design of the studies on Pre-conditioning (Effects of DEM pretreatment on neurotoxicant-induced damage (Fig 7)

DEM (1 mmol/kg, ip) dissolved in DMSO
OTA (4 mg/kg, ip) dissolved in $NaHCO_3$

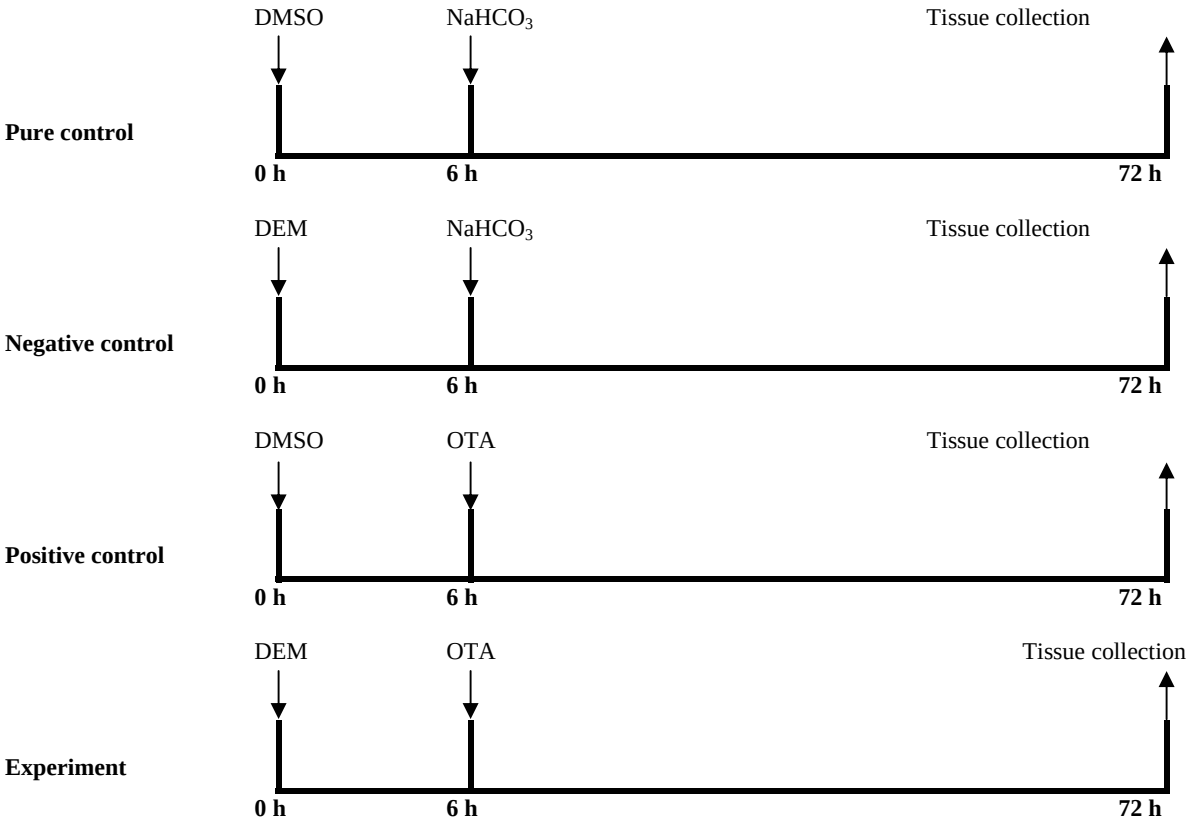

Fig 7 Experimental design for the assessment of the effect of pre-conditioning with a mild pro-oxidant DEM on OTA toxicity. DEM (1 mmol/kg, ip) was dissolved in DMSO and OTA (4 mg/kg, ip) was dissolved in.$NaHCO_3$ Animals were euthanatized 72 hrs after treatment and midbrains were harvested and micro-dissected.

RESULTS

Three groups of mice (n=6) were injected with single doses of OTA (4 mg/kg), Dieldrin (16 mg/kg) or MPTP (20 mg/kg) and extent of DNA damage in total midbrain was assayed. Each of the toxicants caused DNA damage, but the effect of dieldrin was much greater than the other two (Fig 8).

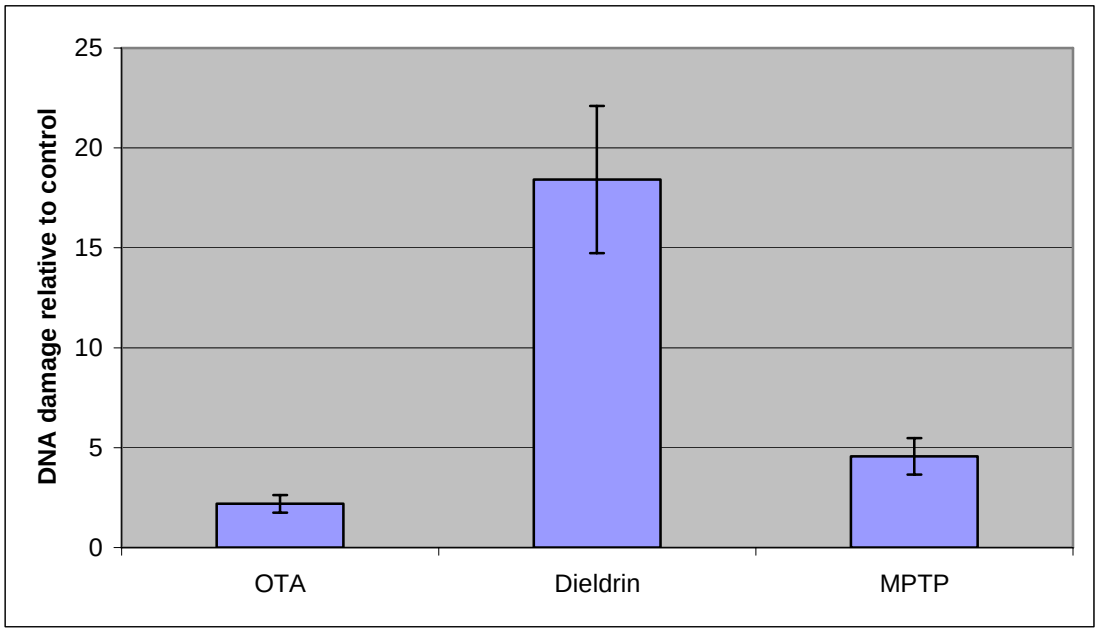

Fig. 8. Relative oxidative DNA damage in midbrain caused by different neurotoxicants (OTA= 4 mg/kg; Dieldrin = 6 mg/kg; MPTP = 20 mg/kg). Bars illustrate mean ±SD (n=6). DNA damage was evaluated with Poly(ADP-ribose) Polymerase Assay Kit (Trevigen, Gaithersburg, MD).

To assess the effects of pre-conditioning, four groups of mice (n= 6 per group) were injected i.p. with DEM (1 mmol/kg), the specific neurotoxicant (OTA, dieldrin or MPTP) or a combination of both according to the experimental design illustrated in Fig 7. DEM was dissolved in DMSO and OTA (4 mg/kg, ip) was dissolved in $NaHCO_3$ In the pre-conditioning group, mice were injected with DEM 6 hrs before the toxicant. All animals were euthanatized 72 hrs after the first injection. Entire midbrain and micro-punches of midbrain (SN and VTA) from another set of mice were harvested.

Total oxidative DNA damage in midbrain samples was estimated and shown to increase following administration of the toxicant (Fig 9). OTA, but not DEM caused a significant increase in total midbrain DNA damage. Pretreatment with DEM 6 hrs before administration of OTA potentiated the total DNA damage caused by OTA (Fig 9, top panel).

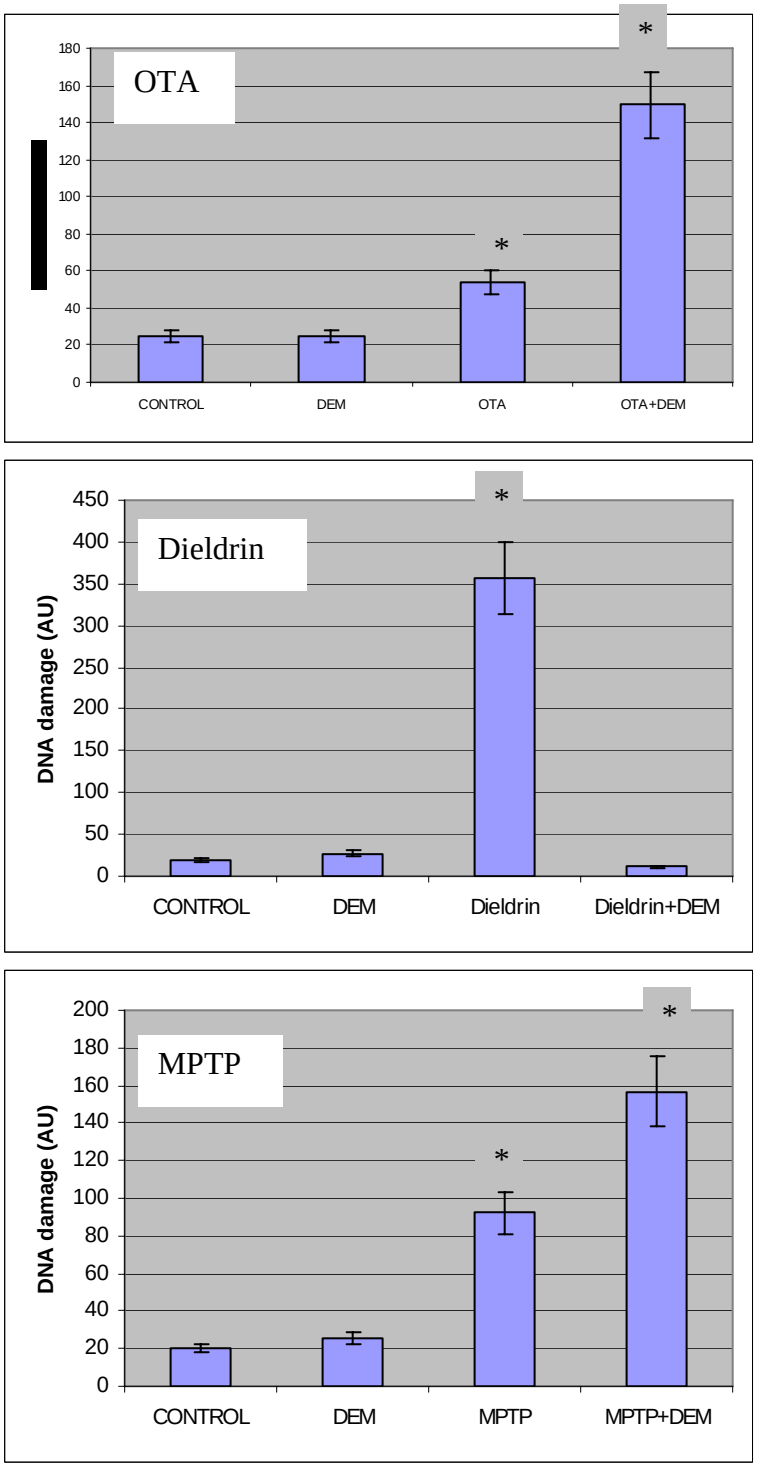

Fig. 9. Effects of pre-conditioning with DEM on oxidative DNA damage caused by OTA (4 mg/kg), Dieldrin (6 mg/kg) and MPTP (20 mg/kg) in whole midbrain. **Top panel:** OTA treatment and pre-conditioning with DEM each significantly increased DNA damage compared to control. **Middle panel:** Dieldrin alone significantly increased DNA damage and pre-conditioning reduced DNA damage to control levels. **Lower panel:** MPTP significantly increased DNA damage and pre-conditioning with DEM further increased damage. One-way ANOVA followed by t-tests was performed for each panel. Asterisk indicates significant difference from control values ($p < 0.05$) Oxidative DNA damage was assayed with Poly(ADP-ribose) Polymerase Assay Kit (Trevigen, Gaithersburg, MD).

Dieldrin administered alone significantly increased DNA damage and pre-conditioning with DEM reduced DNA damage to control levels (Fig 9, middle panel). MPTP significantly increased DNA damage and pre-conditioning with DEM further increased damage (Fig 9, lower panel).

To assess the effects of DEM pre-conditioning on redox status of the midbrain, total (GSSG+GSH), reduced (GSH) and oxidized glutathione (GSSG) was measured. DEM, as expected of a mild pro-oxidant, caused a decrease in reduced glutathione (GSH), but did not significantly affect total glutathione (GSH+GSSG). See Fig 12. OTA also caused a similar reduction in GSH, showing that each of these agents increased oxidative stress. Interestingly, pre-conditioning with DEM increased levels of reduced glutathione (GSH) a result that suggests a potential protective effect of pre-conditioning. Consistent with this result, the oxidized glutathione (GSSG) was significantly reduced by the pre-conditioning. Paradoxically, the improvement of redox status (less oxidation) promoted by pre-conditioning with DEM, did not diminish the extent of DNA damage and lipid peroxidation that was potentiated by pre-conditioning. Our earlier work on the acute effects of OTA did not reveal apoptosis in either SN or VTA and therefore the anti-oxidative and DNA repair responses to OTA may have been robust enough to prevent cell death(6).

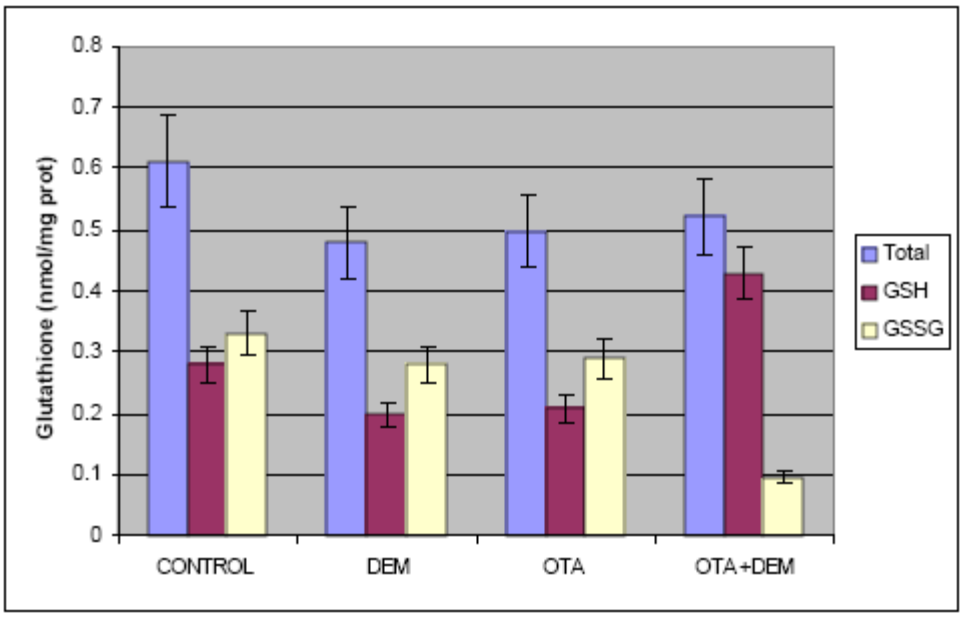

Fig. 10 Changes in in reduced (GSH), oxidized (GSSG) and total concentration of glutathione measured in midbrains of ICR mice exposed to DEM alone, OTA alone and mice pre-conditioned with DEM 6 hrs before OTA injection.

SUMMARY OF RESULTS FROM TASK 4

Task 4: **To measure the effects of neurotoxicant exposure on the DNA repair response in two compartments of the midbrain, the SN-pars compacta and the ventral tegmental area (VTA)**

Rather than using laser capture micro-dissection to removal individual neurons for the gene expression studies of Task 4, we used the micro-punch dissection technique to harvest VTA and SN from sets of 6 mice. Brains were dissected under a dissecting stereo-microscope. The ventral and dorsal parts of midbrain (MB) were dissected at the level of the caudal end of the cerebral peduncles. SN and VTA were dissected from the coronal sections of the brain using micro-punch biopsy method as described (7). All the samples were kept frozen at –70 °C until assayed.

To analyze the role of other DNA repair genes in mediating this phenomenon, quantitative real-time PCR was performed in whole midbrain as well as SN and VTA micro-dissected tissue samples.

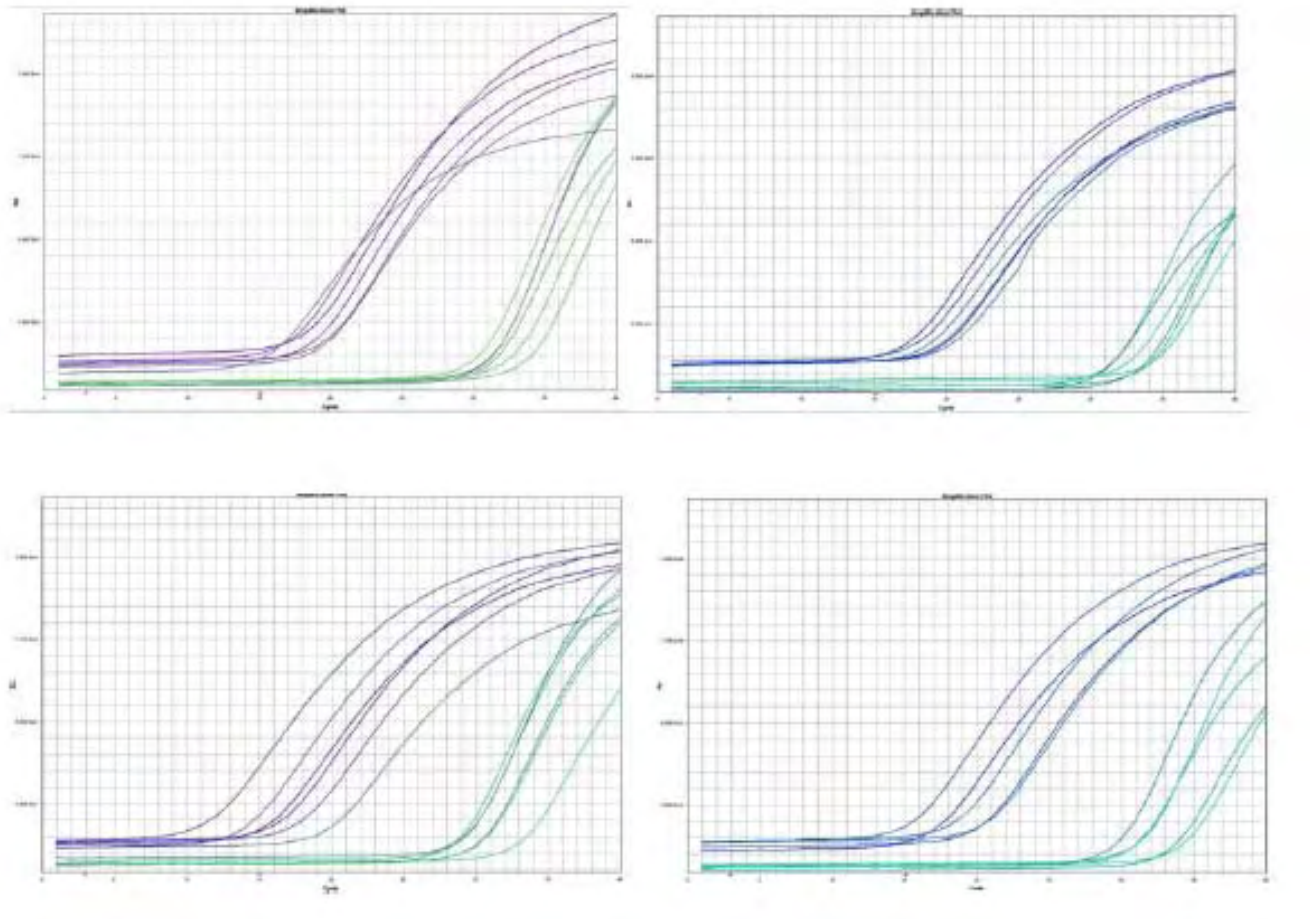

Fig 11. Real time PCR amplification plot for OGG1 mRNA isolated from midbrain of ICR mice given DEM, OTA and combinations of both.. Graphs represent two groups of curves corresponding to 18S housekeeping genes (lower cycle numbers) and OGG1 (higher cycle numbers). Left upper panel depicts control group of animals; right upper panel depicts effect of OTA alone; left lower panel represent effect of DEM alone and right lower panel represents the effects of preconditioning with an injection of DEM 6 hrs before administration of OTA.

Quantitative RT-PCR of DNA Repair Genes (*OGG1, PARP, APEX/Ref1*)

RNeasy Mini KIT (Qiagen, Valencia, CA) was utilized for total RNA isolation from animal brain tissues and for RNA cleanup according to the manufacturer's protocol. The reverse transcription reaction was performed with Superscript III Kit (Invitrogen, Cartsbad, CA) according to manufacturer protocol. Briefly, the reaction mixture I contained the following : 1 µL of 50 µM Oligo dT primers, 1 µL of 10 mM dNTP mix and 1 µL of ddH2O template plus 10 ul from the original samples, was heated to 65°C for 5 min and incubated on ice for 1 min. The mixture was supplemented with 4 µL of 10x Buffer, 1 µL of 40 U/µL RNaseOUT , 1 µl of 0.1 M DTT and 1 µL of Superscript III Reverse Transcriptase (all reagents from Invitrogen, Cartsbad, CA) following incubation at 50 °C for 50 min and reaction was stopped by heating at 70 ºC for 15 min then was added 1 µl of 2 U/µl ribonuclease H (Invitrogen, Cartsbad, CA) incubated samples at 37ºC during 20 min RNA degradation. The reverse-transcription reaction is stored on ice until real-time PCR. For long-term storage reverse-transcription reactions kept at –20 °C.

The quantitative real-time PCR was performed in the ABI PRISM 79000 with cycling as follows: 2 minutes at 50°C, followed by 10 minutes at 95°C, 15 seconds at 95°C and 1 minute at 60°C (40 cycles). Each 96-well plate was divided into two parts, one for each target (OGG1, PARP or APEX) and another part for 18S housekeeping gene. Each part included the following: control (no treatment), negative control (DEM pretreatment), positive control (OTA alone) and experiment (DEM and OTA).
The primers and probe were adapted from sequences used in the TaqMan Gene Expression Kit (Applied Biosystems) as presented in Table 1. Each probe included FAM (6-carboxy-fluorescein, emission 518 nm) at the 5'-end as the reporter and a nonfluorescent quencher at the 3' end of the probe. Primer and probe have been premixed in a concentration of 18 µM for each primer and 5 µM for each probe, with a total volume of 250 µL. Technical characteristics of primers and probes are listed in **Table 1.**
The reaction mixture for real time PCR contained the following in a final volume of 25 µl: 12.5µl of 2x TaqMan universal PCR master Mix, 9.5 µl of RNase-free water and 1.25 µl of housekeeping gene or gene of interest (all from Applied Biosystems) plus 2 µl of diluted samples (10µl of original samples plus 20 µl of dd H2O)

Data Analysis

Results were calculated by the "Comparative Ct Method of Quantitation" ($\Delta\Delta$Ct) as published by Applied Biosystems: www.wzw.tum.de/gene-quantification/pe-rel-quan.pdf). In this method no standard curve is used, instead all results are calculated relative to a reference standard, called a "calibrator." Each of the three targets is analyzed separately, and then OGG1, PARP and APEX were each normalized to 18S. The normalization is necessary to account for variabilities in RNA quantity and quality, and

variabilities in reverse transcription efficiency among samples. In this study we required that the 18S Ct of less than 30 to be considered an interpretable specimen. In our experience using 18S in real time assays, higher Cts for the 18S indicate insufficient template quantity, quality, and/or the presence of inhibitors. Samples were excluded if failed to meet this criterion.

Table 1. TaqMan Gene Expression Kit (Applied Biosystems) employed for this study.

Assay ID	**Gene Name**	**GenBank mRNA**	Assay location **Assay As**	**Amplification Length**
: Mm00500154_m1	PARP1 poly (ADP-ribose) polymerase family, member 1	NM_007415.2	346	74
Hs99999901_s1	Eukaryotic 18S rRNA	X03205.1	609	187
Mm00501781_m1	8-oxoguanine DNA-glycosylase 1	NM_010957.2	348	106
Mm00507805_g1	apurinic/apyrimidinic endonuclease 1	NM_009687.1	123	115

Results

The regulation of OGG1, PARP and APEX mRNA in SN and VTA triggered by OTA in the pre-conditioning paradigm is summarized in Fig. 12.

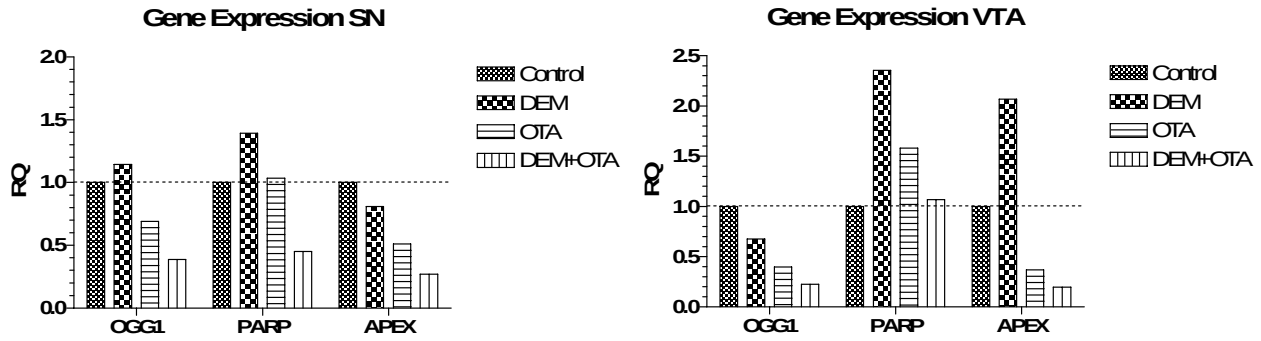

Fig 12. Quantitative real time PCR of OGG1. PARP and APEX mRNA measured in SN (left panel) and VTA (right panel) of mice exposed to DEM alone, OTA alone and mice pre-conditioned with DEM 6 hrs before OTA injection. Horizontal dashed line indicates the RQ value of the control samples. RQ (relative quantity) of the mRNA was calculated using the "Comparative Ct Method of Quantitation" as described in the methods section.

Pre-conditioning with DEM resulted in down regulation of all three DNA repair genes in SN (Fig 14, left panel). DEM administration alone up-regulated PARP 1.4 fold. OTA administered alone also down-regulated OGG1 and APEX, but not PARP. By contrast, OGG1 was down-regulated by all treatments in the VTA (Fig 14, right panel), with the DEM pre-conditioning causing the greatest degree of down-regulation in this compartment of the midbrain. The biggest contrast between SN and VTA in the profile of DNA repair was in the regulation of PARP. For example, DEM treatment alone markedly increased levels of PARP mRNA, and when given 6 hrs before OTA (pre-conditioning), the expression of PARP mRNA was returned to a control level. APEX regulation also was distinct in VTA compared to SN. APEX was upregulated in VTA following administration of DEM but was markedly down-regulated in the DEM pre-conditioning experiment.

OGG1 gene expression was also analyzed in whole midbrain utilizing the pre-conditioning paradigm (Fig 13). OGG1 mRNA was down-regulated by OTA and DEM treatments alone, but when DEM was given in the pre-conditioning paradigm, there was marked up-regulation of the gene. It is worth noting that at the same time OTA caused down-regulation of OGG1 mRNA, the total amount of DNA damage in midbrain was increased (Fig 9). This observation is consistent with earlier work from our lab that indicates an inverse relationship between OGG1 enzymatic activity and DNA damage (9).

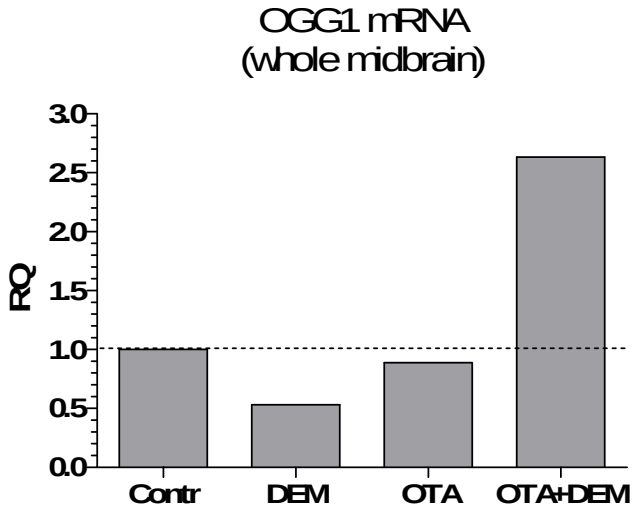

Fig 13 Quantitative real time PCR of OGG1 mRNA measured in whole midbrain tissue (includes SN, VTA and dorsal compartments of midbrain) exposed to DEM alone, OTA alone and mice pre-conditioned with DEM 6 hrs before OTA injection. Horizontal dashed line indicates the RQ value of the control samples. RQ (relative quantity) of the mRNA was calculated using the "Comparative Ct Method of Quantitation" as described in the methods section.

These effects of the pre-conditioning paradigm on OGG1 mRNA regulation in **whole midbrain** were in stark contrast to the effects on the two DA neuron compartments (compare Figs 13 and 14). The OGG1 mRNA in the whole midbrain increased with pre-conditioning, but the expression of OGG1 mRNA was markedly down-regulated in both SN and VTA by the pre-conditioning. This could be interpreted as evidence of successful repair in these compartments, requiring a dampening down of OGG1 by 72 hrs. On the other hand, up-regulation of OGG1 mRNA in VTA and SN might indicate increased DNA damage. The marked difference between sub-compartment analysis and whole midbrain analysis underscores the importance of examining well-defined populations of neurons. Despite the suggestion of increased DNA damage in VTA and SN following OTA, there was insufficient damage to result in cell death as indicated by the absence of apoptotic profiles or caspace- expressing neurons in the SN and VTA(6). The pre-conditioning paradigm caused an up-regulation of OGG1 mRNA, suggesting that the total amount of DNA damage was diminished and also did not result in cell death in either compartment.

The question as to the relative vulnerability of SN DA neurons compared to VTA DA neurons to agents which caused oxidative stress remains a puzzle. However, the distinctive VTA profile of PARP regulation may provide a clue as to the relative resistance of VTA DA neurons to oxidative stress (Fig 16). Here it is clear that PARP mRNA was markedly upregulated by DEM, and in the pre-conditioning paradigm PARP mRNA was regulated to levels measured in the control condition. In the case of the SN, pre-conditioning resulted in a marked down-regulation of PARP mRNA below control levels.

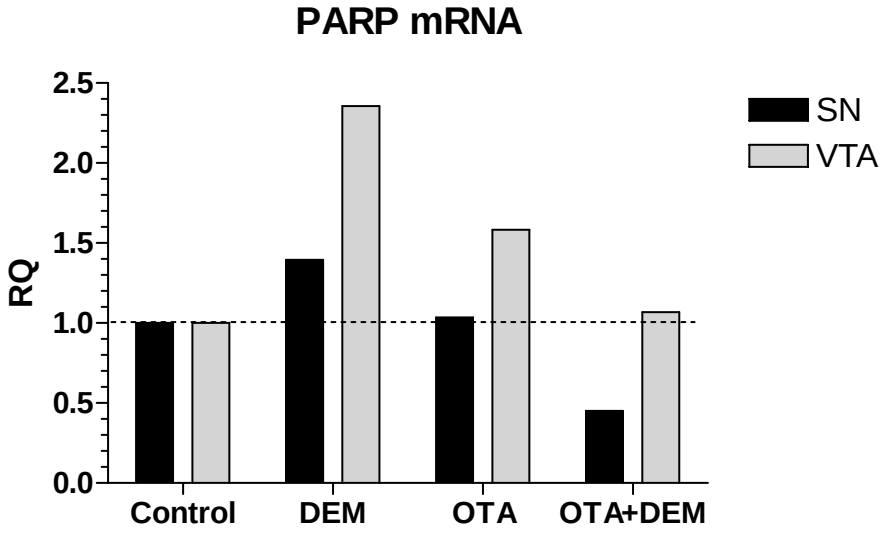

Fig 14. Quantitative real time PCR of PARP mRNA measured in SN and VTA of mice exposed to DEM alone, OTA alone and mice pre-conditioned with DEM 6 hrs before OTA injection. Horizontal dashed line indicates the RQ value of the control samples. RQ (relative quantity) of the mRNA was calculated using the "Comparative Ct Method of Quantitation" as described in the methods section.

Interestingly, the pre-conditioning paradigm restored the total amount of DNA damage in midbrain to levels measured in normal midbrain (Fig 9, middle panel). Hence, it is likely that the total amount of DNA damage in VTA was less than that of SN.

Pre-conditioning with DEM before injection of the pesticide dieldrin revealed a profile of gene expression in SN and VTA that was distinct from the profile elicited by the mycotoxin OTA (See Fig 15).

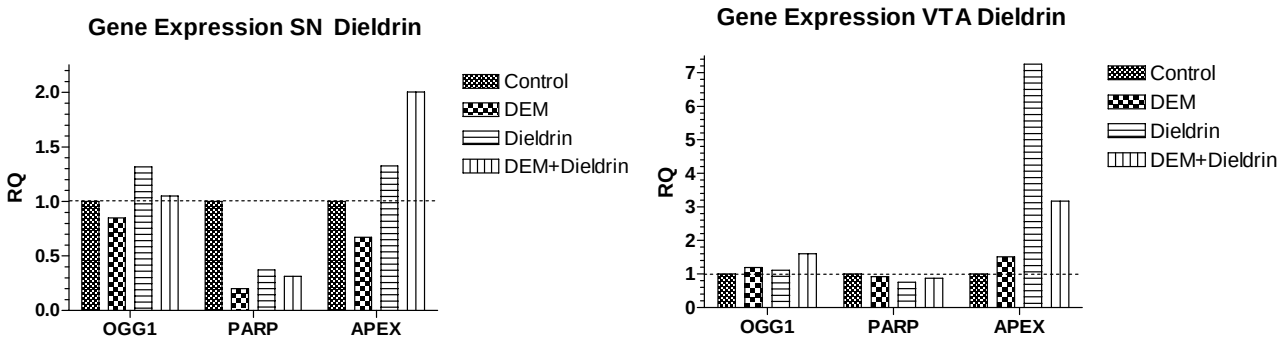

Fig 15 Quantitative real time PCR of OGG1. PARP and APEX mRNA measured in SN (left panel) and VTA (right panel) of mice exposed to DEM alone, Dieldrin alone and mice pre-conditioned with DEM 6 hrs before Dieldrin injection. Horizontal dashed line indicates the RQ value of the control samples. RQ (relative quantity) of the mRNA was calculated using the "Comparative Ct Method of Quantitation" as described in the methods section.

In the SN, OGG1 mRNA levels were normalized by pre-conditioning with DEM, but in the VTA, OGG1 mRNA was upregulated by pre-conditioning compared to the control condition. Also in the SN, PARP mRNA was markedly down-regulated by DEM alone, by dieldrin alone and by pre-conditioning. However, in the VTA, PARP was not down-regulated by any of the conditions. With respect to APEX, a 7 fold up-regulation was elicited by dieldrin in the VTA but in the SN the up-regulation was only 1.3 fold. Despite the clear difference between SN and VTA in the profile of expression of 3 DNA repair genes, there was no difference with respect to cell death (no evidence for apoptosis in either compartment).

KEY RESEARCH ACCOMPLISHMENTS

1. **Distribution of OTA in brain**: Pharmacokinetic parameters for ochratoxin-A (OTA) in each brain region were determined based on OTA concentrations measured at 3, 6, 12, 24 and 72 hrs after administration of the toxin. There were no correlations between parameters of oxidative stress (lipid peroxidation, oxidative DNA damage, OGG1 activity) and pharmacokinetic parameters such as elimination half life, area under the curve (reflecting cumulative concentration over time) and clearance. ***Therefore the regional brain concentrations of OTA were not critical determinants of the degree of oxidative stress (and oxidative DNA damage and repair) elicited by the toxin in specific brain regions.***

2, **Effects of OTA on striatal DA and metabolites and tyrosine hydroxylase immunoreactivity**; The mycotoxin OTA produced a dose- and time-dependent depletion of striatal dopamine (DA), a decrease in striatal DA turnover and qualitatively diminished striatal tyrosine hydroxylase immunoreactivity without the appearance of apoptotic profiles in s. nigra or striatum. These data are consistent with the finding that striatum (caudate/putamen) was the most sensitive of all brain regions to OTA in terms of the ability to increase OGG1 activity (the striatum had lowest ED50 for stimulation of OGG1 activity). In addition, these alterations in DA levels were not due to degeneration of neurons in the SN.

3. Studies on the **chronic OTA infusion** on oxidative stress, oxidative DNA damage and repair were completed:

a) **Effects on glutathione**: Chronic OTA infusion resulted in a cumulative dose-dependent decrease in total glutathione levels in all brain regions. Despite the depletion of total glutathione, the proportion of reduced glutathione relative to total glutathione remained relatively constant in each region with a trend towards an increase following chronic infusion with the highest dose of OTA. This reflects the capacity of the cells to maintain redox homeostasis in the face of chronic oxidative stress. Hence differences in a brain region's capacity to maintain anti-oxidative redox status through the glutathione system does not appear to play an important role in determining vulnerability to OTA.

b) **Effects on SOD (as well as mitochondrial and cytoplasmic component of the total SOD)**: Chronic OTA infusion elicited increases of SOD (both cytoplasmic and mitochondrial) activity in all regions of brain, but the greatest change from baseline was seen in the mitochondrial SOD (mSOD) activity of the pons. The pons was the region with the slowest elimination contstant (T1/2) and very high cumulative exposure (AUC) following acute doses of OTA. This result suggests that there is a relationship between cumulative exposure and the degree of upregulation of mitochondrial SOD in the pons, but this relationship does not hold for other regions of brain.

c) **Effects on OGG1:** Chronic OTA infusion resulted in a dose-dependent increase in OGG1 activities in all brain regions. No region of brain showed an inhibition or decrease in OGG1 activity at any dose, unlike the early responses to acute doses of OTA, when all regions showed initial and transient inhibition of OGG1 activity. Even though all brain regions were capable of marked increases

in OGG1 activity, not all regions were equally sensitive to the toxin. Using the dose-response curve functions generated from each brain region to estimate an ED50 (the dose of OTA that resulted in half the maximal rate of OGG1 activity), it was clear that the caudate/putamen (CP) was most sensitive to the toxin.

4. **Effects of Dieldrin:** Chronic infusion of this pesticide resulted in a dose-dependent increase in OGG1 activity. However, the midbrain, caudate/putamen and cerebral cortex did not differ with respect to the extent of increase of OGG1.

5. **Effects of MPTP:** After mapping the normal distributions of OGG1 and superoxide dismutase (SOD) across 44 loci dissected from mouse brain, MPTP, a mitochondrial toxicant with selective dopamine (DA) neuron cytotoxicity was used to elicit focal oxidative stress and DNA repair responses. A single dose of MPTP (20 mg/kg, i.p.) elicited time- and region dependent changes in both SOD and OGG1, with early increases in DNA repair and anti-oxidant activities throughout all regions of brain. In some sampled loci, notably the substantia nigra (SN) and hippocampus, the heightened DNA repair and antioxidant responses were not maintained beyond 48 h. Other loci from cerebellum, cerebral cortex and pons maintained high levels of activity up to 72 h. Levels of dopamine (DA) were decreased significantly at all time points and remained below control levels in nigro-striatal and mesolimbic systems (ventral tegmental area and nucleus accumbens). Assessment of apoptosis by TUNEL staining revealed a significant increase in number of apoptotic nuclei in the substantia nigra at 72 h and not in other loci. The marked degree of apoptosis that became evident in SN at 72 h was associated with large decreases in SOD and DNA repair activity at that locus. In conclusion, MPTP elicited global effects on DNA repair and antioxidant activity in all regions of brain, but the most vulnerable loci were unable to maintain elevated DNA repair and antioxidant responses.

6. **Effects of pre-conditioning with a mild pro-oxidant on the DNA damage caused by OTA, Dieldrin and MPTP** Each of the toxicants caused acute oxidative DNA damage, with dieldrin administration resulting in the highest degree of DNA damage in whole midbrain samples at 72 hrs after administration. In the pre-conditioning paradigm, DEM potentiated the extent of DNA damage in midbrain caused by the toxicants OTA and MPTP. However, pre-conditioning with DEM reduced the amount of DNA damage in midbrain produced by a single injection of dieldrin.. Even though pre-conditioning with DEM increased oxidative DNA damage caused by OTA administration, measurements of glutathione (reduced, oxidized and total) revealed an augmentation of reduced glutathione (GSH) in whole midbrain. Apparently, the DEM pre-conditioning 6 hrs before administration of OTA allowed recovery of redox status in whole midbrain that normally would be shifted towards decreased GSH levels by the toxicant (OTA). Hence, it appears that mild pro-oxidant conditioning provided some degree of protection against a subsequent challenge of OTA. This conclusion was consistent with our earlier

findings that OTA did not cause apoptosis in midbrain.

7. Effects of OTA (and pre-conditioning) on DNA repair gene expression in VTA and SN: OTA administration resulted in down-regulation of OGG1 and APEX, but not PARP (at 72 hrs). Pre-conditioning with DEM resulted in down regulation of all three DNA repair genes in SN. DEM administration alone up-regulated PARP 1.4 fold. By contrast, OGG1 was down-regulated by all treatments in the VTA, with the DEM pre-conditioning causing the greatest degree of down-regulation in this compartment of the midbrain. The biggest contrast between SN and VTA in the profile of DNA repair was in the regulation of PARP. For example, DEM treatment alone markedly increased levels of PARP mRNA, and when given 6 hrs before OTA (pre-conditioning), the expression of PARP mRNA was returned to a control level.. In addition, the effects of pre-conditioning on dieldrin-triggered DNA repair gene expression revealed a distinct profile in SN compared to VTA.

REPORTABLE OUTCOMES

Acute neurotoxic effects of the fungal metabolite Ochratoxin-A This report is the first to describe depletion of striatal dopamine following single doses of OTA. In addition, the regional vulnerability to OTA was explored in the context of regional differences in oxidative DNA repair, and other parameters of oxidative stress.

Neuroanatomical mapping of DNA repair and antioxidative responses in mouse brain: **effects of a single dose of MPTP**. Results obtained demonstrate that OGG1 is activated across many brain regions in response to MPTP. This response was completely unexpected because MPTP is considered to be a selective nigro-striatal dopamergic neurotoxin and such a widespread activation of antioxidant and OGG1 activity had never been reported. However, by 72 h, there was a decrease of repair capacity, most notably in the nigro-striatal DA system. In SN, the drop in SOD and OGG1 activity at 72 h was associated with a significant increase in the number of apoptotic cells in that nucleus. To summarize, the temporal and spatial profile of MPTP-triggered DNA repair and antioxidant activity at 72 h was consistent with the well-known localized toxicity for the nigro-striatal DA system.

Pharmacokinetics of Ochratoxin-A distribution in mouse brain. This is the first report in which pharmacokinetic parameters of OTA distribution in brain were determined. Interestingly, those regions of brain with the highest cumulative exposure are *not* those most sensitive to the toxin.

Effects of chronic OTA infusion on parameters of oxidative stress in brain regions. This report will be a thorough documentation of the effects of chronic infusion of low doses of OTA, and will be contrasted with the effects of acute OTA administration in explaining striatal vulnerability to the toxin.

Effects of acute and chronic Dieldrin administration on parameters of oxidative stress in brain regions (manuscript submitted to J. Biochem Mol Tox). Dieldrin has been shown to be toxic for DA neurons *in*

vitro and this manuscript assesses the role of regional anti-oxidative capacity and DNA repair in determining vulnerability to the toxin *in vivo.*

Effects of OTA, Dieldrin and MPTP on gene expression were studied in whole midbrain and in sub-compartments (VTA and SN). The profiles of gene expression were complex but differences between VTA and SN were measured in the response to pre-conditioning with the pro-oxidant DEM . These results provide new clues to understanding the greater vulnerability of the SN DA neurons to agents that increase oxidative stress.

CONCLUSIONS Three toxicants (ochratoxin-A, Dieldrin, MPTP) from distinct chemical families were chosen for study on the basis of their reported capacity to interfere with mitochondrial function. The patterns of oxidative stress across brain regions elicited by each of these agents was distinct and unique. The profiles of DNA repair gene expression elicited by each of the toxicants in SN and VTA were specific for the toxicant and unique for each compartment of midbrain. These results provide additional clues that will improve understanding of the mechanism for the vulnerability of specific regions of brain to toxicants that impact mitochondrial function. In particular, understanding the mechanism(s) responsible for the vulnerability of specific populations of DA neurons may lead to new ways to protect against neurotoxicity and even to protect against onset and/or slow progression of Parkinson's Disease.

REFERENCES

1. Reiderer P, Wuketic S. Time course of nigrostriatal degeneration in Parkinson's disease. J Neural Trans 1976;3:277-301.

2. Hornykiewicz O. Brain neurotransmitter changes in Parkinson's disease. Boston: Butterworth, 1982.

3. McGeer PL, McGeer EG, Suuki JS. Aging and extrapyramidal function. Arch Neurol 1977;34:33-35.

4. Bennett JW, Klich M. Mycotoxins. Clin Microbiol Rev 2003;16(3):497-516.

5. Sava V, Mosquera D, Song S, Stedeford T, Calero K, Cardozo-Pelaez F, et al. Rubratoxin B elicits antioxidative and DNA repair responses in mouse brain. Gene Expr 2004;11(5-6):211-219.

6. Sava V, Reunova O, Velasquez A, Harbison R, Sanchez-Ramos J. Acute neurotoxic effects of the fungal metabolite ochratoxin-A. Neurotoxicology 2006;27(1):82-92.

7. Sava V, Reunova O, Velasquez A, Song S, Sanchez-Ramos J. Neuroanatomical mapping of DNA repair and antioxidative responses in mouse brain: Effects of a single dose of MPTP. NeuroToxicology 2006;27(6):1080-1093.

8. Sava V, Reunova O, Velasquez A, Sanchez-Ramos J. Can low level exposure to ochratoxin-A cause parkinsonism? J Neurol Sci 2006;249(1):68-75.

9. Cardozo-Pelaez F, Brooks PJ, Stedeford T, Song S, Sanchez-Ramos J. DNA damage, repair, and antioxidant systems in brain regions: a correlative study. Free Radical Biology & Medicine 2000;28(5):779-785.

APPENDIX

Published and Pending Manuscripts

Gene Expression(2004)11: 211-219

RUBATOXIN-B ELICITS ANTI-OXIDATIVE AND DNA REPAIR RESPONSES IN MOUSE BRAIN

V. Sava[1,2]; D. Mosquera[1,2]; S. Song[1,2]; T. Stedeford [2,4], K. Calero[1];
F. Cardozo-Pelaez[3]; R. Harbison[4], J. Sanchez-Ramos[1,2*]

[1]Neurology, University of South Florida, Tampa, FL
[2]Research Service, James Haley VA, Tampa, FL
[3]Department of Pharmaceutical Sciences, University of Montana, Missoula, MT
[4]College of Public Health, University of South Florida, Tampa, FL, USA

[*] **Corresponding author:** Dr. Juan R. Sanchez-Ramos, The Helen E. Ellis Professor of Neurology, University of South Florida, Department of Neurology (MDC 55), 12901 Bruce B. Downs Blvd., Tampa, FL 33612, USA; Tel: (813) 974-6022; Fax: (813) 974-7200; E-mail: jsramos@hsc.usf.edu

Abstract

Rubratoxin-B (RB) is a mycotoxin with potential neurotoxic effects that have not yet been characterized. Based on existing evidence that RB interferes with mitochondrial electron transport to produce oxidative stress in peripheral tissues, we hypothesized that RB would produce oxidative damage to macromolecules in specific brain regions. Parameters of oxidative DNA damage and repair, lipid peroxidation and superoxide dismutase (SOD) activity were measured across 6 mouse brain regions 24 hrs after administration of a single dose of RB. Lipid peroxidation and oxidative DNA damage was either unchanged or decreased in all brain regions in RB-treated mice compared to vehicle-treated mice. Concomitant with these decreased indices of oxidative macromolecular damage, SOD activity was significantly increased in all brain regions. Oxyguanosine glycosylase activity (OGG1), a key enzyme in the repair of oxidized DNA, was significantly increased in three brain regions cerebellum (CB), caudate/putamen (CP), and cortex (CX) but not hippocampus(H), midbrain(MB), and pons/medulla(PM). The RB-enhanced OGG1 catalytic activity in these brain regions was not due to increased OGG1 protein expression, but was a result of enhanced catalytic activity of the enzyme. In conclusion, specific brain regions responded to an acute dose of RB by significantly altering SOD and OGG1 activities to maintain the degree of oxidative DNA damage equal to, or less than, that of normal steady-state levels.

Running Head: Rubratoxin-B elicits anti-oxidative response

Keywords: Rubratoxin-B, oxidative stress, DNA damage and repair, SOD, mouse brain regions

INTRODUCTION

Mycotoxins are toxic fungal metabolites which are structurally diverse, common contaminants of the ingredients of animal feed and human food. These fungal products exhibit a range of pharmacological activities that have been utilized in development of mycotoxins or mycotoxin derivatives as antibiotics, growth promoters, and other kinds of drugs; still others have been developed as biological and chemical warfare agents [1]. Bombs and ballistic missiles laden with biological agents including aflatoxin were believed to be deployed by Iraq during Operation Desert Storm[2]. In light of the excess incidence of amyotrophic lateral sclerosis in young Gulf War veterans [3], it is important not to forget the potential neurotoxic effects of low doses of mycotoxins. Although much is known about the lethal effects of the aflatoxins, little is known about the acute and long-term effects of less potent mycotoxins, such as Rubratoxin B (RB), on adult nervous system.

Rubratoxin B (RB) is a metabolite of the molds *Penicillum rubrum and Penicillum purpurogenum*. These molds commonly contaminate cereals, foodstuffs and grow on damp tents and fabrics. RB is not known to produce a serious health hazard in this naturally occurring form, but pure RB is a bisanhydride lactone with hepatotoxic [4] and teratogenic properties [5, 6, 7]. Investigation of the effects of acute and chronic exposure to RB on the nervous system has been scarce, even though neuronal tissue appears to be very susceptible to the deleterious effect of RB in teratogenic studies [8].

RB has numerous biochemical actions including the inhibition of (Na^+- K^+)-ATPase [9], inhibition of the hepatic cytochrome P-450-dependent monooxygenase system[10], reduction of hepatic and renal nonprotein sulfhydryl content [11] and inhibition of gap junctional intercellular communication [12]. It was found that RB caused shifts in the

ultraviolet absorption spectra of DNA and RNA [13]. The observed binding properties of RB can disrupt the integrity of DNA and RNA. RB has been shown to induce apoptosis [14, 15] and internucleosomal fragmentation of DNA [14].

Studies with isolated mouse liver mitochondria revealed that RB disrupted mitochondrial respiration and depressed oxygen consumption[8]. The principal site of action of RB in the mitochondrial electron transport system was found to be between cytochrome C1 and the termination of electron flow [8]. Ochratoxin, a related mycotoxin, has been reported to alter mitochondrial respiration and oxidative phosphorylation through impairment of the mitochondrial membrane and inhibition of the succinate-dependent electron transfer activities of the respiratory chain [16].

The overall objective was to study RB neurotoxicity in the context of oxidative stress induced by inhibition of mitochondrial electron transport in brain tissues. Inhibition of oxidative phosphorylation would be expected to result in increased generation of oxyradicals and decreased production of ATP[17]. We hypothesized that RB-induced alteration of oxidative processes would not be homogeneous across all brain regions but would reflect the capacity of distinct brain regions to upregulate anti-oxidative mechanisms and repair processes. Parameters of oxidative stress measured included lipid peroxidation (thiobarbituric acid-reactive substances or TBARS), SOD activity, oxidative DNA damage and repair in each of six brain regions cerebellum (CB), cortex (CX), hippocampus (HP), midbrain (MB), caudate/putamen (CP) and pons/medulla (PM). Accumulation of 8-oxodG was chosen as an indicator of DNA damage and activity of DNA glycosylase was used as an index of DNA repair.

MATERIALS AND METHODS

Materials

Rubratoxin-B, superoxide dismutase, xantine oxidase, ribonuclease T1, HEPES, dithiotreitol, bovine serum albumin and acrylamide/bisacrylamide (19:1) mixture were purchased from Sigma (St. Louis, MO). TEMED was from Bio-Rad Laboratories (Hercules, CA). Protease inhibitors and 8-oxoguanine DNA glycosylase (mOGG1) were from Boehringer Mannheim (Indianapolis, IN). Synthetic oligonucleotide contained 8-oxodG was from Trevigen (Gaithersburg, MD). ^{32}P-ATP (7, 000 Ci/mmol) was from ICN Biomedical, Inc. (Costa Mesa, CA). Phosphorylation buffer, 3'-phosphate free T4 polynucleotide kinase, RNase, proteinase K, nuclease P1, alkaline phosphatase were from Roche Diagnostic Co. (Indianapolis, IN). G-25 Microcentrifuge Spin Column was from Shelton Scientific (Shelton, CT). mOGG1 antibody was from Alpha Diagnostic (San Antonio, TX). ECL western blotting analysis system was from Amersham Biosciences (Piscataway, NJ). All other reagents were ACS grade and from Sigma Chemical Co.

Animals and Treatment

The animal protocol used in this study was approved by the University of South Florida (USF) IUCAC committee. The protocol was also reviewed and approved by the USF Division of Comparative Medicine which is fully accredited by AAALAC International and managed in accordance with the Animal Welfare Regulations, the PHS Policy, the FDA Good Laboratory Practices, and the IACUC's Policies. Male Swiss ICR mice (22 ?2 g) were obtained from the Jackson Laboratories (Bar Harbor, ME). They were housed five per cage at the temperature of 21?2 ?C with 12 light/dark cycle and free access to food and water. Mice were divided into experimental (n=10) and control (n=5) groups. Animals were injected with

either RB dissolved in DMSO (5 mg/kg ip) or vehicle. Mice were sacrificed with CO_2 twenty four hours after treatment. The brains were removed and immediately dissected in a Petri dish on ice (~ 0▾ C).

Isolation of Brain Regions

Brain was separated into 6 regions under a dissecting microscope in following order. The cerebellar peduncles were cut first, and brain stem was removed from the diencephalon. The ventral and dorsal parts of midbrain (MB) were dissected at the level of the caudal end of the cerebral peduncles at the junction with the pons. The pons and medulla (PM) were separated together by cutting the ponto-medullary junction. The cerebral hemispheres were opened with a sagittal cut along the longitudinal tissue and hippocampus (HP) was isolated, followed by caudate and putamen (CP). Finally, cerebellum (CB) and cerebral cortex (CX) were harvested and all the samples were kept frozen at –70 ?C until assay.

Measurement of DNA damage

Steady-state level of 8-oxodG was used as a marker of oxidative DNA damage. The procedure for DNA isolation was basically the same as reported before [18]. Approximately 150 mg of brain sample was used for extraction. Briefly, tissue was pulverized in liquid nitrogen, using mortar and pestle, sonicated in 10 mM ethylenediamine tetraacetic acid (EDTA) and centrifuged. The pellet was treated with DNAase-free RNAase followed by digestion with proteinase K. The protein fraction was separated from DNA by three consecutive organic extractions. The DNA was precipitated by ethanol and incubated overnight at -20 °C. The ratio in absorbance at 260/280 nm was employed for qualification of DNA purity.

The purified DNA was digested with nuclease P1 following by treatment with alkaline phosphatase. The mixture of deoxynucleosides was analysed with HPLC using 5% methanol dissolved in 100 mM of sodium acetate (pH 5.2) as a mobile phase, and 8-oxodG was detected with an electrochemical detector (ESA Coulochem Model 5100A) at +0.4 V. 2-dG was detected at 260 nm in the same sample using a Perkin Elmer 785A Programmable Absorbance Detector (Perkin Elmer, Norwalk, CT) connected in series with the electrochemical detector. 8-oxodG level was expressed as ratio of 8-oxodG/2-dG. Data were recorded, stored, and analyzed on a PC Pentium computer using ESA 500 Chromatography Data System Software.

Assessment of 8-oxoguanine-DNA glycosylase activity (OGG1)

The extraction of OGG1 for enzymatic assay was performed as described previously [18]. Briefly, brain tissue was pulverized in liquid nitrogen, using mortar and pestle. Homogenization buffer contained 20 mM Tris-Base (pH 8.0), 1 mM EDTA, 1 mM dithiotrietol (DTT), 0.5 mM spermine, 0.5 mM spermidine, 50% glycerol and protease inhibitors. Homogenates were rocked for 30 min after addition of 1/10 volume 2.5 M KCl and spun at 14,000 rpm for 30 min. The supernatant was aliquoted and specimens were kept frozen at –70 ?C until assay. Protein concentration was measured using the bicinchoninic acid [19].

OGG1 activity was measured by incision assay as previously described [18]. To prepare ^{32}P-labeled duplex oligonucleotide, twenty pmol of synthetic probe contained 8-oxodG (Trevigen, Gaithersburg, MD) was incubated at 37 ?C with ^{32}P-ATP and polynucleotide T4 kinase. To separate the unincorporated free ^{32}P-ATP, the reaction mixtures were spun through a G25 spin column. Complementary oligonucleotides were annealed in 10

mM Tris, (pH 7.8), 100 mM KCl, 1 mM EDTA by heating the samples 5 min at 80 °C and gradually cooling at room temperature.

Incision reaction (20 ?L) contained 40 mM HEPES (pH 7.6), 5 mM EDTA, 1 mM DTT, 75 mM KCl, purified bovine serum albumin, 100 fmol of ^{32}P-labeled duplex oligonucleotide, and protein extract (30 ? g). The reaction mixture was incubated at 37 °C for 2 h and placed on ice to terminate the reaction. A 20 ?L of loading buffer containing 90% formamide, 10mM NaOH and blue-orange dye was added to each sample. After 5 min of heating at 95 ^{o}C the samples were resolved in a denaturing 20% polyacrylamide gel containing 7 M urea. The gel was visualized using Biorad-363 Phosphoimager System and OGG1 incision activity was calculated as the amount of radioactivity in the band corresponding to the specific cleavage product over the total radioactivity in the lane.

Kinetic study of OGG1 incision reaction

Reaction mixtures and conditions used for kinetic studies were identical to OGG1 incision activity assay, but amounts of the appropriate ^{32}P-labeled oligonucleotide duplex were varied. The enzyme concentration and reaction time was adjusted so as to cleave no more than 10% of the substrate. Kinetic parameters were calculated using a Jandel SigmaPlot version 5.00 nonlinear fit routine. Three independent experiments were performed for each analysis.

Western immunoblotting

The 8-oxoguanine DNA glycosylases extracted from different regions of brain were

separated on a 12% SDS-PAGE and transferred onto a nitrocellulose membrane using a Biorad Semi-Dry Transblot technique. The membranes were blocked overnight at 4 ^{o}C in a solution containing 5% dry milk and Tris-Buffered Saline (TBS) composed of 200 mM NaCl and 50 mM Tris-HCl (pH7.4), and supplemented with 0.04% Tween-20. The membranes were rinsed in TBS-Tween mixture and incubated overnight at 4 ^{o}C with mOGG1 antibody (Alpha Diagnostic, TX) using 1:1000 dilution by 1% dry milk prepared on TBS-Tween. After washing (3 x 10 min) with TBS-Tween at 4 ^{o}C, the membranes were incubated with goat anti-mouse antibody (1:2000 dilution) conjugated to horseradish peroxidase (Santa Cruz Biotechnology, CA) for 1 hr at room temperature. The blot was developed by ECL kit (Amersham Biosciences, Piscataway, NJ).

Native PAGE

OGG1 extracted from different regions of brain mixed with native buffer composed of 0.1 M Tris-HCl (pH6.8), 30% glycerol, and 0.01% bromophenol blue and separated on a non-denaturing 10% polyacrylamide gel at 120 V. Gel were sliced by a razor blade along the lanes into section 1 mm thick. A single 1 mm thick section was homogenized with a teflon hand homogenizer in 20 ? L of incision reaction mixture and enzymatic activity of OGG1 was assayed as described above.

Lipid peroxidation

Formation of lipid peroxide derivatives was evaluated by measuring thiobarbituric acid-reactive substances (TBARS) according to [20]. Briefly, the different regions of brain were individually homogenized in ice-cold 1.15% KCl (w/v); then 0.4 mL of the homogenates were mixed with 1mL of 0.375% TBA, 15% TCA (w/v), 0.25 N HCl and 6.8 mM butylated-

hydroxytoluene (BHT), placed in a boiling water bath for 10 min, removed and allowed to cool on ice. Following centrifugation at 3000 r.p.m. for 10 min, the absorbance in the supernatants was measured at 532 nm. The amount of TBARS produced was expressed as nmol TBARS per milligram of protein using malondialdehyde bis(dimethyl acetal) for calibration.

Superoxide dismutase (SOD) assay

Determination of superoxide dismutase activity in mouse brain regions was based on inhibition of nitrite formation in reaction of oxidation of hydroxylammonium with superoxide anion radical [21]. Nitrite formation was generated in a mixture contained 25 ?L xanthine (15 mM), 25 ?L hydroxylammonium chlorode (10 mM), 250 ?L phosphate buffer (65 mM, pH 7.8), 90 ?L distilled water and 100 ?L xanthine oxidase (0.1 U/mL) used as a starter of the reaction. Inhibitory effect of inherent SOD was assayed at 25?C during 20 min of incubation with 10 ?L of brain tissue extracts. Determination of the resulted nitrite was performed upon the reaction (20 min at room temperature) with 0.5 mL sulfanilic acid (3.3 mg/mL) and 0.5 mL α-naphthylamine (1 mg/mL). Optical absorbance at 530 nm was measured with Ultrospec III spectrophotometer (Pharmacia, LKB). The results were expressed as units of SOD activity calculated per milligram of protein. The amount of protein in the samples was determined using the bicinchoninic acid [19].

Statistical analysis

The results were reported as mean ± SE for at least five different preparations, assayed in duplicate. For electrophoresis two different gels were run. The differences between samples were analyzed by the Student's *t*-test, and a $P<0.05$ was considered as statistically significant.

RESULTS

Administration of a single dose of RB to mice (ip injection, 5 mg/kg body weight) was chosen on the basis of a dose-toxicity curve (data not shown) that resulted in no visible gross damage to brain. This single dose did, however, produce alterations in brain biochemistry. Lipid peroxidation, indicated by TBARS levels, was decreased in all regions of brain of the animals exposed to RB as compared to control mice (Fig. 1). In HP, MB and PM the TBARS levels were significantly ($P<0.05$) different from the control. In PM region, a 2.2 fold decrease in TBARS was observed.

Oxidative DNA damage, indicated by steady-state levels of 8-oxodG, showed a trend towards decreased levels across all brain regions (Table 1). Statistically significant differences in 8-oxod-dG were found in only the PM region, where levels were reduced to 30% below control. Oxidative damage in MB was also distinctly decreased, but did not reach statistical significance.

The decreased levels of oxidative DNA damage were associated with increased activity of the repair enzyme OGG1 (Table 1). There was a statistically significant increase in OGG1 activity in CB, CP and CX regions as compared to the respective controls. In HP the activity of OGG1 was higher than in control though the difference did not reach statistical significance. The OGG1 activity was reduced in MB and PM. The trend of reduced OGG1

activity within the MB-PM array presented in Table 1 was unexpectedly associated with decreased levels of 8oxodG in those regions. Nevertheless, we observed that relative extent of DNA damage decreased linearly (Fig. 2) with relative activity of OGG1 (correlation factor was - 0.9545). For both specific OGG1 and 8-oxodG relative indices were calculated as follows:

$$\textbf{Relative indices} = \frac{100 \cdot (V_{RB} - V_C)}{V_C}$$

where V_{RB} are values obtained in RB experiment and V_C – in control

The results in Table 1 demonstrated up-regulation of SOD activity in RB-treated animals as compared to control. The extent of increased SOD activity in different regions of brain revealed a negative correlation with the level of 8-oxodG. Namely, the association between 8-oxodG and SOD activity can be expressed by the linear equation with the correlation factor of - 0.8521:

$$\textbf{[8-oxodG] = – 0.19·[SOD] + 4.6}$$

Western blot analysis was carried out to elucidate the source of OGG1 activity (Fig.3). It was found that protein expression levels of OGG1 were not significantly affected by RB exposure and there were no differences in regional levels of OGG1 when normalized to the total protein variations. One of the bands in the Western blot attributed to OGG1 matched the single band of pure enzyme. However, we found an additional band that was also labeled with OGG1 antibody. This band may be due to non-specific binding with antibody or otherwise caused by existence of various isoforms of OGG1. To clarify this issue, we resolved OGG1

in native PAGE followed by cutting the gel into 1 mm strips and assaying the strips for OGG1 enzymatic (incision) activity. Fig. 4 indicates presence of two distinct bands with incision activity, which likely can be attributed to different isoforms of OGG1. Assaying the pure enzyme with the same procedure showed one single band possessing electrophoretic mobility identical to the major band of the tested sample (not shown).

The data are in agreement with kinetic behavior of OGG1 extracted from mouse brain. As can be seen from Fig. 5 the oligonucleotide incision activity plotted against concentration reveals bi-modal curves. The first part of incision activity reached saturation level in a range between 0 and 120 pM of substrate, but second part needed higher concentrations of substrate (up to 500 pM). Computer modeling generated kinetic curves representing the experimental curve as a superposition of low- and high-saturated enzymatic isoforms. Separated incision activities were analyzed using Michaelis-Menten kinetics with the corresponding calculation of kinetic constants as shown in Table. 2.

DISCUSSION

Until the present report, the toxic effects of RB in adult brain had not been investigated. Administration of a single dose (5mg/kg) did not produce gross pathological changes in brain, but resulted in paradoxically less oxidative damage to both lipids and DNA. In fact the level of lipid peroxidation in hippocampus, midbrain and pons/medulla was significantly less than that found in vehicle-treated controls. Similarly, RB did not increase oxidative DNA damage in any region of brain after the injection rather tended to lower the degree of damage. These results were unexpected in light of the putative pro-oxidant effects of the mycotoxin, but were explained by the robust upregulation of anti-oxidative and repair

systems. RB treatment elicited an increase in activity of SOD, a major oxyradical scavenger, across all brain regions. In addition, measures of oxidative DNA repair were observed to increase in three of six brain regions following RB treatment.

Measurement of oxidative DNA damage revealed a trend towards decreased steady-state levels of 8-oxodG across all brain regions with a statistically significant decreased level in pons/medulla (PM). The DNA repair response assessed from the change in OGG1 activity was significantly increased in three brain regions (CX, CB, CP) but it is noteworthy that maintenance of normal steady state levels of 8-oxodG was facilitated by the greatly enhanced SOD activity in regions of brain where OGG1 did not increase.

The index of DNA damage utilized in this study was 8-oxodG, a major pre-mutagenic DNA lesion generated from the reaction of oxyradicals with guanosine. Repair of this DNA lesion involves DNA N-glycosylases that hydrolyse the N-glycosylic bond between the 8-oxoG and deoxyribose, releasing the free base and leaving an apurinic/apyrimidinic (AP) site in DNA. Such AP sites are cytotoxic and mutagenic, and must be further processed. Some DNA glycosylases also have an associated AP lyase activity that cleaves the phosphodiester bond 3' to the AP site [22]. Formamidopyrimidine glycosylase (fpg, also named fapy-DNA glycosylase) is a prokaryotic protein originally identified in *E. coli* that catalyzes the excision of damaged purine bases such as 8-oxodG and 2,6-diamino-4-hydroxy-5-N-methylformamidopyrimidine from double stranded DNA. Two distinct homologues of fpg were identified in yeast, OGG1 and OGG2 (8-oxo-guanine glycosylase). The counterpart of yeast OGG1 has been identified in eukaryotes, and in particular human brain (hOGG1). hOGG1 has been cloned and shares 50% homology with mouse 8-oxoguanine glycosylase

(mOGG1) [22, 23]. In the present report, the role of the brain's DNA response to RB focused on the activity and regulation of the mammalian base excision repair enzyme OGG1.

In addition to the enzymatic assay, the expression of OGG1 protein was measured by Western immunobloting. However, the detection of a second band with molecular weight essentially different from mOGG1 required more careful characterization. Separation of DNA glycosylases with native PAGE followed by assays of incision activity in various portions of gel disclosed heterogeneity of enzyme activity. Thus, enzymatic incision activity of tested extracts from mouse brain was comprised of two distinct isoforms of OGG1.

A detailed characterization of the isoforms of DNA glycosylase was performed by enzymatic kinetic analysis. Calculation of kinetic constants showed that RB treatment caused an increase in catalytic efficacy in both isoforms of OGG1. The response to RB-induced oxidative DNA damage was to enhance OGG1 catalytic activity (V_{max}/K_m) by a factor of 1.74. RB also increased affinity of OGG1 for the substrate that was demonstrated by decrease in magnitudes of the Michaelis-Menten constant, K_m.

The augmentation of SOD activities in all brain regions and the increased affinity and catalytic activity of OGG1 elicited by RB treatment maintained 8-oxodG levels equal to, or below, the levels found in control animals. In the hippocampus, the levels of oxidative DNA damage following RB treatment was 2.7 fold less than that found in control mice. A similar phenomenon in mouse brain has been reported following treatment with the pro-oxidant diethylmaleate [18]. A single treatment with diethylmaleate elicited a significant increase in the activity of OGG1 in three brain regions with low basal levels of activity. There was no change in the activity of OGG1 in those regions with high basal levels of activity (HP, CP,

and MB). This protective response elicited by proxidants such as DEM and RB demonstrate efficient homeostatic mechanisms that maintain a healthy redox status in brain tissues.

The capacity to regulate OGG1 may be important for maintaining genomic integrity in the face of oxidative stress, but endogenous antioxidant defenses also played a role in the brain's response to RB. In fact, the magnitude of the increases in SOD activity across all regions of brain was greater than the observed increases in OGG1 activity. There was a correlation between OGG1 and SOD activities in different regions of brain, suggesting that both enzymes may be regulated by a common signal triggered by oxidative stress.

The mechanisms underlying the vulnerability of the brain to different neurotoxicants is complex, but we hypothesize that the capacity to regulate and repair oxidative DNA damage, and to modulate endogenous anti-oxidant enzymes, are important determinants of a brain region's susceptibility to RB. In the present study, which focused on a single time point 24 hrs after injection with RB, it was not the intent to determine the earliest signals for triggering and amplifying SOD and OGG1 activities. We imposed the limitation of a single time point for this study in order to focus on the differential response across brain regions. The robust anti-oxidant response and enhanced OGG1 catalytic activity in some regions resulted in much lower levels of oxidized base in those brain regions, providing a clue as to the selective vulnerability of specific neuronal populations located in those regions.

The data presented here clearly raises many questions that drive on-going and future investigations. In order to further characterize the regulation of OGG1 in response to RB and similar neurotoxicants, it will be important to discover whether the earliest changes in SOD and OGG1 activity (3 to 6 hrs after exposure) are due to modification in catalytic activities of the protein and to what extent the response requires upregulation of SOD and OGG1 mRNA

and protein expression. Just as importantly, the effects of RB on viability of specific populations of neurons (e.g., dopaminergic neurons, striatal neurons) in the specific brain regions will need to be investigated and correlated with measures of oxidative DNA damage and repair. Finally, studies with graded doses of RB will determine whether RB can produce a rigid-akinetic parkinsonian syndrome similar to that produced by other mitochondrial toxicants such as rotenone.

ACKNOWLEDGEMENTS

This study was supported by VA Merit Grant and DOD grant USAMRMC 03281031.

REFERENCES

[1] Bennett, J. W. and Klich, M., Mycotoxins. Clin Microbiol Rev. 16: 497-516; 2003

[2] Zilinskas, R. A., Iraq's biological weapons. The past as future? Jama. 278: 418-424; 1997

[3] Haley, R. W., Excess incidence of ALS in young Gulf War veterans. Neurology. 2003; 61: 750-756.

[4] Natori S, Sakaki S, Kurata H, Udagawa SI and Ichinoe M. Production of rubratoxin B by *Penicillium purpurogenum Stoll*. Appl Microbiol. 19:613-617;1970

[5] Hood RD, Innes JE and Hayes AW. Effects of rubratoxin B on prenatal development in mice. Bull Environ Contam Toxicol 1973; 10: 200-207;1973

[6] Hood RD. Effects of concurrent prenatal exposure to rubratoxin B and T-2 toxin in the mouse. Drug Chem Toxico. l 9: 185-190;1986

[7] Koshakji RP, Wilson BJ and Harbison RD. Effect of rubratoxin B on prenatal growth and development in mice. Res Commun Chem Pathol Pharmacol; 5: 584-592; 1973

[8] Hayes AW. Action of rubratoxin B on mouse liver mitochondria. Toxicology.6:253-561;1976

[9] Phillips TD, Hayes AW, Ho IK and Desaiah D. Effects of rubratoxin B on the kinetics of cationic and substrate activation of (Na+-K+)-ATPase and p-nitrophenyl phosphatase. J Biol Chem. 253: 3487-3493; 1978

[10] Siraj MY and Hayes AW. Inhibition of the hepatic cytochrome P-450-dependent monooxygenase system by rubratoxin B in male mice. Toxicol Appl Pharmacol 48: 351-359;1979

[11] Engelhardt JA, Carlton WW, Carlson GP and Hayes AW. Reduction of hepatic and renal nonprotein sulfhydryl content and increased toxicity of rubratoxin B in the Syrian hamster and Mongolian gerbil. Toxicol Appl Pharmacol. 96: 85-92; 1988

[12] Nagashima H, Nishida M, Ishizaki Y, Morita I, Murota S, Goto T. Cytological effects of rubratoxin B: morphological change and gap Junctional intercellular communication. In: Funatsu K, Shirai Y, Matsushita T (eds.) Animal Cell Technology: Basis & Applied Aspects 1997; vol. 8. Kluwer Academic Publishers, Dordrecht, pp. 571-575

[13] Watson SA and Hayes AW. Evaluation of possible sites of action of rubratoxin B-induced polyribosomal disaggregation in mouse liver. J Toxicol Environ Health. 2(3): 639-650;1997

[14] Nagashima H and Goto T. Rubratoxin B induces apoptosis in HL-60 cells in the presence of internucleosomal fragmentation. *Mycotoxins*. 46: 17–22; 1998

[15] Nagashima H, Ishizaki Y, Nishida M, Morita I, Murota S, Goto T. Rubratoxin B induces apoptosis in p53-null cells. *Mycotoxins* 46: 35–37;1998

[16] Wei YH, Lu CY, Lin TN and Wei RD. Effect of ochratoxin A on rat liver mitochondrial respiration and oxidative phosphorylation. Toxicology 36: 119-30; 1985

[17] Hasegawa, E., Takeshige, K., Oishi, T. and et al., MPP+ induces NADH-dependent superoxide formation and enhances NADH-dependent lipid peroxidation in bovine heart submitochondrial particles. Biochem Biophys Res Com. 170: 1049-1055, 1990

[18] Cardozo-Pelaez F, Stedeford TJ, Brooks PJ, Song S and Sanchez-Ramos JR. Effects of diethylmaleate on DNA damage and repair in the mouse brain. Free Radical Biology and Medicine 33: 292-298;2002

[19] Smith PK, Krohn RI, Hermanson GT, Mallia AK, Gartner FH, Provenzano MD, Fujimoto EK, Goeke NM, Olson BJ, Klenk DC. Measurement of protein using bicinchoninic acid. Analytical Biochemistry 150: 76-85;1985

[20] Cascio C, Guarneri R, Russo D, De Leo G, Guarneri M, Piccoli F, Guarneri P. Pregnenolone sulfate, a na;turally occurring excitotoxin involved in delayed retinal cell death. J Neurochem. 74(6): 2380-2391;2000

[21] Elstner EF and Heupel A. Inhibition of nitrite formation from hydroxylammoniumchloride: a simple assay for superoxide dismutase. Anal. Biochem. 70: 616–620; 1976

[22] Krokan HE, Standal R. and Slupphaug G. DNA glycosylases in the base excision repair of DNA. Biochem Journal 325: 1-16;1997

[23] Dianov G, Bischoff C, Piotrowski J and Bohr VA. Repair pathways for processing of 8-oxoguanine in DNA by mammalian cell extracts. J Biol Chem 273: 33811-33816;1998

Table 1. Evaluation of Oxidative DNA damage, Oxidative DNA Repair (OGG1) and Superoxide Dismutase Activities across different regions of mouse brain exposed to RB in comparison with control.

Brain regions	Animal groups	DNA damage* (ppm)	OGG1 incision activity (pM?min^{-1}?mg prot^{-1})	Activity of SOD (U/mg prot.)
CB	Control	18.4?2.2	2.6?0.2	42.5?4.6
	RB intoxication	16.7?2.1	4.06?0.55**	63.8?7.5**
CP	Control	20.6?3.8	3.05?0.24	42.4?2.7
	RB intoxication	18.2?1.8	4.27?0.45**	72.6?6.1**
CX	Control	20.7?0.8	2.52?0.4	34.8?1.5
	RB intoxication	20.1?5.1	3.86?0.32**	64.5?11.25**
HP	Control	19.4?1.2	2.86?0.31	32.6?3.2
	RB intoxication	16.1?1.9	3.42?0.33	78.14?12.1**
MB	Control	26.9?8.3	2.79?0.22	48.6?2.1
	RB intoxication	20.2?6.4	2.43?0.19	112.5?16.4**
PM	Control	33.0?2.4	3.4?0.26	38.7?3.8
	RB intoxication	22.7?0.9**	3.0?0.27	105.5?14.8**

*The extent of DNA damage was calculated from the amount of 8-oxodG (fmol) contained in 1 nmol of 2-dG and expressed as parts per million (ppm)
**The values are significantly ($P<0.05$) different compared to controls. All results represented by mean ? SE.

Table 2. Kinetic characterization of OGG1 isoforms obtained from CP of control mouse and from CP of mouse subjected to RB

Isoforms of OGG1	Samples tested	Kinetic constants		
		K_m (pM)	V_{max} (pM?min^{-1}?mg^{-1})	V_{max}/K_m (min^{-1}?mg^{-1})
High-saturated	CP exposed to RB	147.7?12	20.1?2.1	0.136?0.01
	CP control	312.9?29	24.7?2.6	0.078?0.007
Low-saturated	CP exposed to RB	105.3?9	17.7?2	0.16?0.02
	CP control	140.5?11	16.2?1.5	0.11?0.01

Figure Captions

Fig. 1. Content of TBARS in different regions of mouse brain exposed to RB (closed bars) in comparison to control (opened bars). All values represent by mean ? SE. The significantly ($P< 0.05$) different levels of TBARS in comparison to control indicated by asterisks.

Fig.2. Relationship between relative indices of OGG1 activity and accumulation of 8-oxodG in various regions of mouse brain. Relative indices represent values normalized to the correspondent controls.

Fig. 3. OGG1 expression in different regions of mouse brain. The Western blot lanes depicted by $C_{CB} - C_{PM}$ array show the level of OGG1 in control mouse, and lanes from R_{CB} to R_{PM} represent OGG1 expression in the brain of RB-intoxicated animal. Pure enzyme presented as a positional marker for OGG1 identification.

Fig. 4. Determination of OGG1 on native PAGE. Enzymatic activity of OGG1 was assayed in every single fraction by using ^{32}P-duplex oligonucleotide. Upper panel represent ^{32}P-duplex oligonucleotide products visualized with Biorad-363 Phosphoimager System. Lower panel represent the averaged data of three experiments with OGG1 extracted from HP of control mouse. OGG1 activity was calculated as the % of radioactivity in the band of specifically cleaved product over the total radioactivity in the lane.

Fig. 5. Kinetic behavior of OGG1 extracted from different regions of brain. Circles represent OGG1 obtained from CP of mouse exposed to RB. Squares represent OGG1 obtained from CP of control mouse. Data expressed by means of 3 replications.

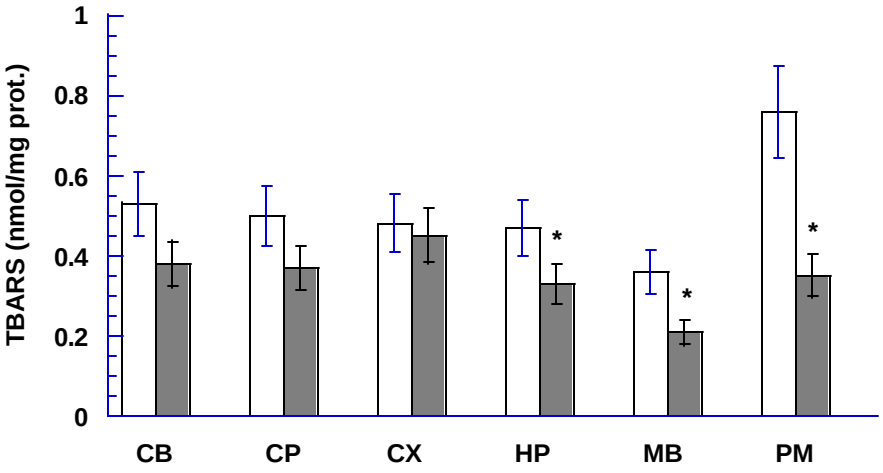
TBARS (nmol/mg prot.)
1
0.8
0.6
0.4
0.2
0
CB
CP
CX
HP
MB
PM
*
*
*

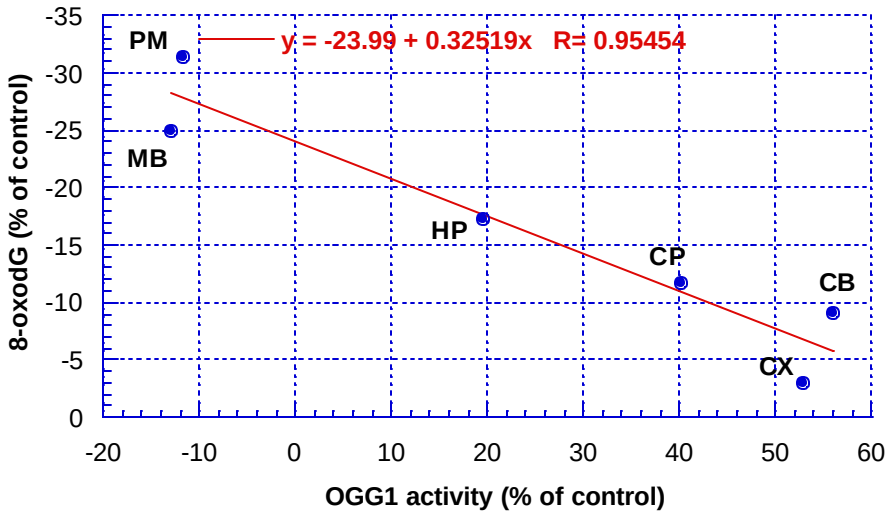
8-oxodG (% of control)
-35
-30
-25
-20
-15
-10
-5
0
-20
-10
0
10
20
30
40
50
60
OGG1 activity (% of control)
y = -23.99 + 0.32519x R= 0.95454
PM
MB
HP
CP
CB
CX

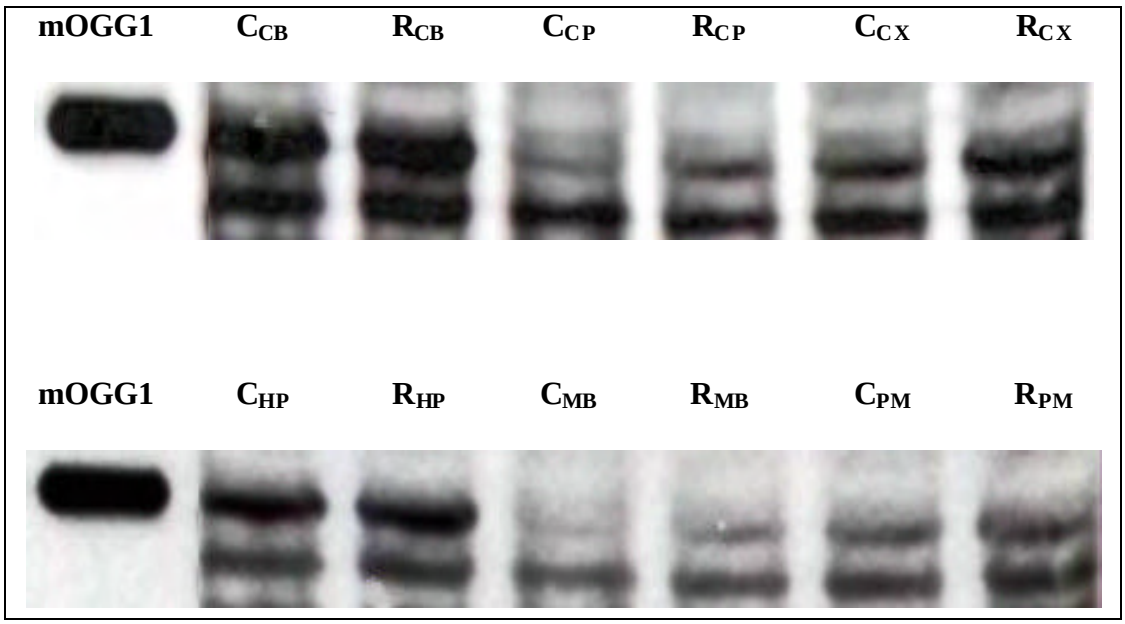
mOGG1
C_{CB}
R_{CB}
C_{CP}
R_{CP}
C_{CX}
R_{CX}
mOGG1
C_{HP}
R_{HP}
C_{MB}
R_{MB}
C_{PM}
R_{PM}

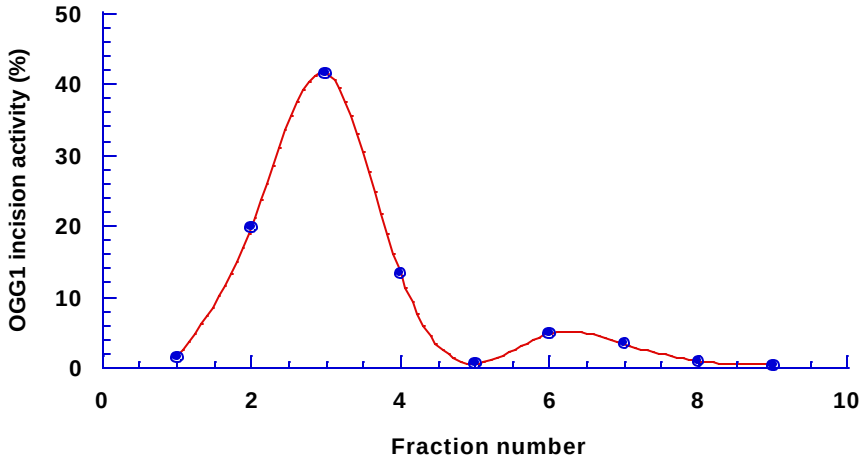
OGG1 incision activity (%)
0
10
20
30
40
50
0
2
4
6
8
10
Fraction number

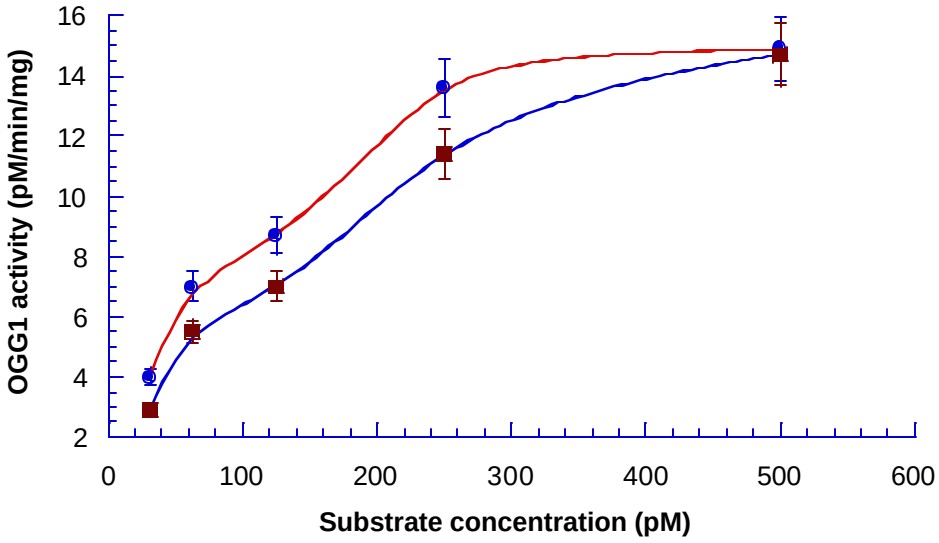
OGG1 activity (pM/min/mg)
16
14
12
10
8
6
4
2
0
100
200
300
400
500
600
Substrate concentration (pM)

Available online at www.sciencedirect.com
SCIENCE DIRECT
NeuroToxicology 27 (2006) 82–92
NeuroToxicology

Acute neurotoxic effects of the fungal metabolite ochratoxin-A

V. Sava [a,c], O. Reunova [a,c], A. Velasquez [a,c], R. Harbison [b], J. Sánchez-Ramos [a,c,*]

[a] University of South Florida, Department of Neurology (MDC 55), 12901 Bruce B. Downs Blvd., Tampa, FL 33612, USA
[b] College of Public Health, University of South Florida, Tampa, FL, USA
[c] Research Service, James Haley VA, Tampa, FL, USA

Received 31 January 2005; accepted 12 July 2005
Available online 2 September 2005

Abstract

Ochratoxin-A (OTA) is a fungal metabolite with potential toxic effects on the central nervous system that have not yet been fully characterized. OTA has complex mechanisms of action that include evocation of oxidative stress, bioenergetic compromise, inhibition of protein synthesis, production of DNA single-strand breaks and formation of OTA–DNA adducts. The time course of acute effects of OTA were investigated in the context of DNA damage, DNA repair and global oxidative stress across six brain regions. Oxidative DNA damage, as measured with the ''comet assay'', was significantly increased in the six brain regions at all time points up to 72 h, with peak effects noted at 24 h in midbrain (MB), CP (caudate/putamen) and HP (hippocampus). Oxidative DNA repair activity (oxyguanosine glycosylase or OGG1) was inhibited in all regions at 6 h, but recovered to control levels in cerebellum (CB) by 72 h, and showed a trend to recovery in other regions of brain. Other indices of oxidative stress were also elevated. Lipid peroxidation and superoxide dismutase (SOD) increased over time throughout the brain. In light of the known vulnerability of the nigro-striatal dopaminergic neurons to oxidative stress, levels of striatal dopamine (DA) and its metabolites were also measured. Administration of OTA (0–6 mg/kg i.p.) to mice resulted in a dose-dependent decrease in striatal DA content and turnover with an ED50 of 3.2 mg/kg. A single dose of 3.5 mg/kg decreased the intensity of tyrosine hydroxylase immunoreactivity (TH+) in fibers of striatum, TH+ cells in substantia nigra (SN) and TH+ cells of the locus ceruleus. TUNEL staining did not reveal apoptotic profiles in MB, CP or in other brain regions and did not alter DARPP32 immunoreactivity in striatum. In conclusion, OTA caused acute depletion of striatal DA on a background of globally increased oxidative stress and transient inhibition of oxidative DNA repair.

Keywords: Ochratoxin-A; Oxyguanosine glycosylase; Superoxide dismutase; Dopamine; Tyrosine hydroxylase; Apoptosis; Substantia nigra; Striatum

1. Introduction

Ochratoxin-A (OTA) is a metabolite produced by *Aspergillus ochraceus* and *Penicillium verrucosum* that accumulates in the food chain because of its long half-life (Galtier, 1991; Kuiper-Goodman and Scott, 1989). In view of its ubiquity, the possible contribution of OTA to the development of human and animal diseases has been investigated (see review Marquardt and Frohlich, 1992). OTA has been shown to induce a tubulointerstitial nephropathy in animals (Krogh et al., 1974) and enzymuria (Kane et al., 1986a,b) similar to Balkan endemic nephropathy found in humans (Krogh, 1992; Krogh et al., 1974; Petkova-Bocharova et al., 1988). In addition to nephrotoxicity, OTA disrupts blood coagulation (Galtier et al., 1979; Gupta et al., 1979) and glucose metabolism (Pitout, 1968). It is immunosuppressive (Creppy et al., 1983b; Haubeck et al., 1981; Lea et al., 1989; Stormer and Lea, 1995), teratogenic (Arora et al., 1983; Fukui et al., 1992; Szczech and Hood, 1981) and genotoxic (Creppy et al., 1985; Pfohl-Leszkowicz et al., 1991).

Investigation of the effects of acute and chronic exposure to OTA on the nervous system has been scarce, even though development of nervous tissue appears to be very susceptible to the deleterious effects of OTA (Hayes et al., 1974; Wangikar et al., 2004). OTA has been reported to induce teratogenic effects in neonates (rats and mice) exposed in utero, characterized by microcephaly and modification of the brain levels of free amino acids (Belmadani et al., 1998). OTA was also reported to be neurotoxic to adult male rats fed OTA in the diet. Neurotoxicity, indicated by concentration of lactic dehydrogenase released from the dissected brain tissue, was more pronounced in the ventral mesencephalon, hippocampus, and striatum than in the cerebellum (Belmadani et al., 1998).

* Corresponding author. Tel.: +1 813 974 6022; fax: +1 813 974 7200.
E-mail address: jsramos@hsc.usf.edu (J. Sánchez-Ramos).

0161-813X/$ – see front matter © 2005 Elsevier Inc. All rights reserved.
doi:10.1016/j.neuro.2005.07.004

The bio-concentration of OTA in these brain regions did not correlate with toxicity (Belmadani et al., 1998).

The mechanism responsible for toxicity to neural tissues is not clear, but studies in peripheral organs and tissues reveal a spectrum of actions. The mechanisms of toxicity implicated include inhibition of protein synthesis, mitochondrial impairment, oxidative stress and DNA damage (Creppy et al., 1985, 1990; Dirheimer and Creppy, 1991; Gautier et al., 2001).

OTA-induced damage to DNA, evidenced by formation of single-strand breaks, has been reported to occur both in vitro and in vivo (Creppy et al., 1985). The DNA damage was shown to be reversible with time suggesting that variation in capacity to repair DNA may account in part for differences in vulnerability to OTA between tissues. OTA was also reported to induce single-strand breaks in a concentration-dependent manner in canine kidney cells and this effect could be potentiated by inhibition of DNA repair (Lebrun and Follmann, 2002). Other studies have demonstrated OTA–DNA adducts in mouse and monkey kidney after OTA treatment (Grosse et al., 1995). In kidney, liver and spleen, several modified nucleotides were clearly detected in DNA, 24 h after administration of OTA, but their levels varied significantly in a tissue and time-dependent manner over a 16-day period. The OTA–DNA adducts were not quantitatively and qualitatively the same in the three organs examined due to differences of metabolism in these organs and differences in the efficiency of DNA repair processes (Pfohl-Leszkowicz et al., 1993).

OTA treatment can increase oxidative stress in peripheral organs. Administration of OTA (1 mg/kg) to rats resulted in a 22% decrease in alpha-tocopherol plasma levels and a five-fold increase in the expression of the oxidative stress responsive protein heme oxygenase-1, specifically in the kidney (Gautier et al., 2001). More direct evidence of oxidative stress was derived from studies, which utilized electron paramagnetic resonance spectroscopy to measure the generation of hydroxyl radicals, in rat hepatocyte mitochondria and microsomes incubated with OTA and metabolites (Hoehler et al., 1997).

OTA toxicity is associated with inhibition of both protein and RNA synthesis (Dirheimer and Creppy, 1991). OTA is known to interfere with the charging of transfer ribonucleic acids (tRNA) with amino acids (Dirheimer and Creppy, 1991). In particular, OTA has been shown to inhibit bacterial, yeast and liver phenylalanyl-tRNA synthetases (Dirheimer and Creppy, 1991). The inhibition is competitive to phenylalanine and is reversed by an excess of this amino acid. OTA has also been shown to inhibit enzymes that use phenylalanine as a substrate such as phenylalanine hydroxylase (Dirheimer and Creppy, 1991).

Mitochondrial dysfunction has been shown to be involved in the development of OTA-induced toxicity in proximal renal tubule cells (Aleo et al., 1991). Respiration was reduced in the absence and presence of a phosphate acceptor using site I (glutamate/malate) and site II (succinate) respiratory substrates 15 and 30 min after exposure to 10^{-3} M OTA, implicating an action of OTA at both electron transport sites (Aleo et al., 1991). However, in isolated rat liver mitochondria, inhibition kinetic studies revealed that OTA is an uncompetitive inhibitor of both succinate-cytochrome *c* reductase and succinate dehydrogenase while sparing cytochrome oxidase and NADH dehydrogenase activity (Complex I) at concentrations less than 10^{-5} M (Wei et al., 1985).

The objective of the present study was to evaluate the extent of OTA neurotoxicity across mouse brain regions in the context of oxidative stress, oxidative DNA damage and DNA repair. Deficits in DNA repair have long been implicated in a number of neurodegenerative diseases, including Alzheimer's disease and Parkinson's disease. It was our goal to determine whether regional differences in DNA repair capacity predicts vulnerability to the toxin. We hypothesized that OTA-induced oxidative DNA damage would not be homogeneous across all brain regions but would reflect the capacity of distinct regions of brain to respond with antioxidative repair processes. Given the body of evidence that nigro-striatal DA neurons are especially vulnerable to oxidative stress, we also hypothesized that DA levels in striatum would be affected by OTA. Hence, we measured the effects of OTA on striatal dopamine (DA) levels and parameters of oxidative stress in six brain regions cerebellum (CB), cortex (CX), hippocampus (HP), midbrain (MB), caudate/putamen (CP) and pons/medulla (PM). Parameters of oxidative stress measured included lipid peroxidation (thiobarbituric acid-reactive substances or TBARS), SOD activity, oxidative DNA damage and repair. The enzymatic activity of DNA glycosylase served as the index of DNA repair.

2. Materials and methods

2.1. Materials

Ochratoxin-A, SOD and dihydrobenzylamine were purchased from Sigma (St. Louis, MO). Protease inhibitors and DNA glycosylase were from Boehringer Mannheim (Indianapolis, IN, USA). ^{32}P-ATP was from NEN Life Science Products (Wilmington, DE). Rabbit anti-tyrosine hydroxylase was purchased from Pel-Freez Biologicals (Arkansas, AR). Rabbit primary antibodies to DARPP32 (dopamine and cyclic AMP regulated phosphoprotein) were purchased from Chemicon, CA. ApopTag in situ Apoptosis Detection Kit and goat anti-rabbit secondary antibody were from Chemicon, CA. All other reagents were from Sigma Chemical Co.

2.2. Animals and treatment

The animal protocol used in this study was approved by the University of South Florida IUCAC committee. The protocol was also reviewed and approved by the Division of Comparative Medicine of the University, which is fully accredited by AAALAC International and managed in accordance with the Animal Welfare Regulations, the PHS Policy, the FDA Good Laboratory Practices, and the IACUC's Policies.

Male Swiss ICR mice (22 ± 2 g) were obtained from the Jackson Laboratories (Bar Harbor, ME). They were housed five per cage at the temperature of 21 ± 2 °C with 12 light/dark

cycle and free access to food and water. Mice were divided into experimental (total $n = 70$) and control (total $n = 20$) groups. Animals were injected with either OTA dissolved in 0.1 M $NaHCO_3$ mg/kg i.p. or vehicle (0.1 M $NaHCO_3$). After injection with OTA or vehicle, mice were observed for changes in spontaneous behavior three times each day until euthanasia. The response to handling was also noted. In particular, evidence for toxic effects such as clasping of limbs in response to being held by the tail was to be recorded. Groups of mice were euthanized with CO_2 at 6, 24, and 72 h after injection with OTA or vehicle. The brains were removed and immediately dissected on ice.

2.3. Isolation of brain regions

Brains were separated into six regions under a dissecting stereo-microscope in the following order. The cerebellar peduncles were cut first, and brain stem was removed from the diencephalon. The ventral and dorsal parts of midbrain (MB) were dissected at the level of the caudal end of the cerebral peduncles at the junction with the pons. The pons and medulla (PM) were separated together by cutting the ponto-medullary junction. The cerebral hemispheres were opened with a sagittal cut along the longitudinal tissue and hippocampus (HP) was isolated, followed by caudate and putamen (CP). Finally, cerebellum (CB) and cerebral cortex (CX) were harvested and all the samples were kept frozen at −70 °C until assayed (see Fig. 1).

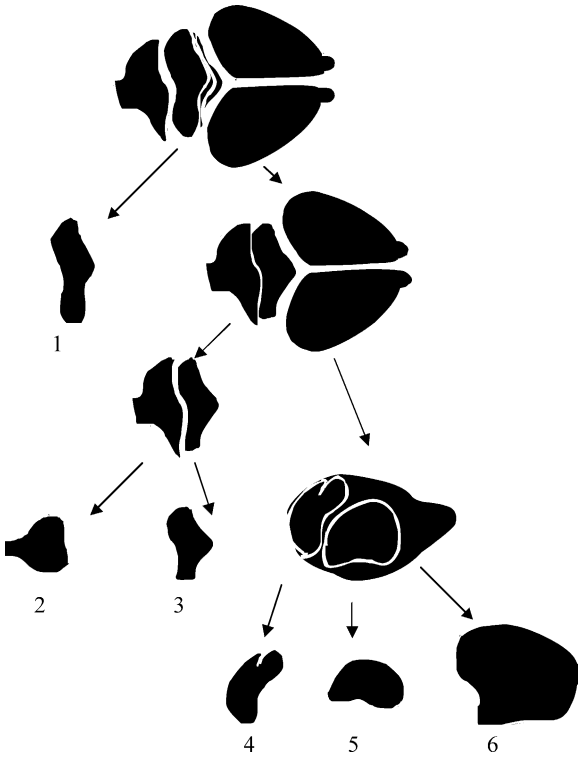

Fig. 1. Each mouse brain was dissected on ice under a stereo-microscope into six regions: (1) cerebellum (CB); (2) pons/medulla (PM); (3) midbrain (MB); (4) hippocampus (HP); (5) caudate/putamen (CP); (6) cerebral cortex (CX).

2.4. Evaluation of OTA neurotoxicity

Mice of either sex were distributed into six groups containing eight animals with an equal number of both sexes in each group. The first group of untreated animals was considered as a control, and the other five groups were treated with OTA given intraperitoneally in doses of 0–6 mg/kg of body weight. Striatal dopamine concentration was measured with HPLC 24 h after OTA administration, and the dose that caused 50% reduction in striatal DA concentrations (ED50) was calculated using the GraphPad Software, Inc. (Sorrento, CA). The ED50 was determined for eight animals in each group.

2.5. DNA damage evaluated by the comet assay

The comet assay was based on a modification of a previously published method (Schindewolf et al., 2000). Two layers of agarose were prepared. For the first layer, 85 μL 1% (w/v) high-melting point (HMP) agarose (Sigma) prepared at 95 °C in PBS was pipetted onto fully frosted microscope slides, covered with coverslip and allowed to set at 4 °C for 10 min. Cells were dissociated with 3% trypsin and RNAse following washing in PBS, centrifuged at $700 \times g$ for 15 min and resuspended at 2×10^5 in 85 μL 1% (w/v) low-melting point (LMP) agarose (Sigma). The cell suspension was then pipetted over the set HMP agarose layer, covered with coverslip and allowed to set at 4 °C for 10 min. After the coverslips were removed, the slides were immersed in pre-chilled lysis solution [2.5 M NaCl, 100 mM sodium EDTA, 10 mM Tris, pH adjusted to 10 using NaOH pellets, 1% Triton X-100 (v/v) (added immediately before use)] for 60 min at 4 °C to remove cellular proteins. Following lysis, slides were placed in a gel electrophoresis unit and incubated in fresh alkaline electrophoresis buffer (300 mM NaOH, 1 mM EDTA, pH 13) for 40 min at room temperature, before being electrophoresed at 25 V (300 mA) for 30 min at 4 °C. All the above procedures were conducted in the dark to minimize extraneous sources of DNA damage. Following electrophoresis, the slides were immersed in neutralization buffer (0.4 M Tris–HCl, pH 7.5) and gently washed three times for 5 min at 4 °C to remove alkalis and detergents. SYBR Green (50 μL; Trevigen, Gaithersburg, MD) was added to each slide to stain the DNA, then covered with a coverslip and kept in the dark before viewing. Slides were examined at 250× magnification on a Zeiss inverted fluorescence microscope (Zeiss, Germany) at 460 nm. One hundred randomly selected nonoverlapping cells were visually assigned a score based on perceived comet tail length migration and relative proportion of DNA in the comet tail. The extent of DNA damage was calculated as follows:

$$\text{DNA damage} = \text{tail length}/\text{diameter of comet head}.$$

2.6. Assessment OGG1 activity

The procedure for extraction of DNA glycosylase was similar to that described previously (Cardozo-Pelaez et al., 2000). Punched tissues were sonicated in homogenization

buffer containing 20 mM Tris, pH 8.0, 1 mM EDTA, 1 mM dithiothrietol (DTT), 0.5 mM spermine, 0.5 mM spermidine, 50% glycerol and protease inhibitors and homogenates were rocked for 30 min after addition of 1/10 volume of 2.5 M KCl. Samples were spun at 14,000 rpm for 30 min and supernatants were collected.

The OGG1 activities in supernatants were determined using duplex oligonucleotide containing 8-oxodG as incision substrate. For preparation of the incision assay, 20 pmol of synthetic probe containing 8-oxodG (Trevigen, Gaithersburg, MD) was labeled with ^{32}P at the 5′ end using polynucleotide T4 kinase (Boehringer Mannheim, Germany). Unincorporated free ^{32}P-ATP was separated on G25 spin column (Prime; Inc., Boulder, CO). Complementary oligonucleotides were annealed in 10 mM Tris, pH 7.8, 100 mM KCl, 1 mM EDTA by heating the samples 5 min at 80 °C and gradually cooling at room temperature.

Incision reactions were carried out in a mixture (20 μL) containing 40 mM HEPES (pH 7.6), 5 mM EDTA, 1 mM DTT, 75 mM KCl, purified bovine serum albumin, 100 fmol of ^{32}P-labeled duplex oligonucleotide, and extracted guanosine glycosylase (30 μg of protein). The reaction mixture was incubated at 37 °C for 2 h and products of the reaction were analyzed on denaturing 20% polyacrylamide gel. Pure OGG1 served as positive control and untreated duplex oligonucleotide was used for negative control. The gel was visualized with a Biorad-363 Phosphoimager System. The incision activity of OGG1 was calculated as the amount of radioactivity in the band representing specific cleavage of the labeled oligonucleotide over the total radioactivity. Data were normalized to equal concentration of protein, the concentration of which was measured using the bicinchoninic acid assay (Smith et al., 1985).

2.7. SOD assay

Determination of superoxide dismutase activity in mouse brain was based on inhibition of nitrite formation in reaction of oxidation of hydroxylammonium with superoxide anion radical (Elstner and Heupel, 1976). Nitrite formation was generated in a mixture contained 25 μL xanthine (15 mM), 25 μL hydroxylammonium chloride (10 mM), 250 μL phosphate buffer (65 mM, pH 7.8), 90 μL distilled water and 100 μL xanthine oxidase (0.1 U/mL) used as a starter of the reaction. Inhibitory effect of inherent SOD was assayed at 25 °C during 20 min of incubation with 10 μL of brain tissue extracts. Determination of the resulted nitrite was performed upon the reaction (20 min at room temperature) with 0.5 mL sulfanilic acid (3.3 mg/mL) and 0.5 mL α-naphthylamine (1 mg/mL). Optical absorbance at 530 nm was measured on Ultrospec III spectrophotometer (Pharmacia, LKB). The results were expressed as units of SOD activity calculated per milligram of protein. The amount of protein in the samples was determined using the bicinchoninic acid (Smith et al., 1985).

2.8. Lipid peroxidation assay

Formation of lipid peroxide derivatives was evaluated by measuring thiobarbituric acid-reactive substances (TBARS) according to a previously reported method (Cascio et al., 2000). Briefly, the different regions of brain were individually homogenized in ice-cold 1.15% KCl (w/v); then 0.4 mL of the homogenates were mixed with 1 mL of 0.375% TBA, 15% TCA (w/v), 0.25N HCl and 6.8 mM butylated-hydroxytoluene (BHT), placed in a boiling water bath for 10 min, removed and allowed to cool on ice. Following centrifugation at 3000 rpm for 10 min, the absorbance in the supernatants was measured at 532 nm. The amount of TBARS produced was expressed as nmol TBARS/mg protein using malondialdehyde bis(dimethyl acetal) for calibration.

2.9. Measurement of dopamine and metabolites

HPLC with electrochemical detection was employed to measure levels of dopamine (DA) as previously reported in our laboratory (Cardozo-Pelaez et al., 1999). Tissue samples were sonicated in 50 volumes of 0.1 M perchloric acid containing 50 ng/mL of dihydrobenzylamine (Sigma Chemical, MA) as internal standard. After centrifugation (15,000 × g, 10 min, 4 °C), 20 μL of supernatant was injected onto a C18-reversed phase RP-80 catecholamine column (ESA, Bedford, MA). The mobile phase consisted of 90% of a solution of 50 mM sodium phosphate, 0.2 mM EDTA, and 1.2 mM heptanesulfonic acid (pH 4) and 10% methanol. Flow rate was 1.0 mL/min. Peaks were detected by a Coulchem 5100A detector (ESA). Data were collected and processed with TotalChrom software (Perkin Elmer Instruments).

2.10. Tissue preparation

Mice were euthanatized after 72 h of a single injection with OTA. They were then perfused via the heart and ascending aorta with 25 mL ice-cold phosphate buffered saline (0.1 M PBS), followed by 50 mL freshly prepared 4% paraformaldehyde in PBS (pH 7.4). Brains were rapidly removed and immersion fixed for 24 h in freshly prepared 4% paraformaldehyde. The brains were then incubated for 24 h in 30% sucrose to cyroprotect them. For tyrosine hydroxylase immunohistochemistry, tissue blocks were cut and mounted in a Leitz cryostat and sectioned using the Paxinos mouse brain atlas as a guide (Paxinos and Franklin, 2001). Tissue sections to be used for tyrosine hydroxylase immunochemistry were selected from the striatal block (Bregma +0.14 at level of anterior commissure to Bregma +1.18); and hippocampal and midbrain block (Bregma −2.8 to −3.46) and the cerebellar/pons block (Bregma −5.84 to −6.24). For TUNEL staining, sagittal sections of 25-μm thickness were placed on Superfrost/Plus Microscope Slides (precleaned) and processed with immunohistochemical staining methods as described below.

2.11. Immunohistochemistry

Mouse brains were placed in ice-cold aluminum brain molds and cut into 2 mm coronal blocks. These tissue blocks were mounted in a cryostat and sectioned using a mouse brain atlas as a guide (Paxinos and Franklin, 2001). In several mouse brains,

tissue was blocked into two mid-sagittal parts and tissue sections (25 μm thin) were cut in the parasagittal plane to include the entire extent of striatum, pallidum and midbrain. Tissue sections to be used for tyrosine hydroxylase immunochemistry were selected from the striatal block (Bregma +0.14 at level of anterior commissure to Bregma +1.18); and hippocampal and midbrain block (Bregma −2.8 to −3.46) and the cerebellar/pons block (Bregma −5.84 to −6.24). For TUNEL staining sections were sampled from all the blocks encompassing forebrain to cerebellum and brainstem. Thin sections (25 μm) were placed on Superfrost/Plus Microscope Slides (precleaned) and processed by using the staining method described below.

2.11.1. Tyrosine hydroxylase (TH) immunoreactivity

Tissue sections were fixed for 30 min at room temperature in 4% paraformaldehyde prepared on PBS (pH 7.4) and then transferred to PBS containing 5% sucrose. After 15 min of incubation sections were treated with 10% H_2O_2 in 95% MeOH for 30 min at room temperature to destroy endogenous peroxidase. Then sections were blocked at room temperature during 60 min with 10% goat serum (Sigma Chemicals, MI) prepared on PBS containing 0.3% Triton X-100. Rabbit anti-tyrosine hydroxylase (Pel-Freez Biologicals, Arkansas) was the primary antibody (1:1000) and it was prepared in PBS containing 10% goat serum and 0.3% Triton X-100. The sections were incubated with primary antibody overnight at 4 °C and then washed in three changes of PBS for 10 min each. Goat anti-rabbit (Chemicon, CA) secondary antibody was prepared on PBS/Triton X-100 buffer (1:300) and incubated with samples for 60 min at room temperature. Then sections were washed for 10 min in three changes of PBS, treated with avidin–biotin-complex (Vectastain ABC Kit (Peroxidase Standard*), Vector Labs, CA) for 60 min and developed with 3,3′-diaminobenzidine (DAB Substrate Kit, Vector Labs, CA) at room temperature during 2–5 min. Finally the sections were rinsed with distilled water to stop reaction and then dehydrated in ethanol, and cleared in xylene. Controls for nonspecific staining were performed for evaluation in which either primary or secondary antibody was applied alone.

2.11.2. TUNEL assay

TUNEL staining was performed following the methods described in ApopTag Plus Fluorescein In Situ Apoptosis Detection Kit (S7111) and ApopTag Peroxidase In Situ Apoptosis Detection Kit (S7100) (Chemicon, CA). Slide-mounted tissue sections were post-fixed in precooled ethanol:acetic acid (2:1) for 5 min at −20 °C in a Coplin jar and rinsed two times for 5 min with PBS. For ApopTag Peroxidase staining slices were quenched in 3.0% hydrogen peroxidase in PBS for 5 min at room temperature and rinsed twice with PBS for 5 min each time. Equilibration buffer was immediately applied directly to the specimen for 20 s at room temperature. TdT enzyme was pipetted onto the sections following by incubation in a humidified chamber for 1 h at 37 °C. Specimens were placed in a Coplin jar containing working strength stop/wash buffer and incubated for 10 min at room temperature. After triple rinsing in PBS, the sections were incubated with anti-digoxigenin conjugate (fluorescence) or anti-digoxigenin peroxidase conjugate accordingly in a humidified chamber for 30 min at room temperature. The specimen for fluorescence apoptosis staining were rinsed with PBS (4× 2 min) and mounted on a glass cover slip with Vectashield mounting medium containing DAPI or PI (Vector Labs, CA). The specimens for peroxidase staining were rinsed with PBS (4× 2 min) and color was provided in peroxidase substrate (DAB Substrate KIT for peroxidase, Vector Labs). Then sections were rinsed in three changes of dH_2O for 1 min each wash and counterstained in methyl green (Vector Labs). The specimens were dehydrated and mounted under a glass coverslip in mounting medium. Samples were then examined with bright field microscopy or in the case of fluorescently tagged antibodies, with a Zeiss Scanning Confocal microscope (Model LSM510).

2.11.3. Rabbit anti-DARPP32

Sections were immunostained for DARPP32, a protein expressed by striatal neurons and which has been used to characterize effects of toxicants on striatal neurons (Haug et al., 1998; Stefanova et al., 2003). Cryosections were rinsed in PBS three times for 10 min each wash. Then the sections were incubated with ''blocking'' solution (PBS containing 10% goat serum (Sigma, Missouri), 0.3% Triton X-100) at room temperature for 60 min. Primary antibody *rabbit anti-DARPP32* (Chemicon, CA) diluted in carrier solution (PBS, goat serum, Triton X-100, primary antibody 1:300) was placed onto the sections and incubated overnight at 4 °C.

Secondary antibody *goat anti-rabbit secondary* (Alexa Fluor 594 (rodamine) Chemicon, CA) was applied to the slides (PBS, Triton X-100, secondary antibody—1:300) for 60 min at room temperature. Finally, the sections were rinsed with PBS (3× 10 min) and mounted on a glass cover slip with Vectashield mounting medium containing DAPI (Vector Labs, CA). Appropriate controls without primary antibodies were also prepared to assess nonspecific immunohistochemical staining. In some sections, propidium iodide (PI) from Molecular Probes (Eugene, OR) was used to counterstain nucleic acid. Laser Scanning confocal microscopy (Zeiss LSM 510) was used to resolve TUNEL-stained tissues counterstained with PI.

2.12. Statistical analysis

The results were reported as mean ± S.E.M. for at least five individual samples of specific brain regions, assayed in duplicate. Two-way ANOVA was performed to assess the contribution of brain region, time of analysis and their interaction on variance. Post-hoc *t*-tests with Bonferroni corrections were performed to compare values at each time point to control (untreated) values.

For electrophoresis, two different gels were run. The differences between samples were analyzed by the Student's *t*-test, and a $p < 0.05$ was considered as statistically significant. The Pearson correlation coefficients between DNA repair

Table 1
Development of TBARS response in different regions of mouse brain following i.p. administration of 3.5 mg/kg of OTA

Brain regions	TBARS (pmol/mg protein)			
	Control	6 h	24 h	72 h
CB	2.44 ± 0.2	3.99 ± 0.35*	5.54 ± 0.48*	8.54 ± 0.77*
PM	2.41 ± 0.17	4.80 ± 0.43*	6.09 ± 0.55*	9.13 ± 0.89*
HP	2.23 ± 0.21	4.69 ± 0.4*	6.03 ± 0.52*	8.57 ± 0.88*
MB	3.17 ± 0.28	4.22 ± 0.33*	6.09 ± 0.53*	9.16 ± 0.81*
CP	2.65 ± 0.22	3.58 ± 0.32*	5.63 ± 0.49*	8.39 ± 0.79*
CX	3.19 ± 0.27	4.01 ± 0.41*	6.78 ± 0.63*	10.31 ± 0.98*

* The values are significantly ($p < 0.05$) different compared to controls. All results represented by mean ± S.E.M.

(OGG1) and basal DNA damage (comet assay) across brain regions were determined at each time point by correlation analysis using GraphPad Software, Inc. (Sorrento, CA).

3. Results

Administration of OTA at doses less than 6 mg/kg i.p. (below the reported LD50 of 39.5 mg/kg i.p. in mice, Moroi et al., 1985) did not elicit obvious alterations in mouse behavior and locomotor activity at any time up to 3 days after treatment. Behavior was not measured instrumentally, but was based on visual inspections over the course of 3 days and response to handling. In particular, there was no abnormal posturing or clasping of limbs when mice were picked up by the tail.

Administration of a single dose of OTA (3.5 mg/kg i.p.) rapidly evoked oxidative stress across all brain regions. TBARS levels, indicators of lipid peroxidation, increased in a monophasic time-dependent manner in all brain regions of animals exposed to OTA as compared to control mice (Table 1). This same dose of OTA caused a rapid upregulation of SOD activities in all regions of brain, with peak values reached after 24 h. However, the elevation of the SOD antioxidative response was maintained only for a short time, returning to control levels or below after 72 h (Table 2).

Oxidative DNA damage, estimated from the comet assay (Fig. 2), was increased early across all brain regions (Fig. 3) and remained elevated at all time points. Peak elevation was observed at 24 h where the magnitude of increase ranged from 1.8 to 2.9 times the control levels. The MB, CP and HP showed the highest levels of oxidative DNA damage.

Concomitant with the increased levels of oxidative DNA damage, the DNA repair enzyme OGG1 was significantly decreased across all brain regions at 6 h with a gradual return to near normal levels by 72 h (Fig. 4). The activity of OGG1 across the six brain regions was inversely correlated to basal levels of DNA damage at all time points except for 72 h (the Pearson correlation coefficients were −0.88 at 0 h; −0.89 at 6 h; −0.85 at 24 h; −0.45 at 72 h—see Fig. 5). Oxidative DNA repair activity recovered completely by 72 h in CB but

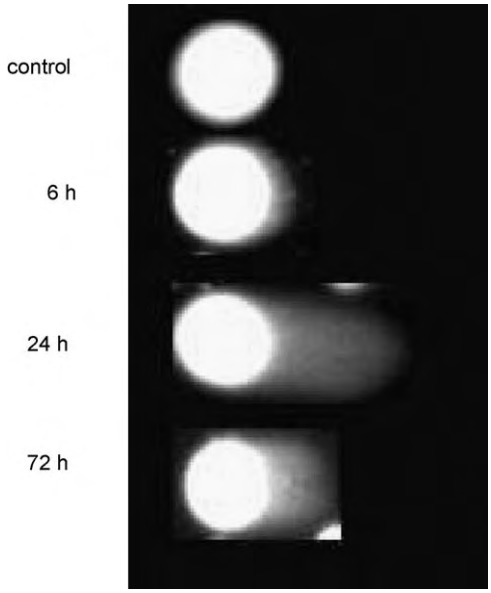

Fig. 2. Representative photomicrographs of "comets" in the substantia nigra obtained at 6, 24 and 72 h after OTA injection (3.5 mg/kg, i.p.).

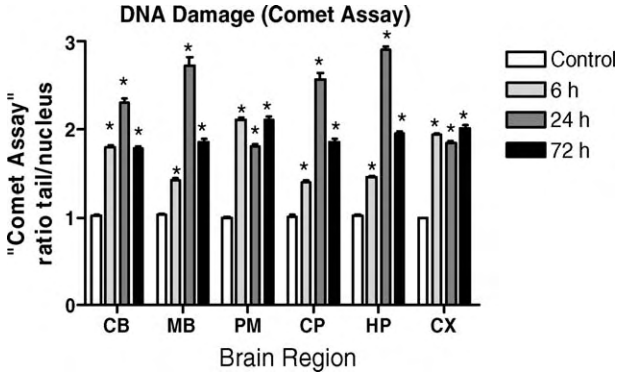

Fig. 3. Time course of effects of OTA on DNA damage across six brain regions mice following administration of OTA (3.5 mg/kg, i.p.). The extent of DNA damage was calculated from relative changes in length of comet tails. The mean ± S.E.M. was determined from the average of 50 cells calculated for three animals in each experimental group (control, 6, 24 and 72 h). Two-way ANOVA revealed that brain region and time each contributed significantly to the variance ($p < 0.0001$); there was no statistically significant interaction between time course and region. Post-hoc comparison of values at each time point compared to controls revealed significant increases at each time point for each region (asterisks indicate $p < 0.05$; *t*-test with Bonferroni correction for multiple comparisons).

Table 2
Development of SOD response in different regions of mouse brain during intoxication caused by i.p. administration of 3.5 mg/kg of OTA

Brain regions	SOD (U/g protein)			
	Control	6 h	24 h	72 h
CB	0.39 ± 0.04	0.38 ± 0.03	0.71 ± 0.07*	0.35 ± 0.03
PM	0.557 ± 0.05	0.61 ± 0.05	0.8 ± 0.08*	0.37 ± 0.03
HP	0.37 ± 0.03	0.39 ± 0.03	0.81 ± 0.07*	0.33 ± 0.03
MB	0.36 ± 0.03	0.44 ± 0.04	0.79 ± 0.07*	0.34 ± 0.02
CP	0.34 ± 0.02	0.36 ± 0.03	0.73 ± 0.06*	0.32 ± 0.02
CX	0.53 ± 0.04	0.55 ± 0.04	0.91 ± 0.08*	0.36 ± 0.04

* The values are significantly ($p < 0.05$) different compared to controls. All results represented by mean ± S.E.M.

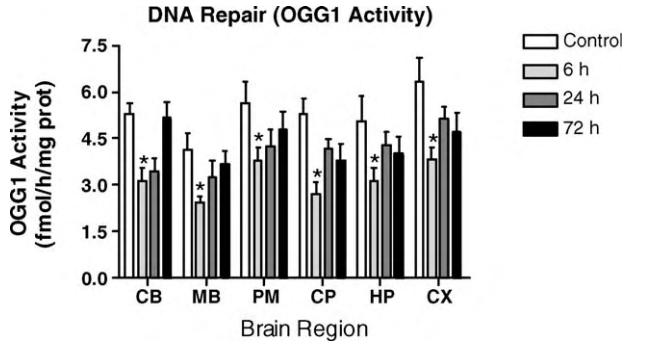

Fig. 4. Time course of OTA effects on OGG1 activity across specific brain regions. Results are expressed as mean ± S.E.M. ($n = 4$–6 samples per brain region). Two-way ANOVA revealed that brain region and time each contributed significantly to the variance ($p < 0.0001$); there was no statistically significant interaction between time course and region. Post-hoc comparison of values at each time point compared to controls revealed significant decreases at 6 h in each region (asterisks indicate $p < 0.05$; t-test with Bonferroni correction for multiple comparisons).

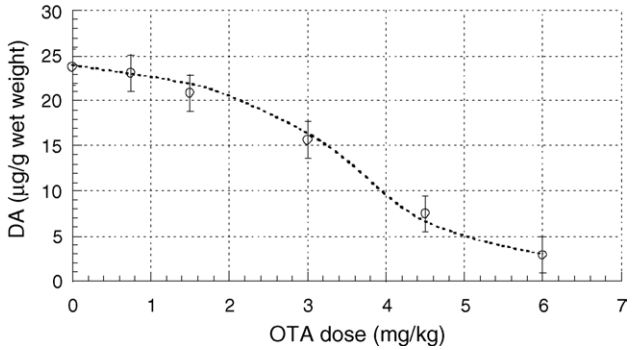

Fig. 6. Dose–response curve obtained following i.p. administration of OTA. DA concentration was measured in CP of ICR mice 24 h after administration of OTA. The results are expressed as mean ± S.E.M. Data averaged for five animals.

remained depressed in all other regions despite a trend towards recovery. The CP, CX and HP exhibited the least degree of recovery of OGG1 activity; at 72 h, the CP remained inhibited by 28%, the CX by 26% and the HP by 21% compared to control OGG1 levels.

In light of the long-standing premise that the nigro-striatal DA system is vulnerable to oxidative stress (a view that has been recently challenged, Ahlskog, 2005), we measured levels of DA and its metabolites in the striatum. OTA administration resulted in a dose-dependent decrease in striatal (caudate/putamen) DA with an ED50 of 3.2 mg/kg (Fig. 6). A time-course study of the effects of a single dose (3.5 mg/kg i.p.) revealed an early (6 h) 1.38-fold elevation of

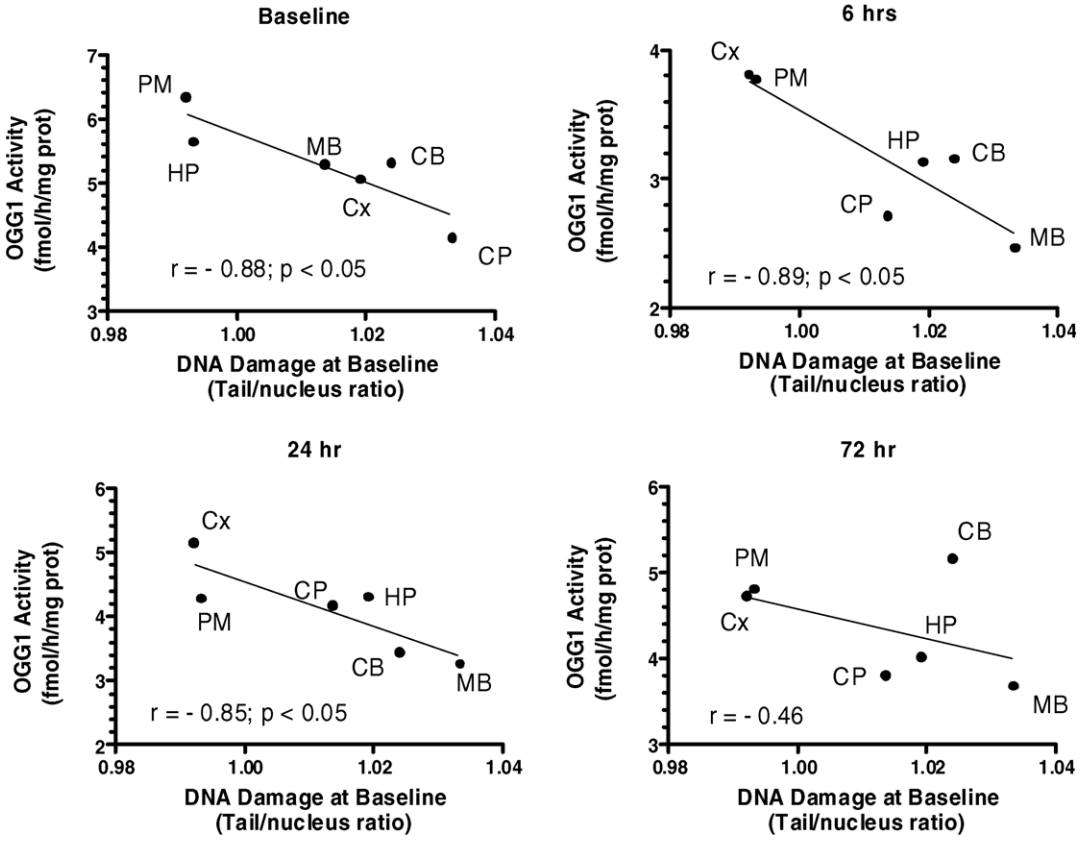

Fig. 5. Relationship between DNA repair (OGG1) and basal levels of oxidative damage in six brain regions. Each panel plots OGG1 activity against the baseline oxidative DNA damage (tail/nucleus ratio of the comet assay) in each brain region at 6, 24 and 72 h after a single dose of OTA (3.5 mg/kg). Pearson correlation coefficients were determined for each time point shown in the four panels. There was a significant inverse correlation between DNA repair activity and baseline level of DNA damage across regions at all time points except 72 h.

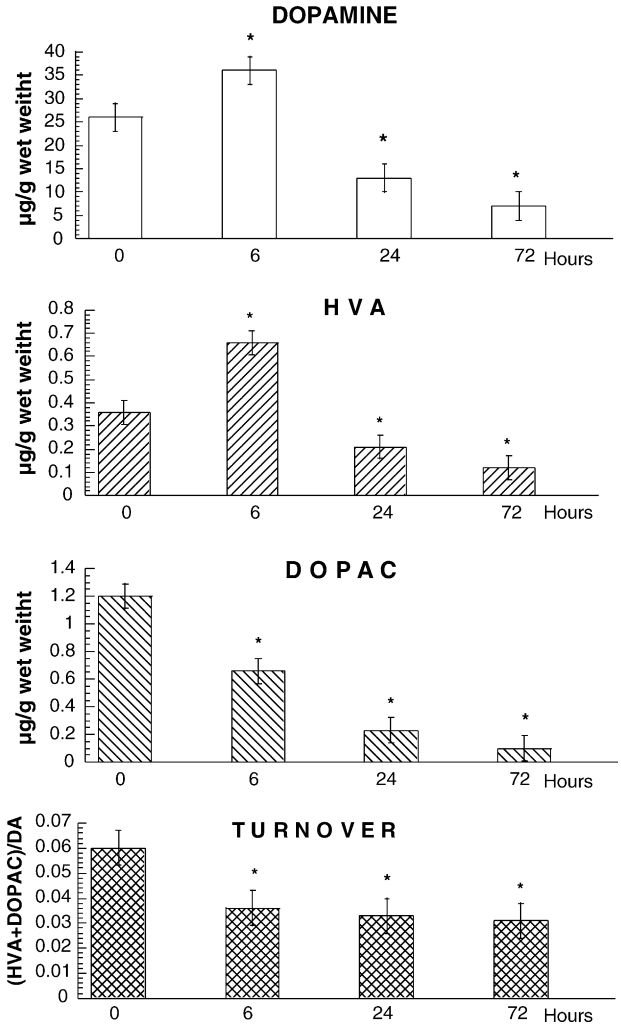

Fig. 7. Effect of OTA administration (3.5 mg/kg, i.p.) on DA metabolism during time course of developed intoxication in brain of ICR mice. Asterisks indicate significance of differences against control ($p < 0.05$). The results are expressed as mean ± S.E.M. ($n = 6$).

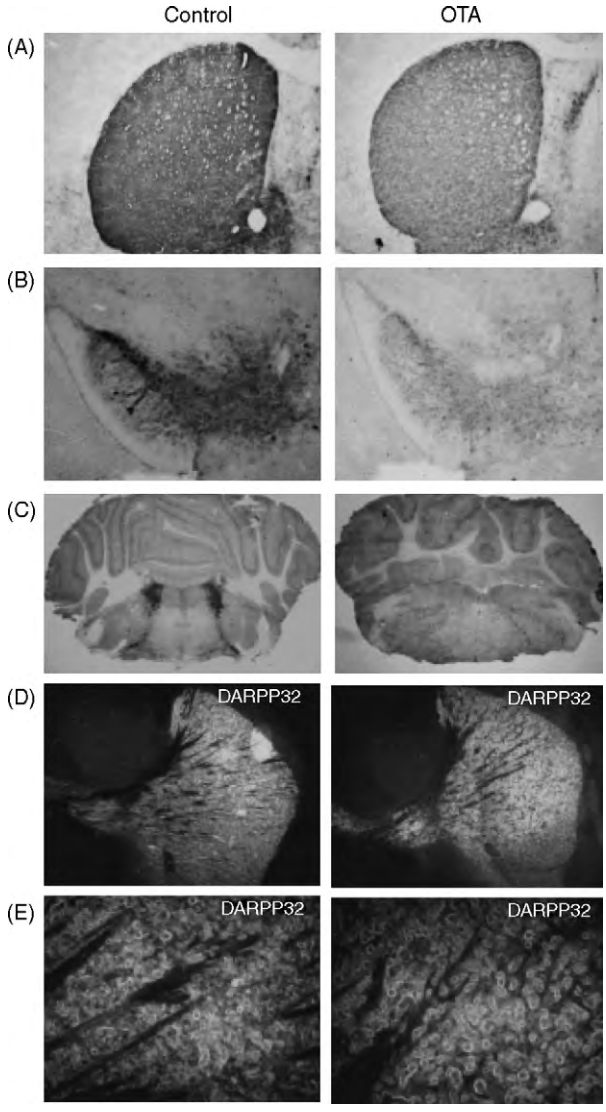

Fig. 8. Representative photomicrographs of TH immunoreactivity in the caudate putamen (row A), substantia nigra (row B) and locus ceruleus (row C) obtained 72 h after OTA injection (3.5 mg/kg, i.p.). Controls are in the left-hand panels. Intensity of TH immunoreactivity is decreased in all three loci in mice treated with OTA. DARPP32 immunohistochemistry is shown in rows D and E. Parasagittal cut through striatum (CP) showing no difference in DARPP32 signal intensity and distribution in OTA-treated compared to control mouse brains (magnification in row D = 40×; in row E = 200×).

DA as compared to control (Fig. 7). After 24 h, DA concentration dropped to 46% of control levels and declined even further by 72 h. A similar kinetic profile was recorded for HVA, while DOPAC levels did not increase at 6 h but showed a steady decline. The turnover of DA calculated as ratio of (HVA + DOPAC)/DA was significantly reduced at all time points (Fig. 7).

Catecholaminergic cells and terminals in the SN, CP and locus ceruleus were affected by OTA as evidenced by a qualitative decrease in tyrosine hydroxylase (TH) immunoreactivity in those structures (Fig. 8, rows A–C). However, the decreased immunostaining was not a result of OTA-induced cell death because TUNEL staining across these and other brain regions failed to reveal apoptotic nuclei (data not shown). DARPP32 immunostaining of cells of the striatum and midbrain (SNpars reticulata) did not reveal differences between OTA and control brains, indicating that there was no direct cytopathic effect on this population of neurons by 72 h after administration (Fig. 8, rows D and E).

4. Discussion

Administration of OTA, at a single dose (3.5 mg/kg) that is approximately 10% of the reported LD50, resulted in widespread oxidative stress across six brain regions. This was evidenced by significant increases in lipid peroxidation and oxidative DNA damage across all brain regions. Furthermore, OTA treatment elicited an early and sustained surge in activity of SOD, a major oxyradical scavenger, across all brain regions. Unlike the monophasic SOD activation, the oxidative DNA repair response exhibited a biphasic response, with an initial inhibition of OGG1 activity followed by a trend towards recovery to normal levels after 3 days. This is quite different

than the acute effects of another pro-oxidant agent, diethyl maleate (DEM), which elicited an early (6 h after injection) and significant upregulation of OGG1 in mouse CB, CX, PM, but not in MB, CP or HP, despite equally decreased glutathione levels in all brain regions (Cardozo-Pelaez et al., 2002). In addition, the DNA repair response to rubratoxin-A (RTA), a mycotoxin with poorly understood complex mechanisms of action in brain, was similar but not identical to that of diethyl maleate. Administration of a single dose of RTA resulted in significant upregulation of the DNA repair enzyme OGG1 in CB, CP, and CX, but not in HP, MB and PM at 24 h, in the presence of *decreased or unchanged levels* of lipid peroxidation in all regions (Sava et al., 2004). In the present study, the OGG1 activity was suppressed equally in all brain regions and only the CB recovered to baseline levels by 72 h, while other regions (CP, HP and CX) approached baseline but stayed mildly suppressed. It should be pointed out that the results in the DEM and RTA experiments cannot be directly compared with the present findings because only a single time point was assessed (6 h in the DEM study and 24 h in the RTA study) and no measurements of DA levels in striatum were made in those earlier experiments (Sava et al., 2004).

Based on our previous work with diethyl maleate and rubratoxin-A, we had expected that the DNA repair response to OTA would show that some regions of brain were more capable of OGG1 upregulation than others. Our working hypothesis was based on the concept that variation in DNA repair was a potential factor in determining neuronal vulnerability; deficient DNA repair processes have been associated with Parkinson's disease (PD) as well as with other neurodegenerative diseases such as Alzheimer's disease, amyotrophic lateral sclerosis (ALS) and Huntington's disease (HD) (Lovell et al., 2000; Mazzarello et al., 1992; Robbins et al., 1985). In addition, we have previously shown that the uneven distribution of oxidative DNA damage across brain regions caused by endogenous or exogenous factors was determined, in part, by the intrinsic capacity to repair oxidative DNA damage (Cardozo-Pelaez et al., 1999, 2000). In those earlier studies, and in the present report, we focused on oxyguanosine glycosylase (OGG1), a key enzyme involved in the repair of the oxidized base, 8-hydroxy-2′deoxoguanosine (oxo8dG). This reaction results in hydrolysis of the *N*-glycosylic bond between the 8-oxoG and deoxyribose, releasing the free base and leaving an apurinic/apyrimidinic (AP) site in DNA. Such AP sites are cytotoxic and mutagenic, and must be further processed. Some DNA glycosylases also have an associated AP lyase activity that cleaves the phosphodiester bond 3′ to the AP site (Dianov et al., 1998). Un-repaired DNA damage in post-mitotic cells, such as neurons, can result in disruption of transcriptionally active genes, cellular dysfunction and apoptosis (Hanawalt, 1994). Hence it was reasonable to hypothesize that diminished DNA repair capacity in populations of neurons would be associated with increased vulnerability to potentially genotoxic agents. Since the CP and MB showed a relatively diminished OGG1 activity and increased oxidative DNA damage (comet assay), we postulated that the DA terminals of the striatum would suffer damage.

This concept was supported by the report of increased oxidative DNA damage in substantia nigra and striatum in post-mortem brain from PD cases (Sanchez-Ramos et al., 1994), and by the observation that MB and CP were less able to upregulate OGG1 repair activity in response to the pro-oxidant, diethylmaleate (Cardozo-Pelaez et al., 2002). To further test this hypothesis, we measured the effects of OTA on striatal DA levels. Administration of OTA caused a dose-dependent decrease of striatal DA and a decrease in DA turnover. The nearly 50% reduction in striatal DA caused by a single dose (3.5 mg/kg i.p.) did not produce observable changes in daytime mouse behavior or locomotor activity, though it is likely that more sensitive, quantitative measures of behavior may reveal alterations. This dose of OTA also resulted in diminished TH immunoreactivity in the CP and MB as well as in the locus ceruleus (which contains noradrenergic neurons). The effects of OTA on catecholaminergic systems appeared to reflect a potentially reversible action rather than a cytotoxic effect because we found no evidence of cell death by 72 h. There were no apoptotic profiles found in SN and CP or any other region of the brain. In addition, there did not appear to be cytotoxic effects on striatal neurons identified by DARPP32 immunostaining.

It may be that the more rapid return of OGG1 activity to normal by 3 days in CB reflects an uneven distribution of the mycotoxin across brain regions. In the present report, the distribution of the toxin itself across brain regions was not investigated. However, previously published reports indicate that the cerebellum, ventral midbrain, and striatum accumulate the highest levels of OTA after 8 days of intragastric administration of a low dose (289 μg/kg/day) (Belmadani et al., 1998). Cerebellar concentrations of OTA accounted for 34% of the total brain OTA and one might expect that this structure would exhibit the greatest degree of oxidative stress and decreased capacity to repair oxidative DNA damage. On the contrary, the present findings demonstrate that the cerebellum exhibited complete recovery of OGG1 activity whereas other regions, reported to accumulate much lower levels of OTA, did not recover DNA repair capacity to as great an extent. Similarly, it has been reported that the cerebellum exhibited the least degree of cytotoxicity evidenced by LDH release; the greatest release of LDH was reported to be in ventral midbrain, hippocampus, and striatum which accumulated much less OTA than the cerebellum (Belmadani et al., 1998). Hence the relationship between regional concentration of OTA and regional vulnerability to the toxin is not clear.

A potential explanation for the observations reported here relates to bioenergetic compromise evoked by OTA. This mycotoxin has been reported to inhibit succinate-dependent electron transfer activities of the respiratory chain, but at higher concentrations will also inhibit electron transport at Complex I (Aleo et al., 1991; Wei et al., 1985). The nigro-striatal dopaminergic system is well known to be especially vulnerable to the mitochondrial toxicants, MPTP and rotenone, especially when the latter toxicant is administered chronically at low doses (Betarbet et al., 2000; Hasegawa et al., 1990; Vyas et al., 1986). Other mitochondrial poisons like nitroproprionic acid

and malonate interfere with succinate dehydrogenase/Complex II. These Complex II inhibitors result in lesions primarily localized to striatum (Calabresi et al., 2001; Schulz et al., 1996). Bioenergetic compromise may lead to persistent activation of NMDA receptors which results in excitotoxicity mediated by the neurotransmitter glutamate in regions of brain richly innervated by glutamatergic fibers, accounting for the vulnerability of the striatum and pallidum, and possibly the SN (Greenamyre et al., 1999; Turski and Turski, 1993). In addition, Ca^{2+} entering neurons through NMDA receptors has 'privileged' access to mitochondria, where it causes free-radical production and mitochondrial depolarization (Greenamyre et al., 1999). Hence the bioenergetic compromise induced by OTA may be responsible for the generation of free radicals and reactive oxygen species that resulted in global oxidative damage to DNA and lipids, as reported here and damage to proteins through generation of oxygen free radicals and nitric oxide, as reported elsewhere (Bryan et al., 2004; Thomas and Mallis, 2001).

Of course OTA may also be toxic through other mechanisms. Due to its chemical structure (chlorodihydroisocoumarin linked through an amide bond to phenylalanine), OTA inhibits protein synthesis by competition with phenylalanine in the aminoacylation reaction of phenylalanine-tRNA (Bunge et al., 1978; Creppy et al., 1983a) and phenylalanine hydroxylase activity (Creppy et al., 1990). These actions could lead to impairment of the synthesis of DOPA, dopamine and catecholamines or enzymes involved in metabolism of DA. Interestingly, the initial effect of OTA was to release DA resulting in increased striatal DA and HVA levels at 6 h, but with a decreased level of striatal DOPAC. It is known that DOPAC levels in striatum decline when DA nerve terminals are exposed to drugs which release newly synthesized DA, possibly because intraneuronal monoamine oxidase is deprived of its main substrate (Zetterstrom et al., 1988). Longer term studies will be required to determine the extent to which the effects of OTA on striatal DA and its metabolites is permanent or reversible.

To summarize, OTA administered at a dose that is 10% of the LD50, resulted in significant reduction of striatal DA, DA turnover and TH immunoreactivity in catecholaminergic neurons and fibers. This was not associated with apoptosis in SN, CP, HP, CB or with loss of striatal neuron immunostaining for DARPP32. OTA evoked pronounced global oxidative stress, possibly related to its inhibition of mitochondrial function. Regional variation in DNA repair did not appear to explain effects on catecholaminergic neurons. The vulnerability of the nigro-striatal system to OTA remains unclear and many questions remain to drive on-going and future investigations. For example, what are the long-term consequences of chronic administration of more clinically relevant low doses of OTA? Does a rigid-akinetic syndrome develop and is it reversible? Given that data derived from analysis of six macro-dissected brain regions are crude approximations for the cellular and molecular events occurring in specific populations of neurons, it will be important to develop refined sampling methods, including microdissection of specific neuro-anatomical loci and laser capture microdissection techniques for analysis of specific neuronal phenotypes.

Acknowledgements

This study was supported by USAMRMC #03281031 and a VA Merit Review Grant.

References

Ahlskog JE. Challenging conventional wisdom: the etiologic role of dopamine oxidative stress in Parkinson's disease. Mov Disord 2005;20:271–82.

Aleo MD, Wyatt RD, Schnellmann RG. Mitochondrial dysfunction is an early event in ochratoxin A but not oosporein toxicity to rat renal proximal tubules. Toxicol Appl Pharmacol 1991;107:73–80.

Arora RG, Frolen H, Fellner-Feldegg H. Inhibition of ochratoxin A teratogenesis by zearalenone and diethylstilboestrol. Food Chem Toxicol 1983;21:779–83.

Belmadani A, Tramu G, Betbeder AM, Steyn PS, Creppy EE. Regional selectivity to ochratoxin A, distribution and cytotoxicity in rat brain. Arch Toxicol 1998;72:656–62.

Betarbet R, Sherer TB, MacKenzie G, Garcia-Osuna M, Panov AV, Greenamyre T. Chronic systemic pesticide exposure reproduces features of Parkinson's disease. Nat Neurosci 2000;3:1301–6.

Bryan NS, Rassaf T, Maloney RE, Rodriguez CM, Saijo F, Rodriguez JR, et al. Cellular targets and mechanisms of nitros(yl)ation: an insight into their nature and kinetics in vivo. Proc Natl Acad Sci USA 2004;101:4308–13.

Bunge I, Dirheimer G, Roschenthaler R. In vivo and in vitro inhibition of protein synthesis in *Bacillus stearothermophilus* by ochratoxin A. Biochem Biophys Res Commun 1978;83:398–405.

Calabresi P, Gubellini P, Picconi B, Centonze D, Pisani A, Bonsi P, et al. Inhibition of mitochondrial complex II induces a long-term potentiation of NMDA-mediated synaptic excitation in the striatum requiring endogenous dopamine. J Neurosci 2001;21:5110–20.

Cardozo-Pelaez F, Brooks PJ, Stedeford T, Song S, Sanchez-Ramos J. DNA damage, repair, and antioxidant systems in brain regions: a correlative study. Free Radic Biol Med 2000;28:779–85.

Cardozo-Pelaez F, Song S, Parthasarathy A, Hazzi C, Naidu K, Sanchez-Ramos J. Oxidative DNA damage in the aging mouse brain. Movement Disord 1999;14:972–80.

Cardozo-Pelaez F, Stedeford TJ, Brooks PJ, Song S, Sanchez-Ramos JR. Effects of diethylmaleate on DNA damage and repair in the mouse brain. Free Radic Biol Med 2002;33:292–8.

Cascio C, Guarneri R, Russo D, De Leo G, Guarneri M, Piccoli F, et al. Pregnenolone sulfate, a naturally occurring excitotoxin involved in delayed retinal cell death. J Neurochem 2000;74:2380–91.

Creppy EE, Chakor K, Fisher MJ, Dirheimer G. The myocotoxin ochratoxin A is a substrate for phenylalanine hydroxylase in isolated rat hepatocytes and in vivo. Arch Toxicol 1990;64:279–84.

Creppy EE, Kane A, Dirheimer G, Lafarge-Frayssinet C, Mousset S, Frayssinet C. Genotoxicity of ochratoxin A in mice: DNA single-strand break evaluation in spleen, liver and kidney. Toxicol Lett 1985;28:29–35.

Creppy EE, Kern D, Steyn PS, Vleggaar R, Roschenthaler R, Dirheimer G. Comparative study of the effect of ochratoxin A analogues on yeast aminoacyl-tRNA synthetases and on the growth and protein synthesis of hepatoma cells. Toxicol Lett 1983a;19:217–24.

Creppy EE, Stormer FC, Roschenthaler R, Dirheimer G. Effects of two metabolites of ochratoxin A, (4R)-4-hydroxyochratoxin A and ochratoxin alpha, on immune response in mice. Infect Immun 1983b;39:1015–8.

Dianov G, Bischoff C, Piotrowski J, Bohr VA. Repair pathways for processing of 8-oxoguanine in DNA by mammalian cell extracts. J Biol Chem 1998;273:33811–6.

Dirheimer G, Creppy EE. Mechanism of action of ochratoxin A. IARC Sci Publ 1991;171–86.

Elstner EF, Heupel A. Inhibition of nitrite formation from hydroxyl-ammonium chloride: a simple assay for superoxide dismutase. Anal Biochem 1976;70:616–20.

Fukui Y, Hayasaka S, Itoh M, Takeuchi Y. Development of neurons and synapses in ochratoxin A-induced microcephalic mice: a quantitative assessment of somatosensory cortex. Neurotoxicol Teratol 1992;14:191–6.

Galtier P. Pharmacokinetics of ochratoxin A in animals. IARC Sci Publ 1991;187–200.

Galtier P, Boneu B, Charpenteau JL, Bodin G, Alvinerie M, More J. Physiopathology of haemorrhagic syndrome related to ochratoxin A intoxication in rats. Food Cosmet Toxicol 1979;17:49–53.

Gautier JC, Holzhaeuser D, Markovic J, Gremaud E, Schilter B, Turesky RJ. Oxidative damage and stress response from ochratoxin a exposure in rats. Free Radic Biol Med 2001;30:1089–98.

Greenamyre JT, MacKenzie G, Peng TI, Stephans SE. Mitochondrial dysfunction in Parkinson's disease. Biochem Soc Symp 1999;66:85–97.

Grosse Y, Baudrimont I, Castegnaro M, Betbeder AM, Creppy EE, Dirheimer G, et al. Formation of ochratoxin A metabolites and DNA-adducts in monkey kidney cells. Chem Biol Interact 1995;95:175–87.

Gupta M, Bandopadhyay S, Paul B, Majumder SK. Hematological changes produced in mice by ochratoxin A. Toxicology 1979;14:95–8.

Hanawalt PC. Transcription-coupled repair and human disease: perspective. Science 1994;266:1957–8.

Hasegawa E, Takeshige K, Oishi T, Murai Y, Minakami S. 1-Methyl-4-phenylpyridinium (MPP+) induces NADH-dependent superoxide formation and enhances NADH-dependent lipid peroxidation in bovine heart submitochondrial particles. Biochem Biophys Res Commun 1990;170: 1049–55.

Haubeck HD, Lorkowski G, Kolsch E, Roschenthaler R. Immunosuppression by ochratoxin A and its prevention by phenylalanine. Appl Environ Microbiol 1981;41:1040–2.

Haug LS, Ostvold AC, Torgner I, Roberg B, Dvorakova L, St'astny F, et al. Intracerebroventricular administration of quinolinic acid induces a selective decrease of inositol(1,4,5)-trisphosphate receptor in rat brain. Neurochem Int 1998;33:109–19.

Hayes AW, Hood RD, Lee HL. Teratogenic effects of ochratoxin A in mice. Teratology 1974;9:93–7.

Hoehler D, Marquardt RR, McIntosh AR, Hatch GM. Induction of free radicals in hepatocytes, mitochondria and microsomes of rats by ochratoxin A and its analogs. Biochim Biophys Acta 1997;1357:225–33.

Kane A, Creppy EE, Roschenthaler R, Dirheimer G. Biological changes in kidney of rats fed subchronically with low doses of ochratoxin A. Dev Toxicol Environ Sci 1986a;14:241–50.

Kane A, Creppy EE, Roschenthaler R, Dirheimer G. Changes in urinary and renal tubular enzymes caused by subchronic administration of ochratoxin A in rats. Toxicology 1986b;42:233–43.

Krogh P. Role of ochratoxin in disease causation. Food Chem Toxicol 1992;30:213–24.

Krogh P, Axelsen NH, Elling F, Gyrd-Hansen N, Hald B, Hyldgaard-Jensen J, et al. Experimental porcine nephropathy. Changes of renal function and structure induced by ochratoxin A-contaminated feed. Acta Pathol Microbiol Scand [A] 1974;1–21.

Kuiper-Goodman T, Scott PM. Risk assessment of the mycotoxin ochratoxin A. Biomed Environ Sci 1989;2:179–248.

Lea T, Steien K, Stormer FC. Mechanism of ochratoxin A-induced immunosuppression. Mycopathologia 1989;107:153–9.

Lebrun S, Follmann W. Detection of ochratoxin A-induced DNA damage in MDCK cells by alkaline single cell gel electrophoresis (comet assay). Arch Toxicol 2002;75:734–41.

Lovell MA, Xie C, Markesbery WR. Decreased base excision repair and increased helicase activity in Alzheimer's disease brain. Brain Res 2000;855:116–23.

Marquardt RR, Frohlich AA. A review of recent advances in understanding ochratoxicosis. J Anim Sci 1992;70:3968–88.

Mazzarello P, Poloni M, Spadari S, Focher F. DNA repair mechanisms in neurological diseases: facts and hypotheses. J Neurol Sci 1992;112:4–14.

Moroi K, Suzuki S, Kuga T, Yamazaki M, Kanisawa M. Reduction of ochratoxin A toxicity in mice treated with phenylalanine and phenobarbital. Toxicol Lett 1985;25:1–5.

Paxinos G, Franklin KBJ. The mouse brain in stereotaxic coordinates. San Diego, CA: Academic Press; 2001.

Petkova-Bocharova T, Chernozemsky IN, Castegnaro M. Ochratoxin A in human blood in relation to Balkan endemic nephropathy and urinary system tumours in Bulgaria. Food Addit Contam 1988;5:299–301.

Pfohl-Leszkowicz A, Chakor K, Creppy EE, Dirheimer G. DNA adduct formation in mice treated with ochratoxin A. IARC Sci Publ 1991;245–53.

Pfohl-Leszkowicz A, Grosse Y, Kane A, Creppy EE, Dirheimer G. Differential DNA adduct formation and disappearance in three mouse tissues after treatment with the mycotoxin ochratoxin A. Mutat Res 1993;289:265–73.

Pitout MJ. The effect of ochratoxin A on glycogen storage in the rat liver. Toxicol Appl Pharmacol 1968;13:299–306.

Robbins JH, Otsuka F, Tarone RE, Polinsky RJ, Brumback RA, Nee LE. Parkinson's disease and Alzheimer's disease: hypersensitivity to X-rays in culture cell lines. J Neurol Neurosurg Psychiatry 1985;48:916–23.

Sanchez-Ramos J, Overvik E, Ames BN. A marker of oxyradical-mediated DNA damage (oxo8dG) is increased in nigro-striatum of Parkinson's disease brain. Neurodegeneration (incorporated into Exp Neurol) 1994;3:197–204.

Sava V, Mosquera D, Song S, Stedeford T, Calero K, Cardozo-Pelaez F, et al. Rubratoxin B elicits antioxidative and DNA repair responses in mouse brain. Gene Expression 2004;11:211–9.

Schindewolf C, Lobenwein K, Trinczek K, Gomolka M, Soewarto D, Fella C, et al. Comet assay as a tool to screen for mouse models with inherited radiation sensitivity. Mamm Genome 2000;11:552–4.

Schulz JB, Henshaw DR, MacGarvey U, Beal MF. Involvement of oxidative stress in 3-nitropropionic acid neurotoxicity. Neurochem Int 1996;29: 167–71.

Smith PK, Krohn RI, Hermanson GT, Mallia AK, Gartner FH, Provenzano MD, et al. Measurement of protein using bicinchoninic acid. Anal Biochem 1985;150:76–85.

Stefanova N, Puschban Z, Fernagut PO, Brouillet E, Tison F, Reindl M, et al. Neuropathological and behavioral changes induced by various treatment paradigms with MPTP and 3-nitropropionic acid in mice: towards a model of striatonigral degeneration (multiple system atrophy). Acta Neuropathol (Berl) 2003;106:157–66.

Stormer FC, Lea T. Effects of ochratoxin A upon early and late events in human T-cell proliferation. Toxicology 1995;95:45–50.

Szczech GM, Hood RD. Brain necrosis in mouse fetuses transplacentally exposed to the mycotoxin ochratoxin A. Toxicol Appl Pharmacol 1981;57:127–37.

Thomas JA, Mallis RJ. Aging and oxidation of reactive protein sulfhydryls. Exp Gerontol 2001;36:1519–26.

Turski L, Turski WA. Towards an understanding of the role of glutamate in neurodegenerative disorders: energy metabolism and neuropathology. Experientia 1993;49:1064–72.

Vyas I, Heikkila RE, Nicklas WJ. Studies on the neurotoxicity of MPTP; inhibition of NAD-linked substrate oxidation by its metabolite, MPP+. J Neurochem 1986;46:1501–7.

Wangikar PB, Dwivedi P, Sharma AK, Sinha N. Effect in rats of simultaneous prenatal exposure to ochratoxin A and aflatoxin B(1). II. Histopathological features of teratological anomalies induced in fetuses. Birth Defects Res B Dev Reprod Toxicol 2004;71:352–8.

Wei YH, Lu CY, Lin TN, Wei RD. Effect of ochratoxin A on rat liver mitochondrial respiration and oxidative phosphorylation. Toxicology 1985;36:119–30.

Zetterstrom T, Sharp T, Collin AK, Ungerstedt U. In vivo measurement of extracellular dopamine and DOPAC in rat striatum after various dopamine-releasing drugs; implications for the origin of extracellular DOPAC. Eur J Pharmacol 1988;148:327–34.

Journal of the Neurological Sciences 249 (2006) 68–75

Journal of the Neurological Sciences

www.elsevier.com/locate/jns

Can low level exposure to ochratoxin-A cause parkinsonism?

V. Sava, O. Reunova, A. Velasquez, J. Sanchez-Ramos *

University of South Florida, Tampa, FL, USA
James Haley VA Hospital, Tampa, FL, USA

Available online 14 July 2006

Abstract

Mycotoxins are fungal metabolites with pharmacological activities that have been utilized in the production of antibiotics, growth promoters, and other classes of drugs. Some mycotoxins have been developed as biological and chemical warfare agents. Bombs and ballistic missiles loaded with aflatoxin were stockpiled and may have been deployed by Iraq during the first Gulf War. In light of the excess incidence of amyotrophic lateral sclerosis (ALS) in veterans from Operation Desert Storm, the potential for delayed neurotoxic effects of low doses of mycotoxins should not be overlooked. Ochratoxin-A (OTA) is a common mycotoxin with complex mechanisms of action, similar to that of the aflatoxins. Acute administration of OTA at non-lethal doses (10% of the LD_{50}) have been shown to increase oxidative DNA damage in brain up to 72 h, with peak effects noted at 24 h in midbrain (MB), caudate/putamen (CP) and hippocampus (HP). Levels of dopamine (DA) and its metabolites in the striatum (e.g., CP) were shown to be decreased in a dose-dependent manner. The present study focused on the effects of chronic low dose OTA exposure on regional brain oxidative stress and striatal DA metabolism. Continuous administration of low doses of OTA with implanted subcutaneous Alzet minipumps caused a small but significant decrease in striatal DA levels and an upregulation of anti-oxidative systems and DNA repair. It is possible that low dose exposure to OTA will result in an earlier onset of parkinsonism when normal age-dependent decline in striatal DA levels are superimposed on the mycotoxin-induced lesion.

Keywords: Mycotoxins; Ochratoxin-A; DNA damage and repair; Parkinson's disease; Oxyguanosine glycosylase; Superoxide dismutase; Glutathione; Dopamine

1. Introduction

Mycotoxins are toxic fungal metabolites known to be common contaminants of animal feed and human food. Some of the fungal products exhibit pharmacological activities that have been utilized in the production of antibiotics, growth promoters, anti-neoplastic agents and many other drugs with therapeutic potential. Some mycotoxins have been developed as bioterrorist weapons [1]. The most studied are the aflatoxins, a family of difuranocoumarin derivatives produced by many strains of *Aspergillus parasiticus* and *Aspergillus flav*us [2]. Acute aflatoxicosis (disease caused by aflatoxin exposure) results in death. Chronic aflatoxicosis results in cancer, immune suppression, and may be responsible for other delayed onset pathological conditions [2].

Aflatoxin has achieved some notoriety in popular literature and public media as a poison, although experts consider its use to be a " toxicologically improbable way to kill someone" [2]. Nevertheless, aflatoxin's reputation as a potent poison may explain why it has been adapted for use in bioterrorism. Iraqi scientists developed aflatoxins as part of their bioweapons program during the 1980s [1]. Toxigenic strains of *A. flavus* and *A. parasiticus* were cultured, and aflatoxins were extracted to produce over 2300 l of concentrated toxin. The majority of this aflatoxin was used to fill warheads; the remainder was stockpiled [1]. Aflatoxins seem an unlikely choice for chemical warfare because the induction of liver cancer is "hardly a knockout punch on the battlefield" [2]. There are certainly more potent mycotoxins, such as those from the trichothecene family (e.g. T-2). These can act immediately upon contact, and exposure to a few milligrams of T-2 is potentially lethal [2]. Even so, the fear

* Corresponding author. Department of Neurology (MDC 55), University of South Florida, 12901 Bruce B. Downs Blvd., Tampa, FL 33612, USA. Fax: +1 813 974 720.
E-mail address: jsramos@hsc.usf.edu (J. Sanchez-Ramos).

0022-510X/$ - see front matter © 2006 Elsevier B.V. All rights reserved.
doi:10.1016/j.jns.2006.06.006

and anxiety caused by the use of any chemical and biological weapon is the kind of psychological response that terrorists seek to inflict on their enemies. Furthermore, if used against rival ethnic groups, such as the Kurds in Iraq, the long-term physical and psychological results would be devastating. Finally, some experts think aflatoxin might have been selected simply because it was the favorite toxin of an influential Iraqi scientist [3].

The extent to which military personnel and civilian populations were exposed to aflatoxin during the first Gulf War is not known, but the incidence of motor neuron disease — amyotrophic lateral sclerosis (ALS) — was increased in returning veterans, suggesting a war-related environmental trigger [4,5]. This observation has provided the impetus to the present project. If low dose exposure to mycotoxins results in progressive neurodegerative disorders in humans, it may be possible to replicate this in the laboratory using mice exposed to another *Aspergillus* derived mycotoxin with mechanisms of action similar to the aflatoxins [4,5].

Ochratoxin-A (OTA) is a metabolite produced by *Aspergillus ochraceus* and *Penicillium verrucosum* that accumulates in the food chain because of its long half-life [6,7]. The possible contribution of OTA to the development of human and animal systemic diseases has been investigated by many authors (See review, [8]). Embryonic development of nervous tissue appears to be very susceptible to the deleterious effects of OTA [9,10]. OTA induces teratogenic effects in neonates (rats and mice) exposed *in utero*, characterized by microcephaly and modification of the brain levels of free amino acids [11]. OTA was also reported to be neurotoxic to adult male rats fed OTA in the diet. Neurotoxicity, indicated by concentration of lactic dehydrogenase released from the dissected brain tissue, was more pronounced in the ventral mesencephalon, hippocampus, and striatum than in the cerebellum [11].

Acute administration of OTA has recently been reported to cause oxidative stress and DNA damage in all brain regions [12]. OTA also caused depletion of striatal dopamine (DA) and its metabolites, as well as decreased tyrosine hydroxylase immunoreactivity in the corpus striatum (caudate/putamen). No evidence for apoptosis was found in the substantia nigra (SN), striatum or hippocampus, suggesting an effect on striatal DA innervation rather than on the neuronal cell bodies in the SN [12].

The primary objectives of the present study were 1) to evaluate the pharmacokinetics of OTA, 2) to assess the effects of chronic low dose OTA administration on parameters of oxidative stress and DNA repair in mouse brain and 3) to determine whether continuous low dose exposure caused DA depletion and parkinsonism in mice. The focus on DNA repair was based on recently published findings on the acute effects of OTA in mouse brain regions [12] and on older reports that deficits in DNA repair underlie a number of neurodegenerative diseases, including Alzheimer's Disease, Amyotrophic Lateral Sclerosis and Parkinson's Disease [13]. The overall goal was to determine the extent to which regional differences in distribution of the toxin and anti-oxidative and DNA repair capacity result in striatal DA depletion and the development of parkinsonism in mice.

2. Materials and methods

2.1. Materials

Ochratoxin-A, SOD and dihydrobenzylamine were purchased from Sigma (St. Louis, MO). Protease inhibitors and DNA glycosylase were from Boehringer Mannheim (Indianapolis, IN, USA). ^{32}P-ATP was from NEN Life Science Products (Wilmington, DE).

2.2. Animals and treatment

The animal protocol was approved by the Division of Comparative Medicine of the University of South Florida, which is fully accredited by AAALAC International and managed in accordance with the Animal Welfare Regulations, the PHS Policy, the FDA Good Laboratory Practices, and the IACUC's Policies.

Male Swiss ICR mice (22±2 g) were obtained from the Jackson Laboratories (Bar Harbor, ME). They were housed five per cage at the temperature of 21±2 °C with 12 h light/dark cycle and free access to food and water. For acute pharmacokinetic studies animals (n=36) were injected by the intraperitoneal route (i.p.) with OTA (3.5 mg/kg) dissolved in 0.1 M $NaHCO_3$) or vehicle (0.1 M $NaHCO_3$). This dose was based on the ED50 for depletion of striatal DA which was recently determined in our laboratory [12]. For *chronic administration of OTA,* four groups of male Swiss ICR mice (n=7 in each group) were implanted with Alzet osotic minipumps. Each group received different cumulative doses of OTA; vehicle alone, 4 mg/kg, 8 mg/kg, or 16 mg/kg over a 2 week infusion period. After injection with OTA or vehicle, mice were observed for changes in spontaneous behavior daily until euthanasia. The response to handling was also noted. In particular, evidence for toxic effects such as clasping of limbs in response to being held by the tail was to be recorded. Animals in the acute pharmacokinetic studies were euthanatized at 3, 6, 12, 24, and 72 h after administration of a single dose of OTA (3.5 mg/kg). In the chronic studies, mice were euthanatized at 2 weeks after initiation of OTA infusions.

2.3. Isolation of brain regions

Brains were separated into 8 regions under a dissecting stereo-microscope in the following order. The cerebellar peduncles were cut first and cerebellum (CB) was removed. The pons (PN) and medulla (MD) were separated by cutting the ponto-medullary junction. The ventral and dorsal parts of midbrain (MB) were dissected at the level of the caudal end of the cerebral peduncles. Cerebral hemispheres were

opened with a sagittal cut. Then caudate/putamen (CP) was isolated, followed by thalamus/hypothalamus (T/H) and hippocampus (HP). Finally, cerebral cortex (CX) was harvested and all the samples were kept frozen at −70 °C until assayed.

2.4. Measurement of dopamine and metabolites

HPLC with electrochemical detection was employed to measure levels of dopamine (DA) as previously reported [14]. In short, tissue samples were sonicated in 50 volumes of 0.1 M perchloric acid containing 50 ng/mL of dihydrobenzylamine (Sigma Chemical, MA) as internal standard. After centrifugation (15,000 ×*g*, 10 min, 4 °C), 20 μL of supernatant was injected onto a C18-reversed phase Microsorb-MV 300-5 column (Varian, CA) operated through Series 200 Autosampler (Perkin Elmer, CT). The mobile phase consisted of 90% of a solution of 50 mM sodium phosphate, 0.2 mM EDTA, and 1.2 mM heptanesulfonic acid (pH 4) and 10% methanol. Flow rate was 1 mL/min. Peaks were detected by a Coulchem 5100A detector (ESA). Data were collected and processed with TotalChrom software (Perkin Elmer Instruments).

2.5. Assessment OGG1 activity

The procedure for extraction of DNA glycosylase was similar to that described previously [15]. Pure OGG1 served as positive control. The incision activity of OGG1 was calculated as the amount of radioactivity in the band representing specific cleavage of the ^{32}P labeled oligonucleotide over the total radioactivity. Results were normalized to equal concentration of protein measured using the bicinchoninicacid assay [16].

2.6. Measurement of ochratoxin concentrations in brain

The method utilized HPLC with fluorescence detection. Brain samples of about 100 mg were sonicated in 2 volumes of absolute ethyl alcohol containing 50 ng/ml of ochtratoxin-A (Sigma Chemical, MA) as internal standard. Supernatants obtained after centrifugation (14,000 ×*g*, 5 min, 4 °C) passed through Acrodisc LC 13 mm syringe filter and 20 μL of supernatant samples were injected onto C18 reverse phase Microsorb-MV 300-5 column (Varian, inc., CA). The mobile phase consisted of 57% of water, 42% of acetonitrile and 1% of acetic acid. Flow rate was 0.9 mL/min. Peaks were detected with Series 200 fluorescent detector and data were collected and processed with TotalChrom software (Perkin Elmer Instruments, CT).

2.7. Statistical analysis

The results were reported as the mean±SEM for at least five individual samples of specific brain regions, assayed in duplicate. Two way ANOVA was performed to assess the contribution of brain region, time of analysis and their interaction on variance. The differences between samples were analyzed by the Student's *t*-test, and a $P<0.05$ was considered as statistically significant. The Pearson correlation coefficients between DNA repair (OGG1) and basal DNA damage (comet assay) was calculated using GraphPad Software, Inc. (Sorrento, CA).

3. Results

3.1. Regional distribution of OTA in brain

A single dose of OTA (3.5 mg/kg i.p., the ED_{50} for depletion of striatal DA) was administered to mice. Animals were euthanized in groups of six after 3, 6, 12, 24 and 72 h. Brains were collected, dissected and assayed for levels of OTA. At 3 h, the highest concentrations of OTA were measured in the cerebellum (CB), followed by the pons (PN), cerebral cortex (CX), and medulla (MD) (Fig. 1). Pharmacokinetic parameters were calculated and are summarized in Table 1. The rank order of concentrations of OTA based on area under the curve (AUC) is as follows:

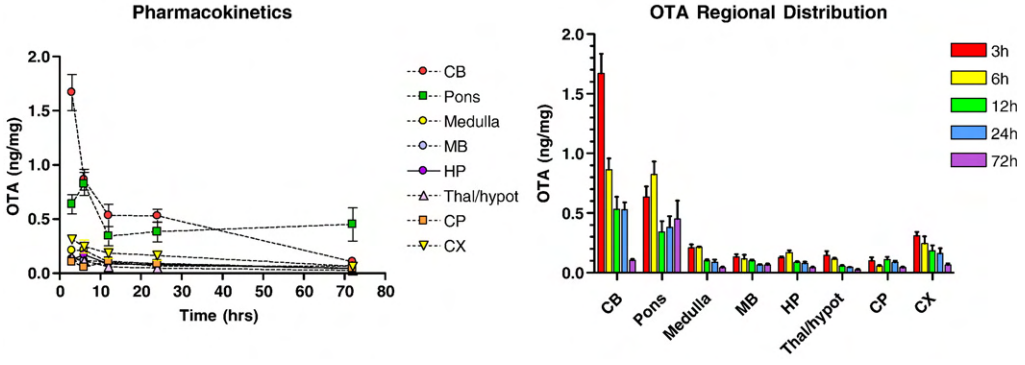

Fig. 1. Left panel summarizes the changes over time in regional brain concentrations of OTA following an acute dose of 3.5 mg/kg (i.p.) The right panel depicts the same data organized according to brain region. CB=cerebellum; MB=midbrain; HP=hippocampus; Thal/hypot=thalamus/hypothalamus; CP=caudate/putamen; CX=cerebral cortex.

Table 1
Pharmacokinetic data for OTA across brain regions

Brain regions	k_{el} (1/h)	$T_{1/2}$ (h)	AUC (ng*h/uL)	CL (uL/mg*h)
CB	0.034	20.175	32.107	0.125
PN	0.003	224.699	31.026	0.129
MD	0.020	33.859	6.175	0.648
MB	0.009	75.107	5.578	0.717
HP	0.016	42.582	5.266	0.760
T/H	0.022	31.104	3.426	1.167
CP	0.015	47.222	5.202	0.769
CX	0.021	32.578	10.087	0.397

The elimination rate constant (k_{el}) was calculated from the slope of the semi-logarithmical plot of OTA concentration versus time using the least square regression analysis.
The half-life of OTA elimination ($T_{1/2}$) was calculated from the equation:

$$T_{1/2} = \ln 2/k_{el}$$

The area under curve (AUC) was calculated by the integration of OTA concentration from time zero to infinity according to the formula:

$$AUC_{0-\infty} = AUC_{0-t} + C_f/k_{el}$$

where C_f represents the final measured OTA concentration made at time t. The clearance (CL) of OTA was determined using the following formula:

$$CL = D/AUC_{0-\infty}$$

where D represents the OTA dose, 3.5 mg/kg.

CB>PN>CX>MD>MB>CP>HP>Tl/H. Comparing the half-life of elimination ($T_{1/2}$) for each region shows that the pons and midbrain eliminated OTA very slowly ($T_{1/2}$=224 and 75 h, respectively) in contrast to the rapid elimination of the toxin from cerebellum ($T_{1/2}$=20 h).

3.2. Relationship between brain regional concentration of OTA and parameters of oxidative stress

Correlation analysis of the present pharmacokinetic data with previously published data on the effects of OTA on parameters of oxidative stress ED_{50} [12] revealed that the distribution of oxidative stress and DNA repair response across brain regions did not correlate with concentrations of the toxin (AUC) in each region (Fig. 2). Therefore the regional vulnerability to the toxin does not bear a linear relationship to the concentration of the toxin in each region. This observation is consistent with the hypothesis that vulnerability to injury induced by this toxin is determined by regional differences in capacity to scavenge oxyradicals and/or to repair oxidative DNA damage caused by the toxin, rather than the actual level of the toxin.

3.3. Effects of chronic OTA on behavior and levels of DA and its metabolites

Continuous sub-cutaneous infusion of OTA with Alzet minipumps resulted in a dose-dependent decrease of DA in caudate/putamen. After 2 weeks of continuous OTA administration (cumulative dose of 8 mg/kg), DA declined by 24% (76% of control level) (Fig. 3). At that dose of OTA, DOPAC concentration was elevated 1.9-fold (as compared to the control). A similar profile was recorded for HVA. The turnover of DA calculated as a ratio of (HVA+DOPAC)/DA was significantly increased at a cumulative dose of 8 mg/kg OTA. However, DA turnover was reduced at both the higher and lower cumulative doses, i.e. 4 and 16 mg/kg.

Notably, chronic exposure did not alter behavior or spontaneous locomotor activity, nor did it result in abnormal clasping or posturing of the limbs when handled by the tail. This is similar to the absence of motor deficits following acute doses of OTA that depleted striatal DA to 50% of control levels [12].

3.4. Effects of chronic OTA infusion on DNA repair (OGG1 activity)

Chronic OTA infusion resulted in a dose-dependent increase in OGG1 activities in all brain regions (Fig. 4). No region of the brain showed an inhibition or decrease in OGG1 activity at any dose, unlike the early responses to acute doses of OTA, when all regions showed initial and transient inhibition of OGG1 activity [12]. Even though all brain regions were capable of marked increases in

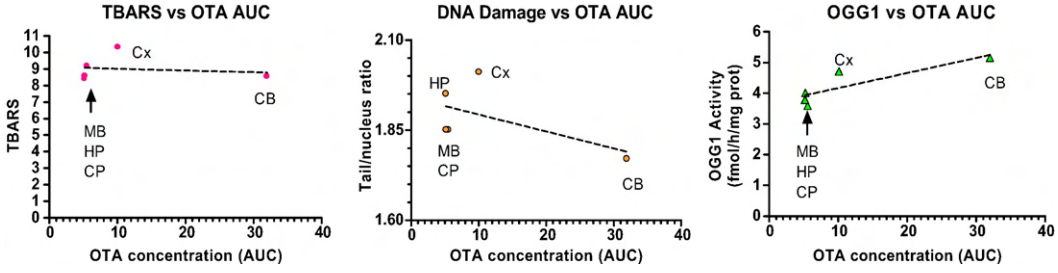

Fig. 2. Parameters of oxidative stress plotted as a function of OTA concentration. The pharmacokinetic parameter that reflects the average concentration of OTA over time in each brain region (“area under the curve” or AUC) s plotted on the *X*-axis. The left panel plots the relationship between TBARS (index of lipid peroxidation) in each brain region as a function of AUC for OTA. The middle and right panels show the plots of DNA damage vs AUC and DNA repair activity (OGG1) vs AUC, respectively. The dashed regression line does not differ significantly from zero in all three panels, indicating that there is no linear relationship between the selected parameter of oxidative stress and the AUC in specific brain regions. This correlation analysis relied on previously published data on TBARS, DNA damage and OGG1 for each brain region [12].

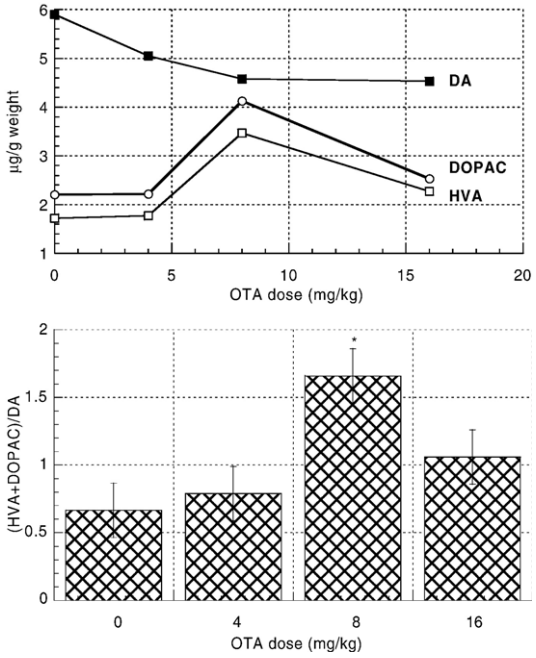

Fig. 3. Effects of chronic infusion of OTA via osmotic minipump on levels of DA and its metabolites across brain regions. Upper panel: Levels of DA and its metabolites in caudate/putamen of ICR mice exposed to different doses of OTA during 2 weeks. OTA was administered using Alzet osmotic minipumps implanted under the skin of animals. Lower panel: Turnover of DA in caudate/putamen of ICR mice subjected to chronic exposure of different doses of OTA during 2 weeks. Asterisk depicted a significantly different value as compared to the control ($P<0.05$).

OGG1 activity, not all regions were equally sensitive to the toxin. Using the dose–response curve functions generated from each brain region to estimate an ED_{50} (the dose of OTA that resulted in half the maximal rate of OGG1 activity), it was clear that the caudate/putamen was most sensitive to the toxin; a cumulative dose of 0.65 mg/kg produced half maximal OGG1 activity. The cerebellum was the least sensitive, with respect to dose of OGG1 required to attain half maximal OGG1 activity (ED_{50}=2.65 mg/kg). See Fig. 4.

4. Discussion

The impetus to this project was provided by reports that veterans of the first Gulf War were developing ALS at a higher frequency than the normal population, suggesting a war-related environmental trigger [4,5]. Since there was no clear evidence of high dose (lethal) exposure to aflatoxin in these veterans, it was possible they were exposed to sub-lethal low doses of the mycotoxin during routine operations in the field or while destroying enemy munition storage facilities. The present project attempted to replicate low dose exposure to a mycotoxin, OTA, with some similarities to aflatoxin in laboratory mice.

Acute administration of OTA has previously been reported to cause widespread oxidative stress in mouse brain, evidenced by significant increases in lipid peroxidation and oxidative DNA damage across 6 brain regions [12]. Furthermore, OTA treatment elicited an early and sustained surge in activity of SOD, a major oxyradical scavenger, across all brain regions [12]. Unlike the monophasic SOD activation, the oxidative DNA repair response exhibited a biphasic response, with an initial inhibition of OGG1 activity followed by a trend towards recovery to normal levels after 3 days. It was hypothesized that variation in DNA repair was a potential factor in determining neuronal vulnerability. Deficient DNA repair processes have been associated with Parkinson's Disease (PD) as well as with other neurodegenerative diseases such as Alzheimer's disease, amyotrophic lateral sclerosis (ALS) and Huntington's disease (HD) [13,17,18]. In addition, it was previously shown that the uneven distribution of oxidative DNA damage across brain regions caused by endogenous or exogenous factors was determined, in part, by the intrinsic capacity to repair oxidative DNA damage [14,15].

Those earlier studies, and the present report on the effects of OTA, were focused on oxyguanosine glyosylase (OGG1), a key enzyme involved in the repair of the oxidized base, 8-hydroxy-2′ deoxoguanosine (oxo8dG). Unrepaired DNA

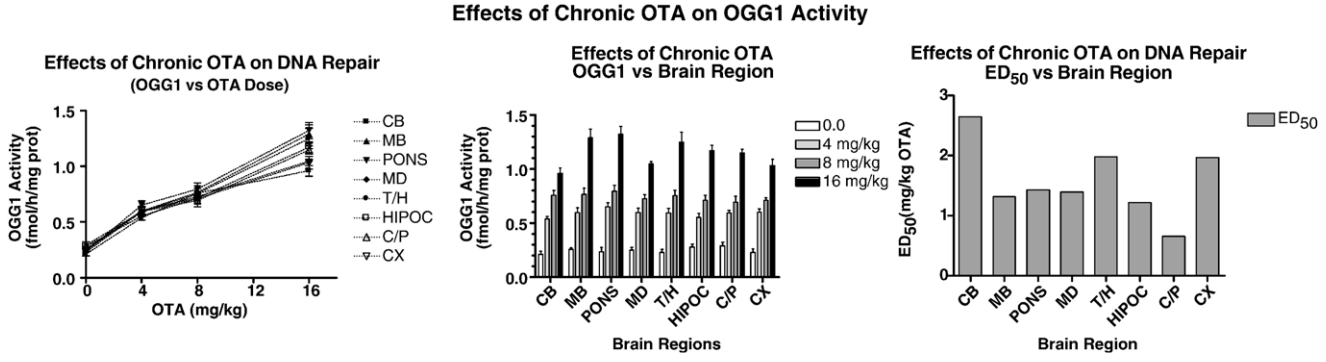

Fig. 4. Effects of chronic infusion of OTA via osmotic minipump on OGG1 activities across brain regions. Left panel: OGG1 activity plotted against cumulative OTA dose delivered over 2 weeks. All brain regions exhibited a dose-dependent increase in OGG1. Middle panel: OGG1 activity plotted against brain region on the *X*-axis. Shading of the bars depicts the cumulative dose administered over 2 weeks as indicated in the legend. Right panel: The ED_{50} (dose of OTA that increased OGG1 to 50% of the maximum response) was determined from the dose–response curves of each brain region. The *X*-axis depicts brain region and the *Y*-axis depicts the ED_{50} of OTA (in mg/kg) for each region. The CB, CX and Thalamus/hypothalamus exhibited the highest ED_{50}s (i.e. higher doses were required to produce half maximal response), while the CP had the lowest ED_{50} (lowest dose required to reach half maximal OGG1 response).

damage in post-mitotic cells, such as neurons, can result in the disruption of transcriptionally active genes, cellular dysfunction and apoptosis [19]. Hence it was reasonable to hypothesize that diminished DNA repair capacity in populations of neurons would be associated with increased vulnerability to potentially genotoxic agents. Since the CP and MB showed a relatively diminished OGG1 activity and increased oxidative DNA damage, it was postulated that the DA terminals of the striatum would suffer damage. This concept was supported by an earlier report of increased oxidative DNA damage in substantia nigra and striatum in post-mortem brain from PD cases [20], and by the observation that MB and CP were less able to upregulate OGG1 repair activity in response to the pro-oxidant, diethylmaleate [21]. This hypothesis was further supported by the report that acute doses of OTA caused a dose-dependent decrease of striatal DA and a decrease in DA turnover [12]. The nearly 50% reduction in striatal DA caused by a single dose (3.5 mg/kg i.p.) did not produce observable changes in daytime mouse behavior or locomotor activity, though it is likely that more sensitive, quantitative measures of behavior may reveal alterations. This dose of OTA also resulted in diminished tyrosine hydroxylase immunoreactivity in the CP and MB as well as in the locus ceruleus (which contains noradrenergic neurons). The effects of OTA on catecholaminergic systems appeared to reflect a potentially reversible action rather than a cytotoxic effect since no evidence of cell death was found by 72 h. There were no apoptotic profiles found in SN and CP or any other region of the brain. In addition, there did not appear to be cytotoxic effects on striatal neurons identified by DARPP32 immunostaining [12].

To determine whether uneven distribution of the toxin across brain regions was responsible for the vulnerability of DA terminals in striatum, pharmacokinetic studies were performed. Surprisingly, the distribution of oxidative stress and the DNA repair response across brain regions did not correlate with regional concentrations of the mycotoxin (AUC). The CB had the highest concentrations and the slowest clearance of OTA and yet was least affected by the toxin. Therefore, the regional vulnerability to the toxin was not directly related to the concentration of the toxin in each region.

Continuous, low dose infusion of OTA resulted in a dose-dependent decrease of striatal DA. After 2 weeks of continuous OTA exposure, DA had declined by 24% (e.g. to 75% of control levels) and DA turnover was significantly increased following delivery of a cumulative dose of 8 mg/kg OTA. The decline of striatal DA following chronic infusion was much less than that caused by a single acute dose of 3.5 mg/kg i.p. This may simply be a result of lower steady-state brain levels of the toxin when infused continuously through the minipump. In addition, chronic, low dose exposure may have permitted a more robust upregulation of the anti-oxidatve and DNA repair systems in the striatum.

Chronic OTA infusion also resulted in a dose-dependent increase in DNA repair (e.g., OGG1 activities) in all brain regions. No region of the brain showed an inhibition or decrease in OGG1 activity at any dose, unlike the early responses to acute doses of OTA, when all regions showed initial and transient inhibition of OGG1 activity [12]. Even though all brain regions were capable of marked increases in OGG1 activity, not all regions were equally sensitive to the toxin. Using the dose–response curve functions generated from each brain region to estimate an ED_{50} (the dose of OTA that resulted in half the maximal rate of OGG1 activity), it was clear that the caudate/putamen (CP) was most sensitive to the toxin; a cumulative dose of 0.65 mg/kg produced half maximal OGG1 activity. The cerebellum was the least sensitive, with respect to dose of OGG1 required to attain half maximal OGG1 activity (ED_{50}=2.65 mg/kg).

What is the most likely mechanism to explain the vulnerability of the caudate/putamen to OTA? These experiments showed that the susceptibility to oxidative stress, oxidative DNA damage and depletion of striatal DA is not directly related to the pharmacokinetics of the mycotoxin. A potential explanation for the observations reported here relates to bio-energetic compromise evoked by OTA. This mycotoxin has been reported to inhibit succinate-dependent electron transfer activities of the respiratory chain, but at higher concentrations will also inhibit electron transport at Complex I. [22,23]. The nigro-striatal dopaminergic system is well known to be especially vulnerable to the mitochondrial toxicants, MPTP and rotenone, especially when the latter toxicant is administered chronically at low doses [24–26]. Other mitochondrial poisons like nitroproprionic acid and malonate interfere with succinate dehydrogenase/Complex II. These Complex II inhibitors result in lesions primarily localized to the striatum [27,28]. Bio-energetic compromise may lead to persistent activation of NMDA receptors which results in excitotoxicity mediated by the neurotransmitter glutamate in regions of brain richly innervated by glutamatergic fibers, accounting for the vulnerability of the striatum and pallidum, and possibly the SN [29,30]. In addition, Ca2+ entering neurons through NMDA receptors has ‘privileged’ access to the mitochondria, where it causes free radical production and mitochondrial depolarization [30]. Hence the bio-energetic compromise induced by OTA may be responsible for the generation of free radicals and reactive oxygen species that resulted in global oxidative damage to DNA and lipids, as reported here and damage to proteins through generation of oxygen free radicals and nitric oxide, as reported elsewhere [31,32].

Of course OTA may also be toxic through other mechanisms. Due to its chemical structure, (chlorodihydroisocoumarin linked through an amide bond to phenylalanine), OTA inhibits protein synthesis by competition with phenylalanine in the aminoacylation reaction of phenylalanine-

tRNA [33,34] and phenylalanine hydroxylase activity [35]. These actions could lead to the impairment of the synthesis of DOPA, dopamine and catecholamines or enzymes involved in the metabolism of DA.

5. Conclusions

The continuous subcutaneous administration of OTA at low doses over a period of 2 weeks caused small, but significant depletion of striatal DA. OTA also caused pronounced global oxidative stress, evoking a strong anti-oxidative and DNA repair response across the entire brain. Even though the depletion of striatal DA did not cause overt parkinsonism in these mice, it is important to consider that the superimposition of normal age-related decline in striatal DA could ultimately result in signs of parkinsonism such as slowness of movement and rigidity in the mice. Without completing the understanding why DA terminals in striatum are especially vulnerable to OTA, it is likely that a toxic insult to the nigro-striatal system will increase the risk of developing Parkinson's Disease at an earlier age than normal. This hypothesis can be tested by studying the long term consequences of episodes of OTA exposure in mice during the aging process. In the real world, it will be important to monitor the neurological status of Gulf War veterans as they age.

Acknowledgements

Supported by the Department of Defense Grant # DAMD17-03-1-0501 and VA Merit Review Grant to J.S-R.

References

[1] Zilinskas RA. Iraq's biological weapons. The past as future? JAMA 1997;278:418–24.
[2] Bennett JW, Klich M. Mycotoxins. Clin Microbiol Rev 2003;16: 497–516.
[3] Stone R. Biodefense. Peering into the shadows: Iraq's bioweapons program. Science 2002;297:1110–2.
[4] Haley RW. Excess incidence of ALS in young Gulf War veterans. Neurology 2003;61:750–6.
[5] Haley RW. Gulf war syndrome: narrowing the possibilities. Lancet Neurol 2003;2:272–3.
[6] Kuiper-Goodman T, Scott PM. Risk assessment of the mycotoxin ochratoxin A. Biomed Environ Sci 1989;2:179–248.
[7] Galtier P. Pharmacokinetics of ochratoxin A in animals. IARC Sci Publ 1991:187–200.
[8] Marquardt RR, Frohlich AA. A review of recent advances in understanding ochratoxicosis. J Anim Sci 1992;70:3968–88.
[9] Hayes AW, Hood RD, Lee HL. Teratogenic effects of ochratoxin A in mice. Teratology 1974;9:93–7.
[10] Wangikar PB, Dwivedi P, Sharma AK, Sinha N. Effect in rats of simultaneous prenatal exposure to ochratoxin A and aflatoxin B(1). II. Histopathological features of teratological anomalies induced in fetuses. Birth Defects Res B Dev Reprod Toxicol 2004;71: 352–8.
[11] Belmadani A, Tramu G, Betbeder AM, Steyn PS, Creppy EE. Regional selectivity to ochratoxin A, distribution and cytotoxicity in rat brain. Arch Toxicol 1998;72:656–62.
[12] Sava V, Reunova O, Velasquez A, Harbison R, Sanchez-Ramos J. Acute neurotoxic effects of the fungal metabolite ochratoxin-A. Neurotoxicology 2006;27:82–92.
[13] Robbins JH, Otsuka F, Tarone RE, Polinsky RJ, Brumback RA, Nee LE. Parkinson's disease and Alzheimer's disease: hypersensitivity to X-rays in culture cell lines. J Neurol Neurosurg Psychiatry 1985;48:916–23.
[14] Cardozo-Pelaez F, Song S, Parthasarathy A, Hazzi C, Naidu K, Sanchez-Ramos J. Oxidative DNA damage in the aging mouse brain. Mov Disord 1999;14:972–80.
[15] Cardozo-Pelaez F, Brooks PJ, Stedeford T, Song S, Sanchez-Ramos J. DNA damage, repair, and antioxidant systems in brain regions: a correlative study. Free Radic Biol Med 2000;28:779–85.
[16] Smith PK, Krohn RI, Hermanson GT, Mallia AK, Gartner FH, Provenzano MD, et al. Measurement of protein using bicinchoninic acid. Anal Biochem 1985;150:76–85.
[17] Mazzarello P, Poloni M, Spadari S, Focher F. DNA repair mechanisms in neurological diseases: facts and hypotheses. J Neurol Sci 1992;112:4–14.
[18] Lovell MA, Xie C, Markesbery WR. Decreased base excision repair and increased helicase activity in Alzheimer's disease brain. Brain Res 2000;855:116–23.
[19] Hanawalt PC. Transcription-coupled repair and human disease: perspective. Science 1994;266:1957–8.
[20] Sanchez-Ramos J, Overvik E, Ames BN. A marker of oxyradical-mediated DNA damage (oxo8dG) is increased in nigro-striatum of Parkinson's disease brain. Neurodegeneration (incorporated into Exp Neurology) 1994;3:197–204.
[21] Cardozo-Pelaez F, Stedeford TJ, Brooks PJ, Song S, Sanchez-Ramos JR. Effects of diethylmaleate on DNA damage and repair in the mouse brain. Free Radic Biol Med 2002;33:292–8.
[22] Wei YH, Lu CY, Lin TN, Wei RD. Effect of ochratoxin A on rat liver mitochondrial respiration and oxidative phosphorylation. Toxicology 1985;36:119–30.
[23] Aleo MD, Wyatt RD, Schnellmann RG. Mitochondrial dysfunction is an early event in ochratoxin A but not oosporein toxicity to rat renal proximal tubules. Toxicol Appl Pharmacol 1991;107:73–80.
[24] Vyas I, Heikkila RE, Nicklas WJ. Studies on the neurotoxicity of MPTP; inhibition of NAD-linked substrate oxidation by its metabolite, MPP+. J Neurochem 1986;46:1501–7.
[25] Hasegawa E, Takeshige K, Oishi T, Murai Y, Minakami S. MPP + induces NADH-dependent superoxide formation and enhances NADH-dependent lipid peroxidation in bovine heart submitochondrial particles. Biochem Biophys Res Commun 1990;170: 1049–1055.
[26] Betarbet R, Sherer TB, MacKenzie G, Garcia-Osuna M, Panov AV, Greenamyre T. Chronic systemic pesticide exposure reproduces features of Parkinson's disease. Nat Neurosci 2000;3:1301–6.
[27] Schulz JB, Henshaw DR, MacGarvey U, Beal MF. Involvement of oxidative stress in 3-nitropropionic acid neurotoxicity. Neurochem Int 1996;29:167–71.
[28] Calabresi P, Gubellini P, Picconi B, Centonze D, Pisani A, Bonsi P, et al. Inhibition of mitochondrial complex II induces a long-term potentiation of NMDA-mediated synaptic excitation in the striatum requiring endogenous dopamine. J Neurosci 2001;21: 5110–20.
[29] Turski L, Turski WA. Towards an understanding of the role of glutamate in neurodegenerative disorders: energy metabolism and neuropathology. Experientia 1993;49:1064–72.
[30] Greenamyre JT, MacKenzie G, Peng TI, Stephans SE. Mitochondrial dysfunction in Parkinson's disease. Biochem Soc Symp 1999;66: 85–97.
[31] Thomas JA, Mallis RJ. Aging and oxidation of reactive protein sulfhydryls. Exp Gerontol 2001;36:1519–26.
[32] Bryan NS, Rassaf T, Maloney RE, Rodriguez CM, Saijo F, Rodriguez JR, et al. Cellular targets and mechanisms of nitros(yl)ation: an insight into their nature and kinetics in vivo. Proc Natl Acad Sci U S A 2004;101:4308–13.

[33] Bunge I, Dirheimer G, Roschenthaler R. In vivo and in vitro inhibition of protein synthesis in *Bacillus stearothermophilus* by ochratoxin A. Biochem Biophys Res Commun 1978;83:398–405.
[34] Creppy EE, Kern D, Steyn PS, Vleggaar R, Roschenthaler R, Dirheimer G. Comparative study of the effect of ochratoxin A analogues on yeast aminoacyl-tRNA synthetases and on the growth and protein synthesis of hepatoma cells. Toxicol Lett 1983;19:217–24.
[35] Creppy EE, Chakor K, Fisher MJ, Dirheimer G. The myocotoxin ochratoxin A is a substrate for phenylalanine hydroxylase in isolated rat hepatocytes and in vivo. Arch Toxicol 1990;64:279–84.

Available online at www.sciencedirect.com
ScienceDirect
NeuroToxicology 27 (2006) 1080–1093
NeuroToxicology

Neuroanatomical mapping of DNA repair and antioxidative responses in mouse brain: Effects of a single dose of MPTP

V. Sava [a,b], O. Reunova [a], A. Velasquez [a], S. Song [a,b], J. Sanchez-Ramos [a,b,*]

[a] *Department of Neurology, University of South Florida, MDC 55, 12901 Bruce B. Downs Blvd., Tampa, FL 33612, USA*
[b] *Research Service, James Haley VA, Tampa, FL, USA*

Received 19 February 2006; accepted 30 May 2006
Available online 9 June 2006

Abstract

The primary objective of this study was to map the normal distribution of the base excision enzyme oxyguanosine glycosylase (OGG1) across mouse-brain regions as a prelude to assessing the effects of various neurotoxicants, ranging from highly selective molecules like MPTP to more global toxic agents. This research is based on the hypothesis that regional brain vulnerability to a toxicant is determined, in part, by variation in the intrinsic capacity of cellular populations to successfully repair oxidative DNA damage. After mapping the normal distributions of OGG1 and superoxide dismutase (SOD) across 44 loci dissected from mouse brain, MPTP, a mitochondrial toxicant with selective dopamine (DA) neuron cytotoxicity was used to elicit focal oxidative stress and DNA repair responses. A single dose of MPTP (20 mg/kg, i.p.) elicited time- and region-dependent changes in both SOD and OGG1, with early increases in DNA repair and anti-oxidant activities throughout all regions of brain. In some sampled loci, notably the substantia nigra (SN) and hippocampus, the heightened DNA repair and antioxidant responses were not maintained beyond 48 h. Other loci from cerebellum, cerebral cortex and pons maintained high levels of activity up to 72 h. Levels of dopamine (DA) were decreased significantly at all time points and remained below control levels in nigro-striatal and mesolimbic systems (ventral tegmental area and nucleus accumbens). Assessment of apoptosis by TUNEL staining revealed a significant increase in number of apoptotic nuclei in the substantia nigra at 72 h and not in other loci. The marked degree of apoptosis that became evident in SN at 72 h was associated with large decreases in SOD and DNA repair activity at that locus. In conclusion, MPTP elicited global effects on DNA repair and antioxidant activity in all regions of brain, but the most vulnerable loci were unable to maintain elevated DNA repair and antioxidant responses.

Keywords: Oxyguanosine glycosylase; Superoxide dismutase; Dopamine; Tyrosine hydroxylase; Apoptosis; *N*-Methyl-4-phenyl-1,2,3,6-tetrahydropyridine (MPTP); Substantia nigra; Striatum

1. Introduction

Aging is associated with increasing levels of oxidative DNA damage in all organs except the brain and testes (Fraga et al., 1990). The stable measures of oxidative DNA damage in whole brain homogenates had masked the variation in DNA damage across neuroanatomically defined brain regions. More refined analysis of DNA damage in specific brain regions revealed increased levels of DNA adducts formed by reaction of oxygen radicals with DNA. In the mouse, there was an age-dependent accumulation of 8-hydroxy-2′-deoxyguanosine (oxo8dG) in total DNA extracted from brain regions involved in locomotor control. These increased levels of the oxidized base relative to the unoxidized 2′-deoxyguanosine were associated with a decline in spontaneous locomotor activity and balance in the aged mice (Cardozo-Pelaez et al., 1999, 2000). In addition, the increase in oxo8dG levels in striatum correlated with decline in striatal dopamine (DA) in old mice (Cardozo-Pelaez et al., 1999). In the human brain, steady-state levels of oxidative DNA damage, indicated by oxo8dG, were increased in the substantia nigra, basal ganglia and cortex of idiopathic Parkinson disease (PD) cases compared to controls (Alam et al., 1997; Sanchez Ramos et al., 1994). Most of the age-dependent increases in oxo8dG measured in total DNA extracted from brain was attributed to the oxidative DNA damage that occurs in mitochondria (Mecocci et al., 1993). More recently, high levels of expression of mitochondrial isoforms of OGG1 enzymes were found in the substantia nigra (SN) in post-mortem brain from cases of PD (Fukae et al., 2005).

* Corresponding author. Tel.: +1 813 974 6022; fax: +1 813 974 7200.
E-mail address: jsramos@hsc.usf.edu (J. Sanchez-Ramos).

0161-813X/$ – see front matter © 2006 Elsevier Inc. All rights reserved.
doi:10.1016/j.neuro.2006.05.023

The enzyme 8-oxoguanine DNA glycosylase 1 (OGG1) participates in a key step of base excision repair, one of many DNA repair mechanisms that maintain the integrity of the genome in proliferating cells and that ensure faithful expression of transcriptionally active genes in post-mitotic cells. OGG1 activity has been shown to be inversely related to the levels of the damaged base (oxo8dG) in macro-dissected brain regions (Cardozo-Pelaez et al., 2000). In addition, OGG1 activity is increased in a region-specific manner following treatment with diethylmaleate, a compound that reduces glutathione levels in the cell (Cardozo-Pelaez et al., 2002). A single treatment with diethylmaleate elicited a significant increase (~2-fold) in the activity of OGG1 in three gross brain regions with low basal levels of activity (cerebellum, cortex, and pons/medulla). There was no change in the activity of OGG1 in those regions with high basal levels of activity (hippocampus, caudate/putamen, and midbrain). These studies clearly demonstrated that base excision repair can be upregulated in the CNS and that the increased repair activity correlated with a reduction in the levels of DNA damage. It is important to point out that alternative repair systems exist to minimize the effects of an increased load of oxo8dG, evidenced by the viability of homozygous OGG1 (−/−) null mice (Klungland et al., 1999). These OGG1 "knockout" mice accumulate abnormal levels of oxo8dG in their genomes, and despite the increase in potentially miscoding DNA lesions, they exhibited only a moderately, but significantly, elevated spontaneous mutation rate in nonproliferative tissues, did not develop malignancies, and showed no marked pathological changes (Klungland et al., 1999). However, the effects of oxidative stress in carefully micro-dissected brains of OGG1 knockout mice has not been reported. In fact, the absence of a neuroanatomical map of OGG1 activity in normal mice provided the impetus for the present study.

The primary objective for the present study was to create a neuroanatomical map of the distribution of base excision repair capacity, indicated by OGG1 activity. Since the response to oxidative stress involves an upregulation of endogenous anti-oxidant activity as well as DNA repair, we also mapped the distribution of superoxide dismutase (SOD) activity across the brain. The assay for OGG1 utilized in the study was sensitive enough to be applied to tissue samples weighing no more than 1 mg. The dissection technique permitted analysis of 44 samples from each brain. The method is limited in that only total OGG1 activity (nuclear and mitochondrial) can be assessed. However, the map of the neuroanatomical distribution of total OGG1 activity will provide a useful baseline for studying an important aspect of the brain's DNA repair capacity under various experimental conditions. The secondary objective was to test the hypothesis that a selective neurotoxicant, such as MPTP, would create oxidative stress localized to the nigro-striatal system. Other regions that escape the toxic effects of MPTP would be expected to have little evidence for oxidative stress or highly efficient antioxidant and DNA repair activities. The effects of a mitochondrial toxicant, oxchratoxin-A, with more global effects on brain have been studied in six major regions of brain and were recently reported (Sava et al., 2006).

In the present report, we investigated the early time-course and neuroanatomical distribution of the DNA repair and anti-oxidative responses in multiple loci across the brain of mice following a single dose of MPTP. In addition, levels of striatal DA and its metabolites were measured at the same time points to determine the relationship between DNA repair and the toxicity for DA neurons in the nigro-striatal system.

2. Materials and methods

2.1. Materials

MPTP, SOD, goat serum and dihydrobenzylamine were purchased from Sigma (St. Louis, MO). Protease inhibitors and DNA glycosylase were from Boehringer Mannheim (Indianapolis, IN, USA). ^{32}P-ATP was from NEN Life Science Products (Wilmington, DE). G25 spin columns were from Prime; Inc. (Boulder, CO). T4 polynucleotide kinase was from Stratagene (Austin, TX). Rabbit Anti-Tyrosine Hydroxylase was purchased from Pel-Freez Biologicals (Arkansas, AR). ApopTag *in situ* Apoptosis Detection Kit, rat anti-DAT primary antibody, and goat anti-rat secondary antibody were from Chemicon International (Temecula, CA). Avidin–biotin-complex Vectastain ABC Kit and DAB-kit was from Vector Labs (Burlingame, CA). All other reagents were from Sigma Chemical Co.

2.2. Animals and treatment

Male C57BL/J6 mice were (22 ± 2 g) obtained from the Jackson Laboratories (Bar Harbor, ME). They were housed at the temperature of 21 ± 2 °C with 12 light/dark cycle and free access to food and water. The animal protocol was approved by the Institutional Animal Care and Use Committee (IACUC) run by the Department of Comparative Medicine at the University of South Florida (USF). Comparative Medicine is fully accredited by the Association for the Assessment and Accreditation of Laboratory Animal Care. Its program and facilities for animal care and use are managed in accordance with the National Research Council Guide for the Care and Use of Laboratory Animals, the Public Health Service (PHS) Policy on Humane Care and Use of Laboratory Animals, and the Animal Welfare Regulations 9 CFR A, 1-3. Comparative Medicine has an assurance of compliance on file with Office of Laboratory Animal Welfare, National Institutes of Health and is a registered research facility with the United States Department of Agriculture.

Mice were divided into control ($n = 8$) and four experimental groups ($n = 8$ per group). Mice received either normal saline (control) or MPTP (20 mg/kg, i.p.) injections. Animals were euthanatized 12, 24, 48 and 72 h after administration of MPTP. Animals were decapitated quickly (in isolation from other mice), brains removed, placed in cold aluminum mouse-brain mold for coronal sectioning as described below. Anesthesia was avoided in these cases because the primary biochemical endpoints were oxidative DNA damage and repair as well as the endogenous anti-oxidative response. Anesthetics may alter the redox status of the brain tissue and artifactually alter the measurement.

2.3. Tissue micro-dissection

Brain coronal sections of 1 mm thickness were prepared at −10 °C in a cryostat chamber using a Brain Matrices mouse-brain mold (Braintree Sci., Inc., MA). The coronal sections were mounted on Superfrost/Plus microscope slides (Fisherbrand, PA) and stored at −70 °C until harvesting of specific brain regions. Prior to freezing, dissection landmarks were briefly confirmed.

The harvesting of brain tissue from specific loci of each coronal section was performed under a stereo microscope (WILD Heerbrugg, Switzerland). Punch micro-dissection of the tissue from the coronal sections utilized a Brain Tissue Punch Set (Vibratome, MO). The stage of the microscope was replaced with a variable temperature thermo-electric Cold Plate (Oven Ind., Inc., PA). The tissue sections were placed on the plate at −15 °C, a temperature that permitted precise punching without rendering the slice brittle and liable to fracture. Punches were obtained from both right and left sides of the brain using a cannula of 1 mm diameter designed for this specific purpose (Vibratome, MO). The cannula was equipped with a spring action inner probe that permitted easy ejection of the sample into a 1.5 mL plastic tube. Collected samples were stored in the 1.5 mL plastic tubes at −70 °C until biochemical procedure. Dissection was documented using a DEI-470 (Optronics Eng., CA) video camera connected to computer and images were processed with MGI VideoWave III software. Selection and identification of the sites for micro-dissection was based on the mouse-brain atlas (Paxinos and Franklin, 2001). In total, 44 different loci were harvested in each mouse brain using micro-punch dissection.

2.4. Assessment of OGG1 activity

The procedure for extraction of DNA glycosylase was similar to that described previously (Cardozo-Pelaez et al., 2000). Micro-punches of brain tissue were sonicated in homogenization buffer contained 20 mM Tris, pH 8.0, 1 mM EDTA, 1 mM dithiotrietol (DTT), 0.5 mM spermine, 0.5 mM spermidine, 50% glycerol and protease inhibitors and homogenates were rocked for 30 min after addition of 1/10 volumes of 2.5 M KCl. Samples were spun at 14,000 rpm for 30 min and supernatants were collected.

The OGG1 activities in supernatants were determined using duplex oligonucleotide containing 8-oxodG as incision substrate. For preparation of the incision assay, 20 pmol of synthetic probe containing 8-oxodG (Trevigen, Gaithersburg, MD) was labeled with P^{32} at the 5′ end using polynucleotide T4 kinase (Boehringer, Mannheim, Germany). Unincorporated free ^{32}P-ATP was separated on G25 spin column (Prime; Inc., Boulder, CO). Complementary oligonucleotides were annealed in 10 mM Tris, pH 7.8, 100 mM KCl, 1 mM EDTA by heating the samples 5 min at 80 °C and gradually cooling at room temperature.

Incision reactions was carried out in mixture (20 μL) containing 40 mM HEPES (pH 7.6), 5 mM EDTA, 1 mM DTT, 75 mM KCl, purified bovine serum albumin, 100 fmol of ^{32}P-labeled duplex oligonucleotide, and extracted guanosine glycosilase (30 μg of protein). The reaction mixture was incubated at 37 °C for 2 h and products of the reaction were analyzed on denaturing 20% polyacrylamide gel. Pure OGG1 served as positive control and untreated duplex oligonucleotide was used for negative control. The gel was visualized on Biorad-363 Phosphoimager System. The incision activity of OGG1 was calculated as the amount of radioactivity in the band representing specific cleavage of the labeled oligonucleotide over the total radioactivity. Data were normalized to equal concentrations of protein, the concentration of which was measured using the bicinchoninic acid assay (Smith et al., 1985).

2.5. SOD assay

Determination of SOD activity in mouse brain was based on inhibition of nitrite formation in reaction of oxidation of hydroxylammonium with superoxide anion radical (Elstner and Heupel, 1976). Nitrite formation was generated in a mixture contained 25 μL xanthine (15 mM), 25 μL hydroxylammonium chloride (10 mM), 250 μL phosphate buffer (65 mM, pH 7.8), 90 μL distilled water and 100 μL xanthine oxidase (0.1 U/mL) used as a starter of the reaction. Inhibitory effect of inherent SOD was assayed at 25 °C during 20 min of incubation with 10 μL of brain tissue extracts. Determination of the resulted nitrite was performed upon the reaction (20 min at room temperature) with 0.5 mL sulfanilic acid (3.3 mg/mL) and 0.5 mL α-naphthylamine (1 mg/mL). Optical absorbance at 530 nm was measured on Ultrospec III spectrophotometer (Pharmacia, LKB). The results were expressed as units of SOD activity calculated per milligram of protein. The amount of protein in the samples was determined using the bicinchoninic acid (Smith et al., 1985).

2.6. Measurement of dopamine

HPLC with electrochemical detection was employed to measure levels of dopamine (DA) as previously reported in our laboratory (Cardozo-Pelaez et al., 1999). Punched tissue samples were sonicated in 50 volumes of 0.1 M perchloric acid containing 50 ng/mL of dihydrobenzylamine (Sigma Chemical, MA) as internal standard. After centrifugation (15,000 × *g*, 10 min, 4 °C), 20 mL of supernatant was injected onto a C18-reversed phase RP-80 catecholamine column (ESA, Bedford, MA). The mobile phase consisted of 90% of a solution of 50 mM sodium phosphate, 0.2 mM EDTA, and 1.2 mM heptanesulfonic acid (pH 4) and 10% methanol. Flow rate was 1.0 mL/min. Peaks were detected by a Coulochem 5100A detector (ESA). Data were collected and processed with TotalChrom software (Perkin-Elmer Instruments).

2.7. Immunohistochemistry

Brains from several animals at each time point was allocated for immunocytochemical study. Following euthanasia, brains were removed, blocked and processed for cryostat sectioning. Tissue was cut in 25 μm thin sections. Every fifth section was selected. Thin sections were placed on Superfrost/Plus

Microscope Slides (precleaned) and processed by using different staining methods as described below.

2.7.1. Tyrosine hydroxylase (TH) immunohistochemistry

Slide-mounted tissue sections were fixed for 30 min at room temperature in 4% paraformaldehyde prepared on PBS (pH 7.4) and then transferred to PBS containing 5% sucrose. After 15 min of incubation sections were treated with 10% H_2O_2 in 95% MeOH for 30 min at room temperature to destroy endogenous peroxidase. Then sections were blocked at room temperature during 60 min with 10% Goat Serum (Sigma Chemicals, MI) prepared on PBS containing 0.3% Triton X-100. Rabbit Anti-Tyrosine Hydroxylase (Pel-Freez Biologicals, Arkansas) was served as primary antibody (1:1000) and it was prepared on PBS containing 10% Goat Serum and 0.3% Triton X-100. The sections were incubated with primary antibody overnight at 4 °C and then washed in three changes of PBS for 10 min each. Goat Anti-Rabbit (Chemicon, CA) secondary antibody was prepared on PBS/Triton X-100 buffer (1:300) and incubated with samples for 60 min at room temperature. Then sections were washed for 10 min in three changes of PBS, treated with avidin–biotin-complex (Vectastain ABC Kit (Peroxidase Standard*), Vector Labs, CA) for 60 min and developed with 3,3′-diaminobenzidine (DAB Substrate Kit, Vector Labs, CA) at room temperature during 2–5 min. Finally the sections were rinsed with distilled water to stop reaction and then dehydrated in ethanol, cleared in xylene and coverslipped for microscopic examination. Controls for nonspecific staining were performed for evaluation in which either primary or secondary antibody were applied alone.

2.7.2. TUNEL assay

TUNEL staining was performed in accordance to Manual of ApopTag *in situ* Apoptosis Detection Kit (Chemicon, CA). Briefly, slide-mounted tissue sections were fixed for 10 min at room temperature with 1% paraformaldehyde prepared on PBS (pH 7.4) and rinsed two times for 5 min of PBS. Slides were post-fixed in precooled ethanol:acetic acid (2:1) for 5 min at −20 °C in a Coplin jar and rinsed two times for 5 min with PBS. Equilibration buffer was immediately applied directly to the specimens for 20 s at room temperature. TdT enzyme was pipetted onto the sections following by incubation in a humidified chamber for 1 h at 37 °C. Specimen were placed in a Coplin jar containing working strength stop/wash buffer and incubated for 10 min at room temperature. After triple rinsing in PBS, the sections were incubated with anti-digoxigenin conjugate in a humidified chamber for 30 min in dark at room temperature. Finally, the specimens were rinsed with PBS (4 × 2 min) and mounted on a glass cover slip with Vectashield mounting medium containing DAPI (Vector Labs, CA).

2.8. Statistical analysis

The results were reported as mean ± S.E.M. for 3–6 sets of brain loci for each time point. Two-tailed *t*-tests were applied in the analysis of the DA and metabolites data. Two-way ANOVA was utilized to evaluate the contribution of time after MPTP and neuroanatomical distribution to the total variance of OGG1 and SOD data (GraphPad Software, Inc, San Diego, CA). This was followed by *t*-tests with Bonferroni corrections to compare results against control values at time zero for each neuro-anatomical locus. One-way ANOVA, followed by Bonferroni-corrected *t*-tests for multiple comparisons, was utilized for analysis of the time-course of apoptosis in the midbrain following MPTP.

3. Results

Tissue samples with consistent dimensions of 1 mm diameter by 1 mm in thickness were harvested with a tissue punch cannula from seven serial coronal sections prepared from each mouse brain. To conform more closely to midline ventral tegmental landmarks, two smaller diameter tangential punches with a smaller needle (0.5 mm diameter) were made in collecting midline loci # 7, 14, 23, 32. Sampling sites were identified with the assistance of a mouse-brain atlas and documented for subsequent confirmation with a microscope-mounted digital camera (see Table 1) (Paxinos and Franklin, 2001). Forty-four loci from each brain were collected and analyzed for DNA repair activity (OGG1) and endogenous antioxidant activity (SOD). Nineteen of the 44 loci were sampled bilaterally (from both the right and left side of the same neuroanatomical site) and analyzed individually. Specific loci from midbrain (s. nigra and ventral tegmental area) and striatum (caudate-putamen and n. accumbens) were analyzed for levels of DA and metabolites.

The distribution of mean OGG1 activities varied significantly across 44 brain loci (one-way ANOVA; $p < 0.01$). The lowest mean OGG1 activity was in locus # 30, caudate-putamen (4.57 ± 1.21 fmol/h/mg protein) and the highest was expressed in locus # 24, comprising sub-thalamic nucleus, nigro-striatal bundle and para-subthalamic nucleus (11.7 ± 1.15 fmol/h/mg protein) (see Table 2). Mean SOD activities at baseline were also distributed unequally across brain regions (one-way ANOVA; $p < 0.0001$) (see Table 3). Locus # 34 (caudate-putamen) expressed the lowest baseline level (5.7 ± 0.38 U/mg protein) and locus # 32 (comprising periventricular hypothalamic nucleus and medial preoptic nucleus) expressed the highest level of activity (14.55 ± 1.25 U/mg protein). Interestingly, there was asymmetry in the baseline OGG1 activities at some loci (more easily visualized in the color-coded, Fig. 6).

A single dose of MPTP (20 mg/kg, i.p.) produced a decrease in DA levels in the nigro-striatal and mesolimbic (VTA–N. Acb) systems (Fig. 1). DA concentration in CP reached its lowest level at 24 h (26% of control levels). In SN, where the DA neuron cell bodies reside, the DA concentration reached its lowest level (15% of control) at a later time, 48 h. Similarly, DA concentration reached the lowest level (52% of control) in the N. Acb at 24 h while the levels in the VTA, where DA neuron cell bodies reside, were reduced to the lowest level (23% of control) at 72 h. The DA levels in N. Acb appeared to be recovering slightly by 72 h. These results are consistent with other reports suggesting that VTA and its projection field in the

Table 1
Neuroanatomical regions sampled with abbreviations

Locus #	Abbreviations	Neuroanatomical region sampled
1	LC + LVe + Mve + MC + PC	Lateral vestibular nu + med vestib nu, magnocell and parvicell
2	3Cb	Third cerebellar lobule
3	LC + LVe + Mve + MC + PC	Lateral vestibular nu + med vestib nu, magnocell and parvicell
4	LEnt + MEnt	Lateral entorhinal + medial entorhinal cortex
5	ECIC	Inferior colliculus
6	MO5 + PnO	Motor trigeminal nu + pontine reticular nu
7	RtTg	Reticulotegmental nu pons
8	MO5 + PnO	Motor trigeminal nu + pontine reticular nu
9	ECIC	Inferior colliculus
10	LEnt + MEnt	Lateral entorhinal + medial entorhinal cortex
11	DG + Mol + LMol	Dentate gyrus + molecular layer dentate gyrus + lacunosum molecular layer
12	CA3	Field CA3 of hippocampus
13	SNC + SNR	Substantia nigra (compact and reticular parts)
14	VTA + IPC + IPR	Ventral tegmental area + interpeduncular nucleus
15	Op + InG + InWh + DpG	Areas of superior colliculus
16	SNC + SNR	Substantia nigra (compact and reticular parts)
17	CA3	Field CA3 of hippocampus
18	DG + Mol + LMol	Dentate gyrus + molecular layer dentate gyrus + lacunosum molecular layer
19	Pir + DEn	Piriform cortex + dorsal endopiriform nu
20	GrDG + Mol + LMol	Granular layer of dentate gyrus + molecular layer dentate gyrus + lacunosum molecular layer
21	Po + PC	Posterior thalamic nu group + parecentral thalamic nu
22	nc + STh + PSTh	Migrostriatal bunble + subthalamic nu + parasubthalamic nu
23	DMC + DM	Dorsomedial nu, compact + dorsomedial hypothalamic nu
24	nc + STh + PSTh	Nigro-striatal bunble + subthalamic nu + parasubthalamic nu
25	Po + PC	Posterior thalamic nu group + parecentral thalamic nu
26	GrDG + Mol + LMol	Granular layer of dentate gyrus + molecular layer dentate gyrus + lacunosum molecular layer
27	Pir + DEn	Piriform cortex + dorsal endopiriform nu
28	Pir + DEn	Piriform cortex + dorsal endopiriform nu
29	S1BF + S1DZ + S1FL	S1 cx, barrel field + S1 cx, dysgranular region + S1 cx, hindlimb region
30	CPu (R)	Caudate putamen (striatum)
31	Cpu + LGP	Caudate putamen (striatum) + lateral globus pallidus
32	Pe + MPOL	Periventricular hypothalamic nu + medial preoptic nu, lateral
33	Cpu + LGP	Caudate putamen (striatum) + lateral globus pallidus
34	CPu (L)	Caudate putamen (striatum)
35	S1BF + S1DZ + S1FL	S1 cx, barrel field + S1 cx, dysgranular region + S1 cx, hindlimb region
36	Pir + DEn	Piriform cortex + dorsal endopiriform nu
37	M1	Primary motor cortex
38	CPu	Caudatum putamen (striatum)
39	CPu + AcbC + aca	Caudatum putamen + accumbens nu, core + anterior commissure, anterior part
40	Cpu + AcbC + aca	Caudatum putamen + accumbens nu, core + anterior commissure, anterior part
41	CPu	Caudatum putamen (striatum)
42	M1	Primary motor cortex
43	LO + VO + M2	Lateral orbital cortex + medial orbital cortex + secondary motor cortex
44	LO + VO + M2	Lateral orbital cortex + medial orbital cortex + secondary motor cortex

N. accumbens are less susceptible to MPTP than the nigro-striatal system (German et al., 1996).

Concomitant with the decreasing DA levels in the nigro-striatal system, the endogenous anti-oxidant SOD activity increased significantly with a peak at 48 h and then a decline below control level at 72 h. In VTA and N. accumbens SOD also increased and peaked at 48 h but then declined below control levels at 72 h (Fig. 2).

Repair of oxidative DNA damage (OGG1) also increased with time in the nigro-striatal DA system, reaching a peak at 48 h and declining, but not dipping below control levels, at 72 h (Fig. 3, upper panel). In particular, OGG1 activity in SN

Table 2
Distribution of OGG1 activity across the mouse brain following a single dose of MPTP (20 mg/kg, i.p.)

Locus #	Control	12 h	24 h	48 h	72 h
1	9.91 ± 2.77	19.6 ± 1.37*	18.9 ± 2.06	16.5 ± 2.99	17.8 ± 5.30
2	6.15 ± 1.06	19.3 ± 5.32*	18.2 ± 3.61*	19.8 ± 2.93*	20.0 ± 3.94*
3	7.45 ± 1.63	12.8 ± 3.31	15.6 ± 3.59	16.0 ± 2.10	14.0 ± 2.11
4	6.35 ± 0.86	18.0 ± 2.00*	7.39 ± 1.05	18.2 ± 2.30*	36.4 ± 1.78*
5	5.02 ± 0.82	11.8 ± 0.70	13.6 ± 1.42	17.9 ± 3.53*	18.6 ± 1.26*
6	7.06 ± 1.88	18.9 ± 0.70*	12.0 ± 2.00	19.3 ± 2.32*	16.1 ± 1.99
7	7.55 ± 1.11	17.7 ± 1.79*	11.6 ± 2.36	8.22 ± 0.82	9.86 ± 0.97
8	6.87 ± 1.39	14.7 ± 0.48	14.4 ± 3.88	13.2 ± 2.08	15.1 ± 1.52
9	5.87 ± 0.91	14.5 ± 2.53	18.5 ± 4.05*	15.3 ± 2.72*	19.1 ± 0.45*
10	5.87 ± 1.68	16.0 ± 0.94*	17.1 ± 1.05*	8.38 ± 0.76	11.1 ± 2.63
11	4.61 ± 0.97	14.9 ± 2.37*	12.6 ± 2.13	9.52 ± 1.00	9.53 ± 1.70
12	7.41 ± 1.23	14.4 ± 2.54	14.7 ± 2.46	11.7 ± 1.37	14.3 ± 2.07
13	5.88 ± 1.38	15.1 ± 1.67*	20.6 ± 4.61*	16.4 ± 1.73*	8.32 ± 1.54
14	6.55 ± 1.80	13.3 ± 2.39	19.7 ± 3.18*	27.0 ± 1.75*	11.2 ± 0.91
15	5.16 ± 1.25	8.08 ± 1.46	21.3 ± 3.28*	26.8 ± 3.27*	14.4 ± 4.02
16	5.78 ± 1.33	3.88 ± 0.64	18.8 ± 2.71*	27.3 ± 1.87*	8.15 ± 0.72
17	7.25 ± 1.42	5.85 ± 0.93	19.3 ± 2.60*	15.0 ± 0.39	12.4 ± 0.96
18	5.77 ± 1.77	7.24 ± 0.89	18.8 ± 3.22*	23.7 ± 5.20*	8.68 ± 0.54
19	7.89 ± 0.97	10.1 ± 0.08	19.1 ± 2.60*	9.75 ± 1.36	32.1 ± 6.64*
20	7.97 ± 1.14	10.0 ± 0.38	12.0 ± 1.16	18.2 ± 3.75*	16.2 ± 1.41
21	6.90 ± 0.56	4.56 ± 0.74	14.9 ± 1.90	24.0 ± 5.76*	7.75 ± 0.81
22	7.50 ± 1.13	6.56 ± 1.51	10.0 ± 2.73	9.31 ± 1.33	17.4 ± 2.54*
23	8.85 ± 1.58	10.2 ± 0.19	14.4 ± 1.78	13.5 ± 2.73	14.5 ± 2.27
24	11.7 ± 1.15	9.29 ± 1.56	11.7 ± 2.46	25.8 ± 2.34*	12.8 ± 1.41
25	5.12 ± 1.49	12.1 ± 1.11	15.6 ± 2.38*	24.8 ± 3.68*	14.8 ± 0.27
26	6.54 ± 1.40	12.6 ± 0.42	19.3 ± 3.06*	13.3 ± 1.12	24.3 ± 2.54*
27	5.81 ± 0.47	19.1 ± 0.76*	12.3 ± 0.65	25.8 ± 2.76	16.3 ± 2.24*
28	8.32 ± 0.91	9.02 ± 1.20	8.37 ± 1.31	12.0 ± 1.31	9.45 ± 0.91
29	7.77 ± 1.59	17.5 ± 0.38	14.9 ± 2.72	9.36 ± 1.28	24.1 ± 2.07*
30	4.57 ± 1.21	11.8 ± 2.17	16.9 ± 1.70*	7.98 ± 0.64	16.1 ± 3.95*
31	10.6 ± 0.52	5.22 ± 1.19	12.9 ± 1.74	9.81 ± 1.90	12.9 ± 2.90
32	12.7 ± 2.81	11.2 ± 2.00	15.9 ± 1.43	29.5 ± 2.38*	11.4 ± 0.31
33	7.69 ± 0.94	7.29 ± 1.44	12.9 ± 2.18	13.9 ± 0.46	11.7 ± 2.27
34	8.03 ± 0.78	9.46 ± 3.19	20.6 ± 4.15*	10.9 ± 1.65	20.3 ± 3.94*
35	7.87 ± 1.67	18.6 ± 2.33*	15.0 ± 1.17	19.1 ± 1.83*	10.4 ± 1.17
36	7.61 ± 1.67	12.3 ± 0.37	5.94 ± 0.93	11.2 ± 1.32	37.2 ± 0.83*
37	5.38 ± 0.61	12.0 ± 0.69	11.7 ± 1.45	20.2 ± 2.06*	37.2 ± 2.55*
38	7.09 ± 1.22	18.5 ± 2.27*	18.3 ± 3.99*	25.2 ± 1.64*	19.6 ± 1.97*
39	7.29 ± 1.66	7.42 ± 2.01	9.20 ± 1.08	17.3 ± 1.01*	11.3 ± 2.28
40	8.89 ± 1.28	19.6 ± 4.13	12.0 ± 1.35	17.1 ± 0.43	12.1 ± 0.45
41	5.82 ± 0.77	14.9 ± 3.96	9.07 ± 1.60	18.9 ± 1.87*	13.4 ± 1.35
42	7.34 ± 1.29	11.3 ± 2.39	11.7 ± 1.76	12.6 ± 0.70	15.7 ± 3.08
43	9.81 ± 1.31	15.1 ± 2.44	2.05 ± 0.38	12.4 ± 0.68	17.8 ± 3.35
44	9.00 ± 1.96	17.1 ± 2.73	15.9 ± 1.95	15.7 ± 1.85	21.7 ± 3.34*

The results expressed as fmol of ^{32}P-labeled duplex oligonucleotide incised by per milligram of protein during 1 h. Values represent mean ± S.E.M. ($n = 6$). Two-way ANOVA revealed that both time and neuroanatomical locus contributed significantly ($p < 0.0001$) to total variance; interaction between time and locus was also statistically significant ($p < 0.0001$). Asterisk (*) indicates significance of the differences against control after Bonferroni correction ($p < 0.05$).

returned to near control levels by 72 h. In caudate-putamen and in the ventral striatum (NAcb), the activity of OGG1 remained higher than control at 72 h. Collating both profiles of OGG1 and SOD responses in SN and VTA loci showed a high correlation between them ($r^2 = 0.9987$) (data not shown).

The SN, striatum (both dorsal and ventral) and locus ceruleus revealed a marked decrease in tyrosine hydroxylase (TH) immunoreactivity (image not shown). Unlike the SN, the site encompassing the locus ceruleus was able to maintain repair of oxidized DNA damage above control levels through 72 h (see Table 2, Loci # 1 and 3).

Examination of all other brain regions also revealed significant increases in OGG1 and SOD activity, a finding that was unexpected given that MPTP is considered to be selectively toxic for the dopaminergic nigro-striatal system, especially when given at a low dose. The extent of OGG1 elevation and the time-course varied across regions. In addition, asymmetry in the OGG1 response to MPTP was noted in some loci (see summary Tables 2 and 3 and Fig. 4). The greatest magnitude of change was seen late (72 h) in primary motor cortex which exhibited a six-fold increase (locus # 27, Table 1). The temporal pattern of change in hippocampal loci revealed early OGG1 and SOD activation followed by decline to control

Table 3
Distribution of SOD activity across the mouse brain following a single dose of MPTP (mg/kg, i.p.)

Locus #	Control	12 h	24 h	48 h	72 h
1	6.64 ± 0.67	12.93 ± 0.88*	13.36 ± 1.72*	6.81 ± 0.31	9.9 ± 0.25*
2	6.54 ± 0.42	9.41 ± 1.07	11.85 ± 2.22*	6.13 ± 0.34	10.57 ± 0.86*
3	7.08 ± 0.47	11.99 ± 1.21*	12.57 ± 2.45*	9 ± 0.24*	11.26 ± 1.23
4	6.76 ± 0.43	12.36 ± 1.81*	8.94 ± 0.67	6.17 ± 0.20	15.77 ± 0.36*
5	6.85 ± 0.39	12.21 ± 1.75*	14.59 ± 1.75*	6.02 ± 0.37	10.21 ± 0.46
6	6.62 ± 0.45	9.47 ± 1.03	13.83 ± 1.92*	6.57 ± 0.34	9.53 ± 0.56*
7	6.48 ± 0.37	10.5 ± 1.30	9.22 ± 0.73	5.99 ± 0.18	10.56 ± 0.33
8	7.02 ± 0.53	9.79 ± 1.75	15.53 ± 1.06*	6.71 ± 0.40	10.71 ± 0.28
9	6.63 ± 0.39	8.99 ± 1.25	14.94 ±0.75*	6.81 ± 0.36	12.02 ± 1.01*
10	6.77 ± 0.49	10.94 ± 1.82	8.33 ± 0.63	6.99 ± 0.31	14.77 ± 0.33*
11	6.54 ± 0.46	8.9 ± 0.61*	14.72 ± 1.17*	9.68 ± 0.53	5.56 ± 0.27
12	6.63 ± 0.48	10.78 ± 0.51	14.43 ± 1.54*	10.98 ± 0.27	8.63 ± 0.19
13	6.56 ± 0.44	10.56 ± 1.77	14.62 ± 2.58*	12.98 ± 0.14*	5.93 ± 0.29
14	6.52 ± 0.41	10.36 ± 1.00	13.16 ± 1.89*	23.46 ± 0.34*	5.74 ± 0.27
15	6.14 ± 0.51	11 ± 1.82*	14.02 ± 2.49*	14.25 ± 0.10*	5.31 ± 0.44
16	6.36 ± 0.40	10.3 ± 1.26	14.18 ± 1.84*	13.06 ± 0.30*	6.19 ± 0.29
17	7.06 ± 0.14	9.54 ± 1.51	12.66 ± 0.94*	6.81 ± 0.53	5.73 ± 0.44
18	6.9 ± 0.29	13.3 ± 0.96*	11.94 ± 1.37*	7.83 ± 0.77	5.71 ± 0.32
19	6.61 ± 0.47	8.98 ± 0.24	9.89 ± 1.79	6.24 ± 0.59	15.08 ± 0.41*
20	7.1 ± 0.46	10.84 ± 1.54	10.09 ± 1.97	6.19 ± 0.54	11.76 ± 1.14
21	6.64 ± 0.41	9.2 ± 1.72	13.42 ± 1.68*	17.86 ± 0.31*	5.92 ± 0.47
22	6.88 ± 0.27	9.82 ± 1.30	10.04 ± 1.60	16.81 ± 2.14*	9.8 ± 0.27
23	6.96 ± 0.30	9.46 ± 1.25	12.14 ± 2.40*	6.29 ± 0.19	14.45 ± 0.14*
24	7.23 ± 0.55	8.99 ± 1.11	13.54 ± 1.14*	15.7 ± 0.40*	8.49 ± 0.28
25	6.62 ± 0.28	9.07 ± 1.35	11.88 ± 1.76*	17.72 ± 0.59*	6.24 ± 0.71
26	7.25 ± 0.59	11.03 ± 2.03	9.84 ± 1.47	9.04 ± 0.98	10.8 ± 0.52
27	6.87 ± 0.73	13.31 ± 1.07*	10.06 ± 1.78	13.7 ± 0.43*	15.76 ± 1.19*
28	6.76 ± 0.28	10.65 ± 0.83	11.1 ± 1.36	5.84 ± 0.33	15.04 ± 1.08*
29	7.02 ± 0.56	11.02 ± 1.32	13.08 ± 1.83*	6.49 ± 0.27	5.46 ± 0.67
30	6.67 ± 0.56	9.28 ± 1.67	11.68 ± 1.73*	5.96 ± 0.37	13.69 ± 0.74*
31	6.92 ± 0.41	10.21 ± 1.75	12.45 ± 1.64*	6.27 ± 0.40	5.81 ± 0.10
32	14.56 ± 1.26	7.43 ± 0.41*	11.65 ± 1.01	19.26 ± 3.36*	5.87 ± 0.25*
33	6.76 ± 0.50	11.65 ± 1.44*	14.13 ± 0.24*	6.09 ± 0.40	5.87 ± 0.33
34	5.74 ± 0.38	7.54 ± 0.97	15.46 ± 0.33*	6.01 ± 0.56	15.95 ± 0.28*
35	6.83 ± 0.49	10.21 ± 1.32	12.46 ± 2.49*	8.29 ± 1.25	5.77 ± 0.24
36	6.2 ± 0.56	9.61 ± 1.22	10.18 ± 1.59	5.9 ± 0.32	14.94 ± 1.29*
37	6.64 ± 0.98	9.04 ± 1.10	10.37 ± 0.25	5.72 ± 0.37	17.99 ± 0.50*
38	6.82 ± 0.70	10.44 ± 1.91	10.11 ± 0.77	14.8 ± 1.35*	5.04 ± 0.57
39	6.77 ± 0.48	11.63 ± 1.99*	9.77 ± 0.86	13.77 ± 2.57*	5.95 ± 0.25
40	6 ± 0.44	10.75 ± 0.27*	11.32 ± 1.29*	14.39 ± 2.52*	5.59 ± 0.42
41	6.64 ± 0.55	9.1 ± 1.05	10.74 ± 0.46	14.59 ± 2.86*	5.7 ± 0.39
42	6.86 ± 1.00	9.52 ± 1.05	9.34 ± 0.05	6.15 ± 0.26	17.34 ± 0.76*
43	8.08 ± 0.42	10.58 ± 1.50	11.53 ± 0.79	6.12 ± 0.44	13.29 ± 0.42*
44	6.74 ± 0.64	8.79 ± 1.41	10.94 ± 0.44	5.77 ± 0.19	14.08 ± 0.51*

Values represent mean ± S.E.M. The SOD activity was calculated per milligram of protein. Two-way ANOVA revealed that both time and neuroanatomical locus contributed significantly ($p < 0.0001$) to total variance; interaction between time and locus was also statistically significant ($p < 0.0001$). Asterisk (*) indicates significance of the differences against control after Bonferroni correction ($p < 0.05$).

levels at 72 similar to that observed in SN (Fig. 5). Other regions such as those in cortical loci (Figs. 6 and 7), exhibited a late rise of OGG1 and SOD whereas loci in ponto-cerebellum had an early and sustained elevation of OGG1 up to 72 h. A biphasic temporal pattern of OGG1 and SOD activity was exhibited in posterior caudate-putamen (loci # 30, 34), in which the activities increased up to 24 h, dropped to slightly above baseline at 48 h and then increased again to reach significantly increased levels at 72 h (Figs. 3 and 5). A similar biphasic response was observed in SOD activities, but not OGG1, in cortical loci # 37, 42, 43, 44 and ponto-cerebellar loci # 1, 2 (Fig. 7).

Assessment of apoptosis using TUNEL staining revealed a large increase in apoptotic nuclei in the SN, but not in striatum or hippocampus, at 72 h (Fig. 8). The proportion of TUNEL-positive cells (ratio between green fluorescent cells and DAPI blue stained nucleus) was significantly increased at 72 h compared to control levels and levels at 12, 23 and 48 h. Apoptotic nuclei were rare at 12, 24 or 48 h. Concomitant with the marked degree of apoptosis that became evident in SN at 72 h, there was a large drop-off of anti-oxidative and DNA repair activity in this locus. Apparently the oxidative challenge elicited by MPTP was unable to be controlled by the vigorous increase in SOD and OGG1 activities in the SN.

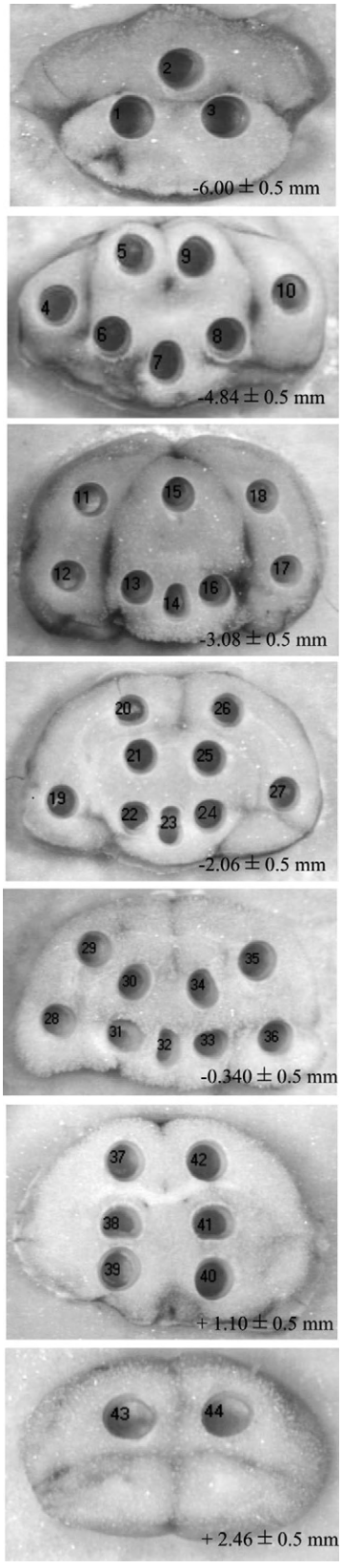

Fig. 1. Representative distribution and numbering system of sampled regions of brain. Photomicrographs of coronal sections (1 mm thick) after sampling of neuroanatomical regions. Each section includes the A-P position relative to Bregma (Paxinos and Franklin, 2001).

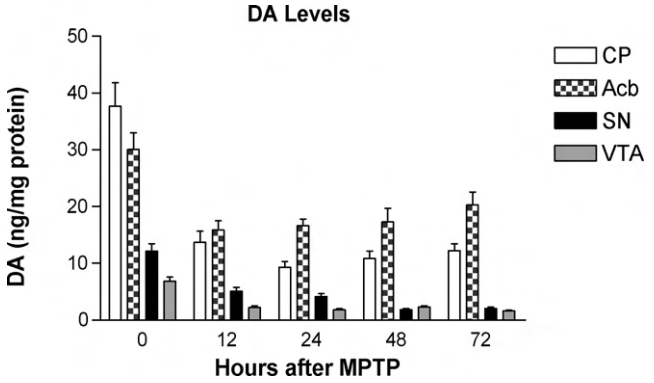

Fig. 2. Temporal profile of DA levels of micro-dissected loci of brain following an acute dose of MPTP. Mean of DA concentrations at all time points were significantly different from the control levels for each region ($p < 0.05$). Error bars = S.E.M. CP, caudate-putamen; Acb, nucleus accumbens; SN, substantia nigra; VTA, ventral tegmental area.

4. Discussion

This is the first study dedicated to mapping the distribution of OGG1 and SOD activities across 44 loci of mouse brain. The goal was to create a neuroanatomical map of the distribution of an important DNA repair enzyme. A second objective was to study the temporal course of DNA repair and SOD activities following administration of neurotoxicants that induce oxidative stress, starting with MPTP, well known to be selective for DA neurons of the nigral-striatal system. A single dose of MPTP elicited oxidative stress across all brain regions, resulting in time- and brain region-dependent changes in DNA repair and anti-oxidative responses. The transient widespread extension of oxidative stress beyond the nigro-striatal system should not be surprising since MPTP is a substrate for monoamine oxidase (MAO) which is distributed throughout the brain. Animal studies have indicated MAO-A is mainly, but not exclusively, located in brain neurons, while MAO-B is preferentially found in glia and astrocytes (Riederer et al., 1987). MAO enzymatic activity generates oxygen free radicals, which when unscavenged, results in lipid peroxidation, oxidation of proteins and DNA (Jenner and Olanow, 1996).

It is important to note that baseline DNA repair and SOD activities were unevenly distributed across brain, consistent with earlier studies on the distribution of oxidative DNA damage in six major structures of the brain (Cardozo-Pelaez et al., 1999, 2000). In these earlier studies, oxidative damage to DNA, indicated by levels of 8-hydroxy-2′-deoxyguanosine (oxo8dG), was measured in pons-medulla (PM), midbrain (MB), caudate/putamen (CP), hippocampus (HP), cerebellum (CB), and cerebral cortex (CX) of mice at ages 3, 18, and 34 months. Steady-state levels of oxo8dG increased significantly with age in MB, CP, and CB, but not in PM, HP, or CX. (Cardozo-Pelaez et al., 1999). These regional differences in basal levels of DNA damage were shown to be inversely correlated with the regional capacity to remove oxo8dG from DNA by the enzyme OGG1 (Cardozo-Pelaez et al., 2000).

In the present study, the distribution of OGG1 and SOD activities changed as a function of time and of neuroanatomical

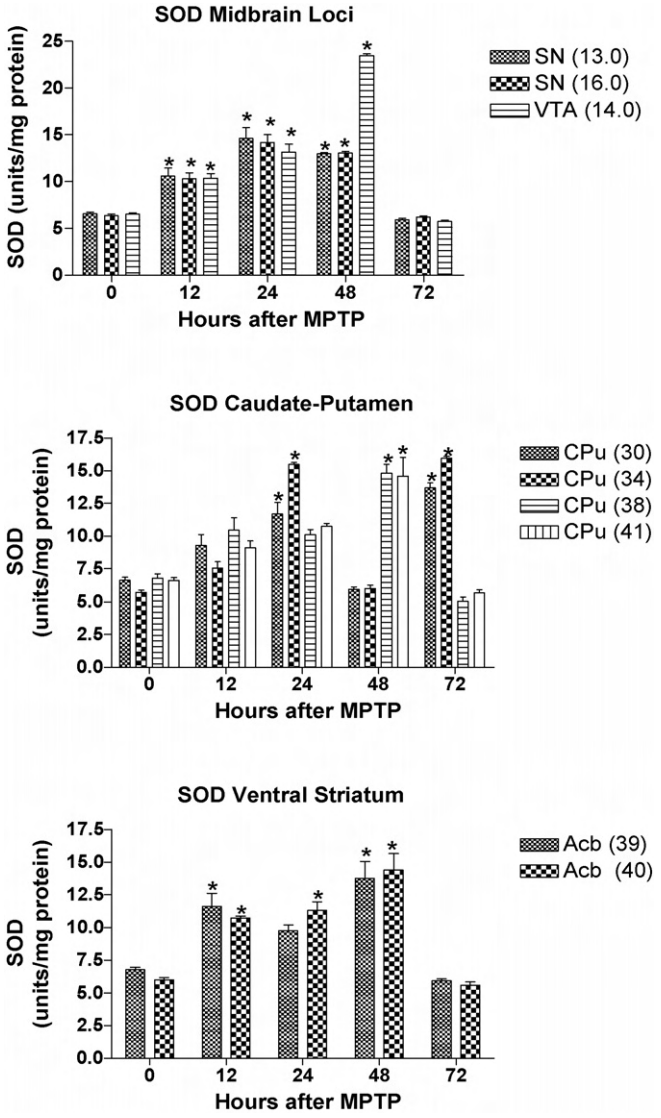

Fig. 3. Temporal profile of SOD activity in midbrain loci (upper panel), caudate-putamen (middle panel) and ventral striatum (lower panel). Neuroanatomical locus # is in parentheses in the key. Error bars = S.E.M. Asterisk (*) indicates statistically significant difference compared to activity at time 0 ($p < 0.05$).

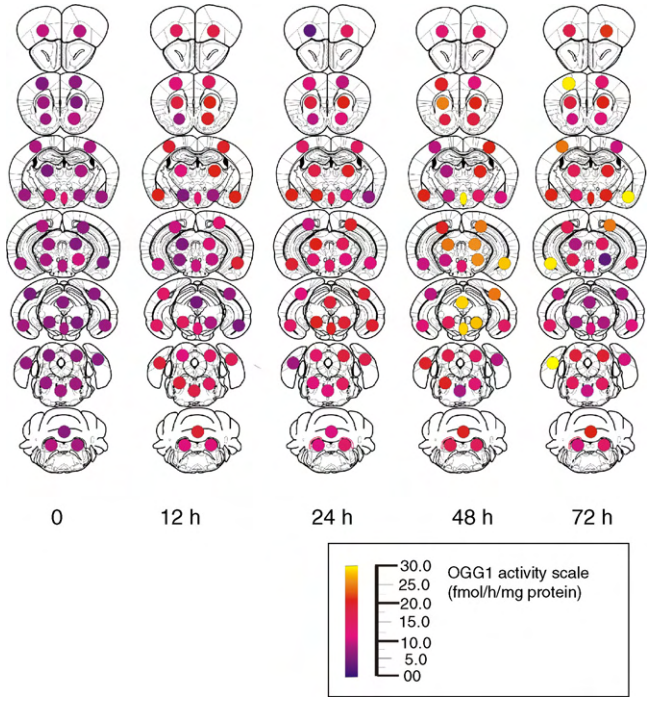

Fig. 4. Summary of temporal profiles of OGG1 activity across 44 brain loci following MPTP administration. Inset is the color key to the OGG1 activity scale. This image illustrates the summary data from Table 2.

locus following a single dose of MPTP. The SN, VTA and hippocampal loci exhibited an early rise in OGG1 and SOD followed by a significant drop to levels equal to or below control levels by 72 h. The significant drop in SN OGG1 and SOD at 72 h corresponded to the appearance of apoptotic nuclei in the SN. In contrast to these sites, many cortical loci exhibited small increases in OGG1 and SOD activities in the early response to MPTP peaking late at 72 h. Another pattern was exemplified by ponto-cerebellar loci (including locus ceruleus), where the increased OGG1 activity occurred early at 12 h and was maintained at a high level up to 72 h after MPTP. An unusual biphasic pattern of OGG1 and SOD activation was observed in loci in cerebral cortex and posterior caudate-putamen (loci # 30, 34). It is difficult to understand the basis for this unusual biphasic response in some loci. Possible explanations include differences in regional metabolism of MPTP, re-distribution of the active agent (MPP+) by injured nerve terminals and variation in the extent of glutamatergic (or other neurotransmitter) innervation of these regions. The magnitude of the increases in SOD activity across all regions of brain was similar to the changes in OGG1 activity, even though there was a weak correlation between OGG1 and SOD activities in the first 24 h following MPTP. The highest correlation between OGG1 and SOD activities was found in the SN. It can be inferred that the generation of superoxide anion and the oxidation of guanosine, signals for activation of SOD and OGG1 respectively, likely occurred in close temporal proximity at this site.

An interesting observation in this study was the asymmetry in distribution of OGG1 activity, both at baseline and following MPTP in some loci. It is known that the anatomy and functional layout of brain are organized asymmetrically, with hemispheric specializations for key aspects of language and motor function. Less well known is the fact that brain asymmetries extend to lateralized differences in maturational rates during development of the nervous system, in dendritic arborization, in rates of metabolism and functional activation (Toga and Thompson, 2003). Moreover, normal hemispheric differences in striatal dopamine levels, metabolites, release, uptake and receptors have been measured and related to rats' circling or rotational behavior, occurring either spontaneously at night or in response to systemically administered drugs (e.g., D-amphetamine, apomorphine) during the day (Glick et al., 1988). Both the regulation of micro-vascular flow and rates of metabolic activity (measured by PET scanning with fluoro-deoxyglucose

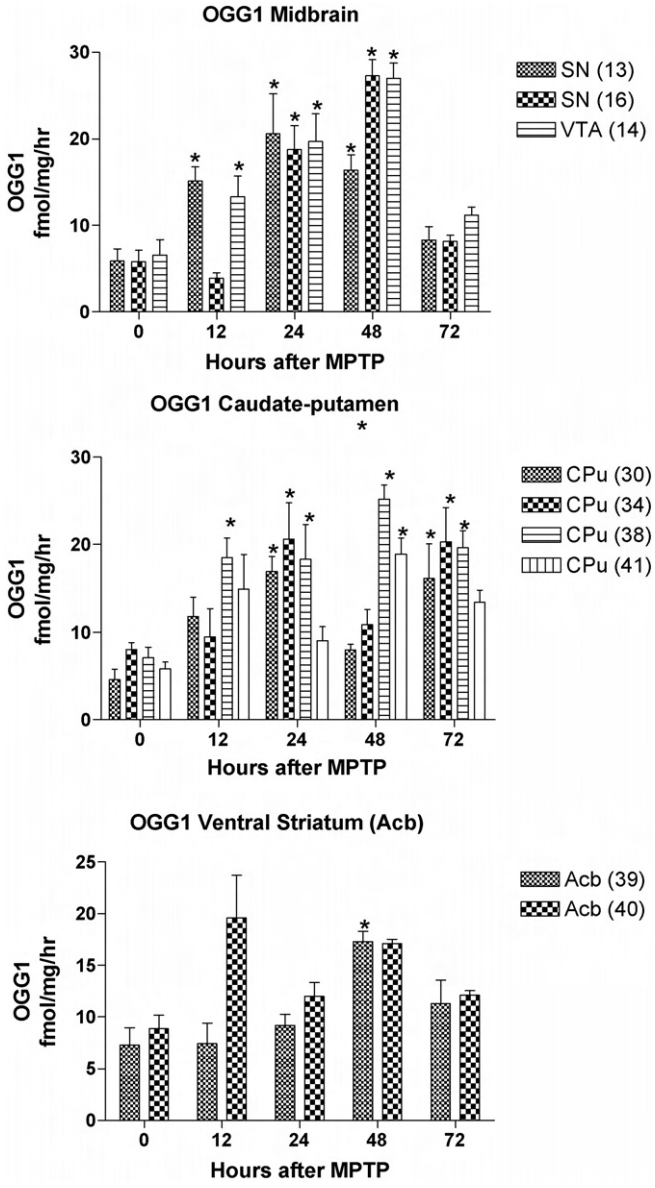

Fig. 5. Temporal profile of OGG1 activity in midbrain loci (upper panel), caudate-putamen (middle panel) and ventral striatum (lower panel). Neuroanatomical locus # is in parentheses in the key. Error bars = S.E.M. Asterisk (*) indicates statistically significant difference compared to activity at time 0 ($p < 0.05$).

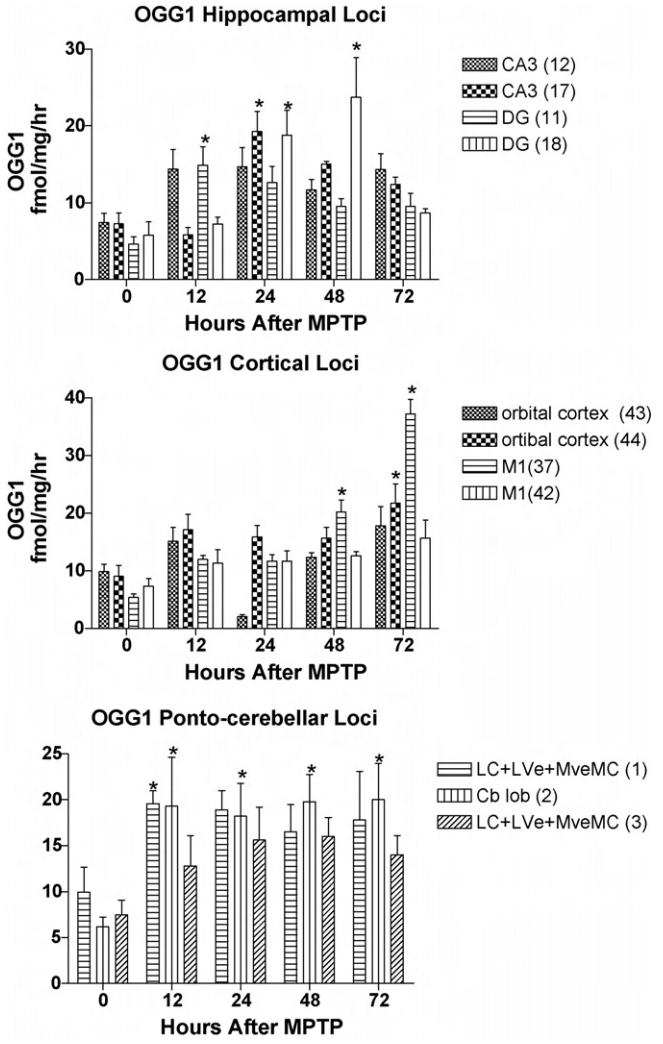

Fig. 6. Temporal profile of OGG1 activity in hippocampal loci (upper panel), cortical loci (middle panel) and ponto-cerebellar loci (lower panel). Neuroanatomical locus # is in parentheses in the key. Error bars = S.E.M. Asterisk (*) indicates statistically significant difference compared to activity at time 0 ($p < 0.05$).

uptake) have been shown to be asymmetric (Toga and Thompson, 2003). Therefore it should not be too surprising that OGG1 activities and the response to MPTP are not symmetrical.

Consistent with its known effects, a single dose of MPTP (20 mg/kg, i.p.) caused a rapid decrease of DA concentration in both the nigro-striatal system and the mesolimbic DA system (VTA–Nac). The depletion of DA occurred earlier in the DA terminal fields of the caudate-putamen and NAc than in the loci which house the cell bodies (SN and VTA). This result has been noted before and suggests that the initial injury occurs in DA terminals with a subsequent dying back phenomenon (Hornykiewicz, 1992). In addition to DA loss, TH immunoreactivity was markedly decreased in both the nigro-striatal and mesolimbic DA systems as well as in the locus ceruleus. The loss of TH in the SN was associated with a sharp rise at 72 h of apoptotic nuclei, suggesting that loss of TH in this locus was due to cell death and not to down-regulation of TH expression.

Research with other neurotoxicants, ochratoxin-A (OTA) and rubratoxin-B (RB), which share at least one mechanism of toxicity (e.g. interference with mitochondrial function), has revealed interesting differences from MPTP in the temporal and neuro-anatomical distribution of DNA repair. OTA, rather than increasing OGG1 like MPTP, produced a transient early depression of OGG1 activity in six brain regions, but with time there was an increase in OGG1 in all regions except for hippocampus, caudate/putamen and cerebral cortex (Sava et al., 2006). These are the brain regions that are most affected following an episode of hypoxia/ischemia (e.g. hippocampus, cerebral cortex and globus pallidus). From this profile of OGG1 reactivity, it may be inferred that OTA toxicity mimics the effects of global hypoxia on brain. Interestingly, OTA treatment

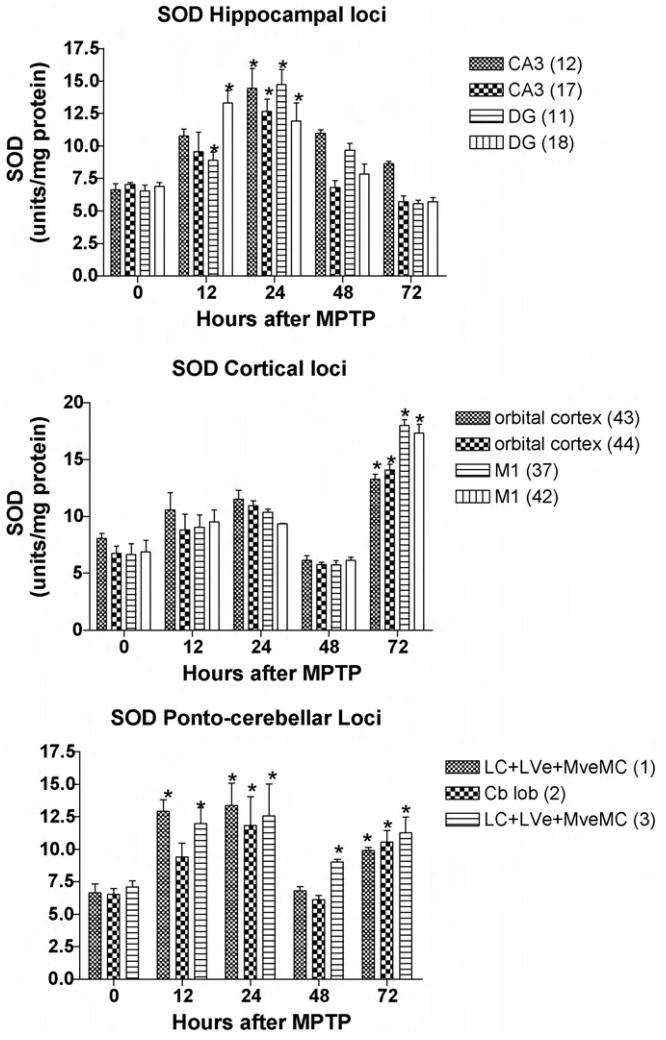

Fig. 7. Temporal profile of SOD activity in hippocampal loci (upper panel), cortical loci (middle panel) and ponto-cerebellar loci (lower panel). Neuroanatomical locus # is in parentheses in the key. Error bars = S.E.M. Asterisk (*) indicates statistically significant difference compared to activity at time 0 ($p < 0.05$).

also resulted in a modest decrease in striatal DA concentration without causing DA neuron cell death (Sava et al., 2006). Very likely, other actions of OTA in addition to its mitochondrial toxicity, contributed to the distinctive DNA repair profile (Sava et al., 2006). These effects were different from the acute effects of RB. Administration of a single dose of RB (5 mg/kg) resulted in significant upregulation of the DNA repair enzyme OGG1 in cerebellum, caudate/putamen and cortex but not in hippocampus, midbrain and pons/medulla at 24 h, in the presence of decreased or unchanged levels of lipid peroxidation in all regions (Sava et al., 2004). In fact, RB resulted in paradoxically less oxidative damage to both lipids and DNA; the level of lipid peroxidation in hippocampus, midbrain and pons/medulla was significantly less than that found in vehicle-treated controls. Similarly, RB did not increase oxidative DNA damage in any region of brain after the injection but tended to lower the degree of damage. These results were unexpected in light of the putative pro-oxidant effects of the mycotoxin, but were explained by the robust upregulation of anti-oxidative and DNA repair enzymes (Sava et al., 2004). However, the study with RB did not examine effects beyond 24 h and did not assay striatal levels of DA, so these effects cannot be compared to those produced by OTA or MPTP.

The value of assessing effects of toxicants on DNA repair systems is based on the hypothesis that vulnerability of neuronal populations can be inferred from the pattern of DNA repair elicited by a specific toxin. However, can differences in vulnerability to toxicants of sub-populations of DA neurons be explained by intrinsic differences in DNA repair? Mesencephalic DA neurons (A9) of the nigro-striatal system are reported to be more vulnerable to the oxidative stress induced by MPTP and other mitochondrial toxicants (like rotenone) than their neighbors in the A10 regions (meso-limbic, meso-cortical DA system). In the case of the neurotoxin MPP+, the relative vulnerability of the SN (pars compacta) has been attributed to their higher density of DA transporters in their terminal fields in the striatum and the relative invulnerability of VTA DA neurons has been attributed to their content of calcium-binding protein, calbindin (Liang et al., 1996). But this explanation may not be applicable in understanding the selective vulnerability of SN DA neurons exposed to rotenone (Betarbet et al., 2000). Unlike MPP+, this mitochondrial toxin is not selectively accumulated by DA neurons alone. Although it has been suggested that the selective toxicity of rotenone to DA neurons of the SN is related to the high density of microglia in this region of the midbrain (Gao et al., 2002; Sherer et al., 2003), it is not clear why DA VTA neurons are more resistant to rotenone than nigral DA neurons.

Recently, analysis of the transcriptional profiles of gene expression in DA neurons from the mesencephalic A9 region (s. nigra) and A10 (mesolimic, mesocortical) has found interesting intrinsic differences between the two populations of DA neurons (Chung et al., 2005). Using a combination of laser capture micro-dissection to harvest the specific DA sub-populations, followed by a DNA micro-array study, the authors identified 42 genes that were relatively elevated in A9 DA neurons and 61 genes elevated in A10 DA neurons. Further studies implicated several molecules in determining relative vulnerability to the active metabolite of the DA neurotoxin MPTP, MPP+ (Chung et al., 2005). A molecule termed GIRK2 (G-protein coupled inwardly rectifying K channel 2) was shown to increase toxicity to MPP+ in the A9 DA neurons. Blocking the molecule ANT2 (adenine nucleotide translocator 2) decreased vulnerability to MPP+ in both A9 and A10 DA neurons (Chung et al., 2005). GIRK2 and ANT-2 may render A9 DA neurons more vulnerable because of their pathophysiological actions on the membrane potential and on the mitochondrial permeability transition, respectively. Interestingly, one of the 61 genes differentially expressed in A10 DA neurons is *single strand DNA binding protein 3* (mRNA accession # AV295012). Though the authors did not elaborate on its potential role in conferring resistance to MPP+, it is worth pointing out that replication protein A [RPA; also known as replication factor A (RFA) and human single-stranded DNA-binding protein] is a single-stranded DNA-binding protein that

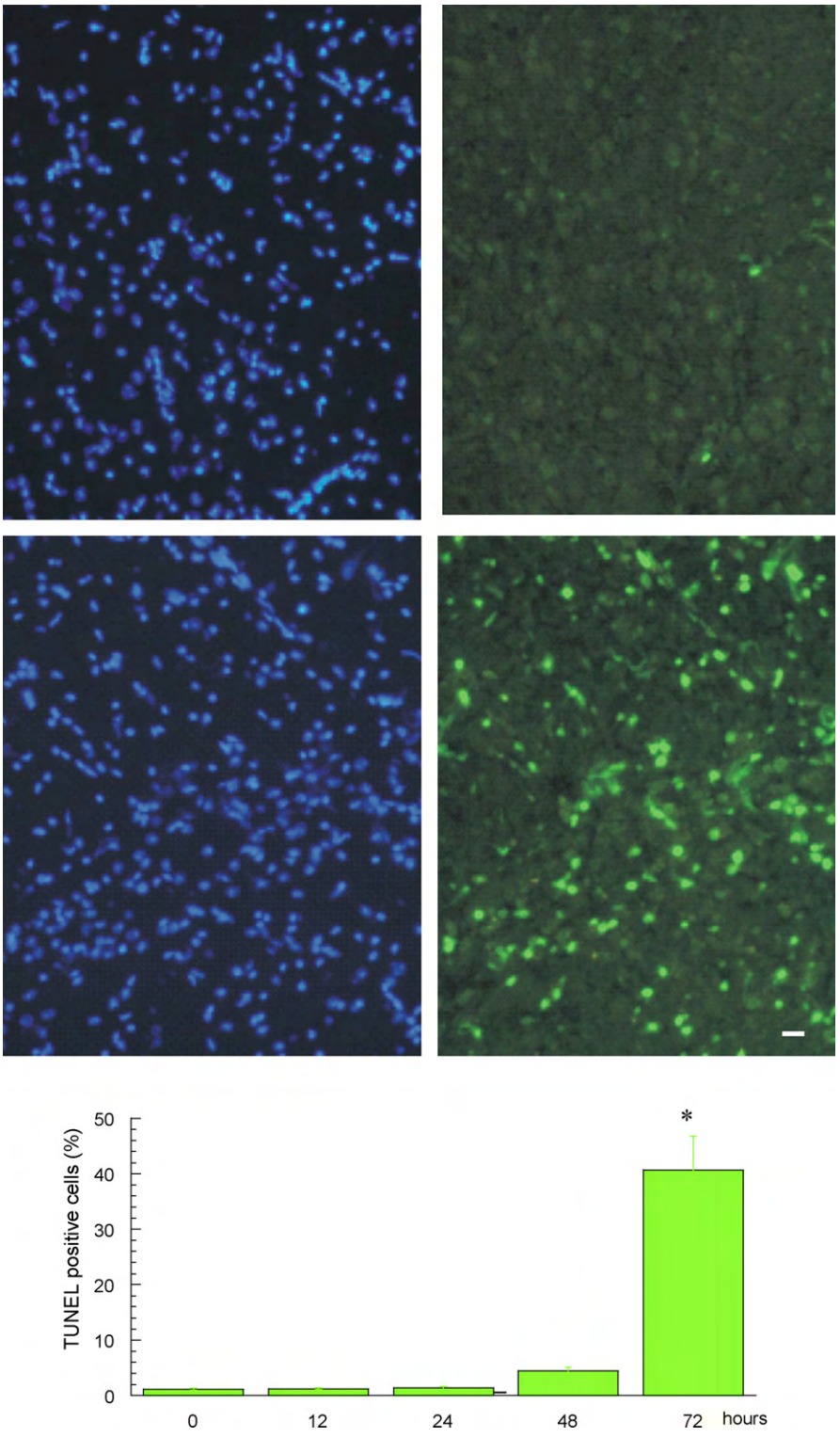

Fig. 8. Representative fluorescence photomicrographs of TUNEL immunoreactivity in substantia nigra of mouse brain exposed to single dose of MPTP (20 mg/kg, i.p.). Left panels represent DAPI stained nuclei and right panels depict TUNEL-positive (apoptotic) cells. Upper panels represent control and lower ones were obtained from animals 72 h after MPTP (scale bar = 20 μm). Graph in lower panel: the *Y*-axis depicts the percentage of TUNEL-positive cells in the substantia nigra (expressed as percent of total number of DAPI + nuclei) following a single dose of MPTP (20 mg/kg, i.p.). The mean percentage (±S.E.M.) of apoptotic cells in SN was determined from the average of the ratio of TUNEL+/DAPI + nuclei in three SN sections obtained from three animals in each experimental group (control 24, 48 and 72 h). Error bars = 1 SEM. One-way ANOVA followed by *t*-tests with Bonferroni correction for multiple comparisons showed a significant increase in TUNEL-positive cells at 72 h compared to each other time point: 0, 12, 24, and 48 h ($^{*}p < 0.001$).

is required for multiple processes in eukaryotic DNA metabolism including DNA repair and recombination (Wold, 1997). Hence, it is possible that differences in DNA repair capacity, in combination with other factors, may contribute to A9 DA neuronal vulnerability to agents (endogenous or exogenous) that increase oxidative stress.

An association between deficient DNA repair and PD, as well as with other neurodegenerative diseases such as Alzheimer's disease, amyotrophic lateral sclerois (ALS) and Huntington's disease (HD) has been previously reported (Lovell et al., 2000; Mazzarello et al., 1992). Fibroblast and lymphoblastoid lines from patients with PD and AD were shown to be hypersensitive to X-rays and this was inferred to be a consequence of diminished DNA repair (Robbins et al., 1985). It is important to point out that early studies focused on DNA repair that occurs in replicating cells and relied on measures of survival of cells, ^{3}H-thymidine incorporation, or breaks in chromosomes, following exposure to ionizing radiation or UV light. The accuracy of overall DNA replication during proliferation is assured by several mechanisms that include nucleotide selection and exonuclease proof-reading activity with DNA polymerases and post-replicative methylation-instructed mismatch repair system (Krokan et al., 1997). However, neurons of adult brain are not proliferative, and post-mitotic cells contain lower levels of DNA repair enzymes and repair DNA slower than proliferating cells (Alexander, 1967; Korr and Schultz, 1989; Stedeford et al., 2001) Repair of oxo^{6}-alkylguanine lesions as well as the damage from UV and ionizing radiations is slower in neurons than in other cultured cell types (Mazzarello et al., 1992). The decline in DNA repair capacity of post-mitotic cells may be related to the development and achievement of their terminal differentiated state. Post-mitotic cells reduce or ''switch-off'' activity levels of some enzymes and proteins directly or indirectly involved in DNA replication. Aging brain tissue has been reported to have diminished capacity to upregulate DNA repair enzymes when challenged with an oxidative stress such as hyperoxia (Edwards et al., 1998). Not all enzymes involved in neuronal DNA synthesis are switched off and some maintain constant activity levels during the life span of the neuron. For example, DNA polymerase-β is responsible for the whole nuclear DNA polymerase activity in adult neurons.

An important aspect of the DNA repair response involved in the demise of DA neurons has been illustrated by a study using transgenic mice lacking the gene for poly(ADP-ribose) polymerase-1 (PARP-1) (Mandir et al., 1999). PARP-1 catalyzes the attachment of ADP ribose units from NAD+ to nuclear proteins after DNA damage. Owing to its ability to bind and be activated by DNA strand breaks, PARP-1 and DNA-dependent protein kinase have long been proposed as DNA damage ''sensors''. Even though these proteins are not considered to be activators of global DNA damage response, upregulation of PARP-1 is clearly involved in the early response to DNA damage. MPTP injections have been shown to activate PARP-1 exclusively in vulnerable dopamine containing neurons of the substantia nigra (Mandir et al., 1999). Animals lacking the gene for PARP-1 were dramatically spared from MPTP neurotoxicity (Mandir et al., 1999). Neuroprotection against MPTP toxicity was also achieved by treatment of mice with PARP-1 inhibitors (Cosi and Marien, 1999). Since, MPTP caused region- and time-dependent changes in levels of NAD+ and ATP in the brain in vivo, it has been suggested that the demise of neurons mediated by PARP-1 is a function of energy depletion. However, the DNA damage response is a complex network involving sensors of DNA damage (e.g. PARP-1), transducers of DNA damage (e.g. ataxia teleangiectasis mutated gene, ATM), and the effectors of DNA repair (e.g., base excision repair ''BER'', and nucleotide excision repair ''NER''). The simplest type of DNA repair removes the damaged base directly, e.g. dealkylation, by a one-step mechanism. Most lesions of DNA are repaired by the much more complex recombination repair or excision repair systems. The latter includes nucleotide excision repair (NER), mismatch repair and base excision repair (BER).

In summary, MPTP was shown to elicit changes in the DNA repair enzyme OGG1 throughout the brain, but only a few regions were unable to maintain repair activity through 72 h. It was postulated that inability to repair oxidative DNA damage is an important factor in determination of neuronal vulnerability to endogenous or exogenous oxidative stressors. Although the evidence partially supports this hypothesis, it is not clear why VTA and hippocampus, regions of brain that do not suffer permanent damage from MPTP, also exhibited an upregulation followed by decline at 72 h in OGG1 and SOD activities. One explanation is that these regions will likely undergo degenerative changes at higher doses of MPTP. Another possibility is that the micro-punch technique employed here cannot assess the behavior of specific neurons in response to the challenge. The harvested samples contained heterogeneous mixtures of cells that include various neuronal phenotypes, astrocytes and very likely, reactive microglia. Although the micro-dissected tissue samples were adequate for profiling enzymatic activities across brain tissue, they are inadequate to supply a satisfactory explanation for the selective vulnerability of DA neurons of the SN.

In light of the observations that oxidative DNA damage (oxo8dG) accumulates in mitochondrial DNA in a OGG1 knockout mouse (de Souza-Pinto et al., 2001) and that alternative repair pathways function to minimize the effects of an increased load of oxo8dG (Klungland et al., 1999), it will be important to expand the study of OGG1 to include expression of other DNA repair genes, especially those involved in maintaining mitochondrial DNA integrity. Future studies will assess a battery of DNA repair genes, including mitochondrial DNA repair genes, in specific neurons from multiple brain loci harvested by the laser capture micro-dissection technique as described in a recent study (Chung et al., 2005).

Acknowledgements

Supported by a Grant from US Army Med Research and Materiel Command (DAMD #17-03-0501), VA Merit Review Grant and the Helen E. Ellis PD Research fund.

References

Alam ZI, Jenner A, Daniel SE, Lees AJ, Cairns N, Marsden CD, et al. Oxidative DNA damage in the parkinsonian brain: an apparent selective increase in 8-hydroxyguanine levels in substantia nigra. J Neurochem 1997;69:1196–203.

Alexander P. The role of DNA lesions in processes leading to aging in mice. Symp Soc Exp Biol 1967;21:29–50.

Betarbet R, Sherer TB, MacKenzie G, Garcia-Osuna M, Panov AV, Greenamyre T. Chronic systemic pesticide exposure reproduces features of Parkinson's disease. Nat Neurosci 2000;3:1301–6.

Cardozo-Pelaez F, Song S, Parthasarathy A, Hazzi C, Naidu K, Sanchez-Ramos J. Oxidative DNA damage in the aging mouse brain. Mov Disorders 1999;14:972–80.

Cardozo-Pelaez F, Brooks PJ, Stedeford T, Song S, Sanchez-Ramos J. DNA damage, repair, and antioxidant systems in brain regions: a correlative study. Free Radic Biol Med 2000;28:779–85.

Cardozo-Pelaez F, Stedeford TJ, Brooks PJ, Song S, Sanchez-Ramos JR. Effects of diethylmaleate on DNA damage and repair in the mouse brain. Free Radic Biol Med 2002;33:292–8.

Chung CY, Seo H, Sonntag KC, Brooks A, Lin L, Isacson O. Cell type-specific gene expression of midbrain dopaminergic neurons reveals molecules involved in their vulnerability and protection. Hum Mol Genet 2005; 14:1709–25.

Cosi C, Marien M. Implication of poly(ADP-ribose) polymerase (PARP) in neurodegeneration and brain energy metabolism decreases in mouse brain NAD+ and ATP caused by MPTP are prevented by the PARP inhibitor benzamide. Ann NY Acad Sci 1999;890:227–39.

de Souza-Pinto NC, Eide L, Hogue BA, Thybo T, Stevnsner T, Seeberg E, et al. Repair of 8-oxodeoxyguanosine lesions in mitochondrial DNA depends on the oxoguanine DNA glycosylase (OGG1) gene and 8-oxoguanine accumulates in the mitochondrial DNA of OGG1-defective mice. Cancer Res 2001;61:5378–81.

Edwards M, Rassin DK, Izumi T, Mitra S, Perez-Polo JR. APE/Ref-1 responses to oxidative stress in aged rats. J Neurosci Res 1998;54:635–8.

Elstner EF, Heupel A. Inhibition of nitrite formation from hydroxyl-ammonium chloride: a simple assay for superoxide dismutase. Anal Biochem 1976; 70:616–20.

Fraga C, Shigenaga M, Park J, Degan P, 'Ames B. Oxidative damage to DNA during aging: 8-hydroxy-2′-deoxyguanosine in rat organ DNA and urine. PNAS 1990;87:4533–7.

Fukae J, Takanashi M, Kubo S, Nishioka K, Nakabeppu Y, Mori H, et al. Expression of 8-oxoguanine DNA glycosylase (OGG1) in Parkinson's disease and related neurodegenerative disorders. Acta Neuropathol (Berl) 2005;109:256–62.

Gao HM, Hong JS, Zhang W, Liu B. Distinct role for microglia in rotenone-induced degeneration of dopaminergic neurons. J Neurosci 2002;22:782–90.

German D, Nelson E, Liang C, Speciale S, Sinton C, Sonsalla P. The Neurotoxin MPTP causes degeneration of specific nucleus A8, A9 and A10 dopaminergic neurons in the mouse. Neurodegeneration 1996;5:229–312.

Glick SD, Carlson JN, Baird JL, Maisonneuve IM, Bullock AE. Basal and amphetamine-induced asymmetries in striatal dopamine release and metabolism: bilateral in vivo microdialysis in normal rats.. Brain Res 1988;473:161–4.

Hornykiewicz O. The primary site of dopamine neuron damage in Parkinson's disease: substantia nigra or striatum? Mov Disorders 1992;7:288–91.

Jenner P, Olanow CW. Oxidative stress and the pathogenesis of Parkinson's disease. Neurology 1996;47:S161–70.

Klungland A, Rosewell I, Hollenbach S, Larsen E, Daly G, Epe B, et al. Accumulation of premutagenic DNA lesions in mice defective in removal of oxidative base damage. Proc Natl Acad Sci USA 1999;96:13300–5.

Korr H, Schultz B. Unscheduled DNA synthesis in various types of cells of the mouse brain in vivo.. Exp Brain Res 1989;573–8.

Krokan HE, Standal R, Slupphaug G. DNA glycosylases in the base excision repair of DNA. Biochem J 1997;325:1–16.

Liang C, Sinton C, Sonsalla P, German D. Midbrain dopaminergic neurons in the mouse that contain calbindin-D 28k exhibit reduced vulnerability to MPTP-induced neurodegeneration. Neurodegeneration 1996;5:313–8.

Lovell MA, Xie C, Markesbery WR. Decreased base excision repair and increased helicase activity in Alzheimer's disease brain.. Brain Res 2000;855:116–23.

Mandir AS, Przedborski S, Jackson-Lewis V, Wang Z-Q, Simbulan-Rosenthal CM, Smulson ME, et al. Poly(ADP-ribose) polymerase activation mediates 1-methyl-4-phenyl-1,2,3,6-tetrahydropyridine (MPTP)-induced parkinsonism. PNAS 1999;96:5774–9.

Mazzarello P, Poloni M, Spadari S, Focher F. DNA repair mechanisms in neurological diseases: facts and hypotheses. J Neurol Sci 1992;112:4–14.

Mecocci P, MacGarvey U, Kaufman AE, Koontz D, Shoffner JM, Wallace DC, et al. Oxidative damage to mitochondrial DNA shows marked age-dependent increases in human brain. Ann Neurol 1993;34:609–16.

Paxinos G, Franklin KBJ. The Mouse Brain in Stereotaxic Coordinates. San Diego, CA: Academic Press; 2001.

Riederer P, Konradi C, Schay V, Kienzl E, Birkmayer G, Danielczyk W, et al. Localization of MAO-A and MAO-B in human brain: a step in understanding the therapeutic action of L-deprenyl. Adv Neurol 1987;45:111–8.

Robbins JH, Otsuka F, Tarone RE, et al. Parkinson's disease and Alzheimer's disease: hypersensitivity to X-rays in culture cell lines. J Neurol Neurosurg Psychiatry 1985;48:916–23.

Sanchez Ramos J, Overvik E, Ames BN. A marker of oxyradical-mediated DNA damage (oxo8dG) is increased in nigro-striatum of Parkinson's disease brain. Neurodegeneration (Exp Neurol) 1994;3:197–204.

Sava V, Mosquera D, Song S, Stedeford T, Calero K, Cardozo-Pelaez F, et al. Rubratoxin B elicits antioxidative and DNA repair responses in mouse brain. Gene Expr 2004;11:211–9.

Sava V, Reunova O, Velasquez A, Harbison R, Sanchez-Ramos J. Acute neurotoxic effects of the fungal metabolite ochratoxin-A. Neurotoxicology 2006;27:82–92.

Sherer TB, Betarbet R, Kim JH, Greenamyre JT. Selective microglial activation in the rat rotenone model of Parkinson's disease. Neurosci Lett 2003;341:87–90.

Smith PK, Krohn RI, Hermanson GT, Mallia AK, Gartner FH, Provenzano MD, et al. Measurement of protein using bicinchoninic acid. Anal Biochem 1985;150:76–85.

Stedeford T, Cardozo-Pelaez F, Nemeth N, Song S, Harbison RD, Sanchez-Ramos JR. Effects of dieldrin on DNA repair in PC12 cells. Free Radic Biol Med 2001;31:1272–8.

Toga AW, Thompson PM. Mapping brain asymmetry. Nat Rev Neurosci 2003;4:37–48.

Wold MS. Replication protein A: a heterotrimeric single-stranded DNA-binding protein required for eukaryotic DNA metabolism. Ann Rev Biochem 1997;66:61–92.

Dr. Ernest Hodgson,
Department of Toxicology
Box 7633,
NC State University
Raleigh, NC 27695

December 22, 2006

Dear Dr. Hodgson:

Enclosed is a manuscript (3 copies and disk) of original research entitled “Dieldrin Elicits a Widespread DNA Repair and Anti-Oxidative Response in Mouse Brain”.

We believe your journal is appropriate for the topic and your readership will appreciate our original findings.

Suggested reviewers include:

Michael A. Collins, PhD
Loyola University Medical School, Chicago, IL
Email: mcollin@lumc.edu

Alexander Storch, MD
Department of Neurology, Technical University of Dresden, Dresden, Germany
alexander.storch@neuro.med.tu-dresden.de

A.G. Kantahsamy, PhD
Department of Biomedical Sciences, Iowa State University, Ames, IA
akanthas@iastate.edu

Sincerely,

Juan Sanchez-Ramos, PhD, MD
Dept of Neurology (MDC 55)
University of South Florida
12901 Bruce B. Downs Blvd
Tampa, FL 33647
jsramos@hsc.usf.edu
phone: 813974-5841

Submitted to Journal of Biochemical and Molecular Toxicology Jan 2007

DIELDRIN ELICITS A WIDESPREAD DNA REPAIR AND ANTI-OXIDATIVE RESPONSE IN MOUSE BRAIN

Vasyl Sava[1], Adriana Velasquez[1], Shijie Song[1, 2], Juan Sanchez-Ramos[1, 2]

University of South Florida[1]
Department of Neurology
12901 Bruce B. Downs Blvd
Tampa, Florida 33612
and
James Haley VA Hospital Research Service[2]
Tampa, Florida

Correspondent
J. Sanchez-Ramos, PhD, MD
Dept of Neurology (MDC55
University of South Florida
12901 Bruce B. Downs Blvd
Tampa, FL 33612
Email: jsramos@hsc.usf.edu

ABSTRACT

Dieldrin is an organochlorine pesticide implicated as a potential etiological agent for Parkinson's Disease (PD) or a PD-like syndrome. The present study was designed to test the hypothesis that a weak DNA repair response to dieldrin by nigro-striatal dopaminergic (DA) neurons results in depletion of striatal DA. The activity of the mammalian base excision repair enzyme oxyguanosine glycosylase (Ogg1) was utilized as the index of DNA repair. Other measures of oxidative stress were also studied, including the regional distribution of lipid peroxidation and superoxide dismutase (SOD) activity. The effects of acute and slow infusion of dieldrin on striatal DA levels were biphasic with a transient initial depression followed by increases beyond normal steady-state levels. Dieldrin administration caused a global oxidative stress evidenced by increased levels of lipid peroxidation in all brain regions, an effect consistent with its capacity to affect mitochondrial bioenergetics. Dieldrin also elicited a strong anti-oxidative and DNA repair responses across the entire mouse brain. Although mitochondrial SOD was not as increased in midbrain as it was in other regions following a cumulative dose of 24 mg/kg, this response, along with the robust DNA repair response, appeared to be sufficient to protect potentially vulnerable DA neurons from cytotoxicity. However, the long-term consequences of chronic dieldrin exposure remain to be studied, especially in light of the concept of "slow excitotoxicity" which postulates that even a mild bioenergetic compromise can over time result in the demise of neurons.

Running Title: *Dieldrin Elicits DNA Repair Response*

Key words: dieldrin, oxidative stress, DNA repair, oxyguanosine glycosylase, superoxide dismutase, brain

INTRODUCTION

Dieldrin, an organochlorine pesticide, has several molecular characteristics that make it a potential etiological agent for Parkinson's Disease. The half life of dieldrin in soil is approximately 5 years(1). This persistence, combined with high lipid solubility, provides the necessary conditions for dieldrin to bioconcentrate and biomagnify in organisms (2-4). Dieldrin appears to be retained for life in lipid-rich tissue (1) and has been measured in human brain (5, 6). It was found at high concentrations in caudate nucleus from post-mortem brain of idiopathic Parkinson's Disease (IPD) cases (7) . Dieldrin has toxic effects for dopaminergic (DA) and monoaminergic neurons in many species, both *in vitro* and *in vivo* (8-12). Like rotenone and the dopaminergic neurotoxin 1-methyl-4-phenyl-pyridinium (MPP^+), dieldrin interferes with mitochondrial oxidative phosphorylation (13-18). Insights derived from studies of 1-methyl-4-phenyl-1,2,3,6-tetrahydropyridine (MPTP) led to the observation that mitochondrial function appears to be compromised in brain and peripheral tissues from PD patients (19-22).

The increased vulnerability of DA neurons to oxidative stress induced by mitochondrial toxicants is not completely understood. These neurons have a combination of factors that are said to make them exquisitely sensitive to bioenergetic compromise (23). DA neurons have a high metabolic rate dependent exclusively on oxidative phosphorylation and high concentrations of metals, especially forms of iron that catalyze oxyradical processes, are found in the substantia nigra (SN). The metabolism of the DA molecule by monoamine oxidase (MAO) generates oxyradicals and the DA neurons are innervated by glutamanergic neurons that contribute to "slow" excitotoxicity (23, 24). However, the relative resistance of other DA neurons that reside nearby, such as those in the ventral tegmental area (VTA), is not well understood. In the case of the neurotoxin MPP+, the relative vulnerability has been attributed to their higher density of DA transporters, which are responsible for the selective uptake of MPP+ into the cells. But this explanation cannot be applied towards understanding the selective vulnerability of substantia nigra (SN) DA neurons exposed to rotenone (18). Unlike MPP+, this mitochondrial toxin is not selectively accumulated by DA neurons of the SN alone. Another hypothesis has been put forth that suggests a diminished capacity to repair oxidative DNA damage may underlie the vulnerability of DA neurons (25, 26). Deficits in DNA repair have long been postulated to play a role in several neurodegenerative diseases including Alzheimer's Disease, Parkinson's Disease and amyotrophic lateral sclerosis (ALS) (27, 28)

The present study was designed to test the hypothesis that the DNA repair response to dieldrin is a determinant of the vulnerability of DA neurons of the nigro-striatal system. The activity of the mammalian base excision repair enzyme oxyguanosine glycosylase (Ogg1) was utilized as the index of DNA repair. Other measures of oxidative stress were also studied, including the regional distribution of lipid peroxidation and superoxide dismutase (SOD) activity. The primary objectives of the study were to determine the effects of acute and slow infusion of dieldrin on a) DA and its metabolites in the striatum and b) to measure the regional distribution of the brain's DNA repair response and parameters of oxidative stress. Secondary objectives were to note observable changes in motor behavior and to measure whole body tremor elicited by dieldrin administration.

MATERIALS AND METHODS

Materials

Dieldrin (1,2,3,4,10,10-Hexachloro-6,7-Epoxy-1,4,4a,5,6,7,8,8a, octahydro-1,4,5,8-dimethanonaphthalene) was purchased from Sigma-Aldrich Co. (St. Louis, MO) and dissolved in corn oil prior to injection or infusion via ALZET osmotic pumps, model 1002 with release rate of 0.25 µL/hr over the course of 2 weeks (Durect, Cupertino, CA). Protease inhibitors and DNA glycosylase were from Boehringer Mannheim (Indianapolis, IN, USA). ^{32}P-ATP was from NEN Life Science Products (Wilmington, DE). All other chemicals were purchased from Sigma-Aldrich Co.

Animals

The animal protocol used in this study was approved by the University of South Florida IUCAC committee. The protocol was also reviewed and approved by the Division of Comparative Medicine of the University, which is fully accredited by AAALAC International and managed in accordance with the Animal Welfare Regulations, the PHS Policy, the FDA Good Laboratory Practices, and the IACUC's Policies. Male Swiss ICR mice (22 ± 2 g) were obtained from Jackson Laboratories (Bar Harbor, ME). They were housed five per cage at the temperature of 21 ± 2 °C with 12 light/dark cycle and free access to food and water. For acute administration studies, animals were injected with either dieldrin dissolved in corn oil or vehicle. After injection with dieldrin or vehicle, mice were observed for changes in spontaneous motor behavior three times each day until euthanasia. The response to handling was also noted. In particular, evidence for toxic effects such as clasping of limbs in response to being held by the tail was to be recorded. Groups of mice were euthanatized with CO_2 at 6, 24, and 72 hrs after injection with dieldrin or vehicle. The brains were removed and immediately dissected on ice. For chronic

infusion of dieldrin, 6 groups of mice containing 6-8 mice per group were implanted with ALZET osmotic pumps. Each group of mice received different cumulative doses of dieldrin (vehicle, 3, 6, 12, 24, 48 mg/kg) delivered over 2 weeks. Animals were euthanatized after 2 weeks.

Tremor Measurements and Analysis

Whole body tremor was recorded for each individual mouse (at one and two weeks after initiation of slow infusion of dieldrin or vehicle infusion) with an accelerometer (Catsys, Ltd, Denmark) mounted on the base of a clear polyethylene chamber (15 X 15 X 12 cm). Each test recording was of 60 sec duration. Data was analyzed using Catsys software, which includes Fast Fourier Transformation to yield a power spectrum function. Parameters derived from this function include a) total intensity of the tremor (m/s^2) and b) distribution of the relative intensity at each frequency. Data from groups of mice was analyzed to obtain a relative intensity at across the frequency spectrum (1-15 Hz). Analysis of the data included ANOVA, followed by t-tests with correction for multiple comparisons.

Isolation of brain regions

Brains were separated into 8 regions under a dissecting stereo-microscope in the following order. The cerebellar peduncles were cut first and cerebellum (CB) was removed. The pons (PONS) and medulla (MD) were separated by cutting the ponto-medullary junction. In some experiments the combined samples of pons and medulla (PM) were employed to provide necessary amount of tissue. The ventral and dorsal parts of midbrain (MB) were dissected at the level of the caudal end of the cerebral peduncles. Cerebral hemispheres were opened with a sagittal cut. Then caudate/putamen (CP) was isolated, followed by thalamus/hypothalamus (T/H) and hippocampus (HP). Finally, cerebral cortex (CX) was harvested and all the samples were kept frozen at –70 °C until assayed

Measurement of DA and metabolites

HPLC with electrochemical detection was employed to measure levels of dopamine (DA) as previously reported in our laboratory (29). Tissue samples were sonicated in 50 volumes of 0.1 M perchloric acid containing 50 ng/mL of dihydrobenzylamine (Sigma Chemical, MA) as internal standard. After centrifugation (15,000 g, 10 min, 4 °C), 20 mL of supernatant was injected onto a C18-reversed phase RP-80 catecholamine column (ESA, Bedford, MA). The mobile phase consisted of 90% of a solution of 50 mM sodium phosphate, 0.2 mM EDTA, and 1.2 mM heptanesulfonic acid (pH 4) and 10% methanol. Flow rate was 1.0 mL/min. Peaks were

detected with analytical 5011A cell on Coulochem II detector (ESA Biosciences, Chelmsford, MA). Data were collected and processed with TotalChrom software (Perkin Elmer Instruments, Boston, MA).

OGG1 Assay

The procedure for extraction of DNA glycosylase was similar to that described previously (30). Brain regions were sonicated in homogenization buffer containing 20 mM Tris, pH 8.0, 1 mM EDTA, 1 mM dithiothrietol (DTT), 0.5 mM spermine, 0.5 mM spermidine, 50% glycerol and protease inhibitors and homogenates were rocked for 30 min after addition of 1/10 volume of 2.5 M KCl. Samples were spun at 14,000 rpm for 30 min and supernatants were collected. The OGG1 activities in supernatants were determined using duplex oligonucleotide containing 8-oxodG as incision substrate. For preparation of the incision assay, 20 pmol of synthetic probe containing 8-oxodG (Trevigen, Gaithersburg, MD) was labeled with ^{32}P at the 5'-end using polynucleotide T4 kinase (Boehringer Mannheim, Germany). Unincorporated free ^{32}P-ATP was separated on G25 spin column (Prime; Inc., Boulder, CO). Complementary oligonucleotides were annealed in 10 mM Tris, pH 7.8, 100 mM KCl, 1 mM EDTA by heating the samples 5 min at 80 °C and gradually cooling at room temperature. Incision reactions were carried out in a mixture (20 mL) containing 40 mM HEPES (pH 7.6), 5 mM EDTA, 1 mM DTT, 75 mM KCl, purified bovine serum albumin, 100 fmol of ^{32}P labeled duplex oligonucleotide, and extracted guanosine glycosylase (30 mg of protein). The reaction mixture was incubated at 37 °C for 2 h and products of the reaction were analyzed on denaturing 20% polyacrylamide gel. Pure OGG1 served as positive control and untreated duplex oligonucleotide was used for negative control. The gel was visualized with a Biorad-363 Phosphoimager System. The incision activity of OGG1 was calculated as the amount of radioactivity in the band representing specific cleavage of the labeled oligonucleotide over the total radioactivity. Data were normalized to equal concentration of protein, the concentration of which was measured using the bicinchoninic acid assay (31).

SOD assay

Determination of superoxide dismutase activity in mouse brain was based on inhibition of nitrite formation in reaction of oxidation of hydroxylammonium with superoxide anion radical (32). Nitrite formation was generated in a mixture contained 25 mL xanthine (15 mM), 25 mL hydroxylammonium chloride (10 mM), 250 mL phosphate buffer (65 mM, pH 7.8), 90 mL distilled water and 100 mL xanthine oxidase (0.1 U/mL) used as a starter of the reaction. Inhibitory effect of inherent SOD was assayed at 25 °C during 20 min of incubation with 10 mL

of brain tissue extracts. Determination of the resulted nitrite was performed upon the reaction (20 min at room temperature) with 0.5 mL sulfanilic acid (3.3 mg/mL) and 0.5 mL α-naphthylamine (1 mg/mL). Optical absorbance at 530 nm was measured on Ultrospec III spectrophotometer (Pharmacia, LKB). The results were expressed as units of SOD activity calculated per milligram of protein. The amount of protein in the samples was determined using the bicinchoninic acid (31).

Lipid peroxidation assay

Formation of lipid peroxide derivatives was evaluated by measuring thiobarbituric acid-reactive substances (TBARS) according to a previously reported method (Cascio et al., 2000). Briefly, the different regions of brain were individually homogenized in ice-cold 1.15% KCl (w/v); then 0.4 mL of the homogenates were mixed with 1 mL of 0.375% TBA, 15% TCA (w/v), 0.25N HCl and 6.8 mM butylated-hydroxytoluene (BHT), placed in a boiling water bath for 10 min, removed and allowed to cool on ice. Following centrifugation at 3000 **g** for 10 min, the absorbance in the supernatants was measured at 532 nm. The amount of TBARS produced was expressed as nmol TBARS/mg protein using malondialdehyde bis(dimethylacetal) for calibration.

Statistical Analysis

The results were reported as mean ± S.E.M. for at least five individual samples of specific brain regions, assayed in duplicate. Two-way ANOVA was performed to assess the contribution of brain region, time of analysis and their interaction on total variance. Post-hoc t-tests with Bonferroni corrections were performed to compare values at each time point to control (untreated) values.

RESULTS

Effects on Striatal DA and metabolites

Four groups (6-8 mice per group) of mice were injected with dieldrin i.p. (6 mg/kg or 30 mg/kg). Animals were euthanatized at 6, 24 and 72 hrs after injections. Brains were dissected and striatal tissue was harvested for assay of DA and metabolites. Striatal DA levels were transiently decreased at 6 hrs, but recovered to levels equal to or greater than baseline by 72 hrs (**Figs 2, 3**). In the group of mice that received the high dose of dieldrin (30 mg/kg) the levels

at 72 hrs far exceeded baseline levels. Striatal DA turnover was initially increased but by 72 hrs was significantly diminished (**Fig 3**). Slow sub-cutaneous infusion of dieldrin with an ALZET osmotic pump over 2 wks (50 mg/kg cumulative dose) resulted in significantly increased levels of striatal DA and HVA but not DOPAC (**Fig 4**). DA turnover was significantly decreased at 14 days (**Fig 4**).

INSERT FIGURES 2, 3, 4

Effects on behavior

Observations of the mice receiving acute and slow infusions of dieldrin did not reveal changes in behavior. There was no dystonic posturing of limbs when the animals were picked up by the tail. Differences in spontaneous locomotor activity between groups was not noted by either observation or by rotometer (data not shown). A transient subtle, fine tremor was noted and instrumental analysis of whole body tremor revealed shifts in the power spectrum (**Fig 5**). These effects on tremor were evident at the highest frequencies 13 and 14 Hz were noted at 1 wk and returned to baseline lines by 2 wks.

INSERT FIGURE 5

Acute and sub-acute effects of dieldrin on oxidative DNA repair:

Four groups of mice (n=6 per group) were injected with 6 or 30 mg/kg of dieldrin i.p. or vehicle. Groups were euthanatized at 6, 24 and 72 hrs after injection. (Data from the low dose is not shown but was similar to the effects of the high dose in the time-course and brain regional pattern). Dieldrin elicited a significant time and brain-region dependent increase in OGG1 activity (**Fig 6**). The greatest extent of increased activity was measured in MB (5 fold), followed closely by PM (4.3 fold) and CP (4.2 fold). These three regions have high levels of monoaminergic neuronal activities. Notably all regions of brain exhibited at least a 2.5 fold increase in OGG1 activity at 72 hrs after dieldrin injection.

INSERT FIGURE 6

Effects of slow infusion of dieldrin over 2 weeks on DNA repair:

Six groups of mice (n=8 per group) were implanted with osmotic pumps loaded with dieldrin and calibrated to deliver 3, 6, 12, 24 and 48 mg/kg over a period of 2 weeks. After euthanasia and rapid dissection of brain, OGG1 activities were determined. Dieldrin infusion elicited a dose-

dependent increase of OGG1 activities in all brain regions, with maximum effects reaching a plateau between 24 and 48 mg/kg (**Fig 7**). The distribution of OGG1 activity across brain regions was fairly homogenous. However, at the 24mg/kg cumulative dose, there was a more heterogeneous distribution of activity, with pons exhibiting significantly greater activity than striatum and cerebral cortex (**Fig 7**).

INSERT FIGURES 7, 8

Effects of slow infusion of dieldrin on lipid peroxidation:

Slow infusion of dieldrin resulted in a dose-dependent increase in oxidative stress across all brain regions as indicated by measurements of lipid peroxidation (**Fig 8**). This curve resembled the DNA repair response shown in **Fig 7**. The maximum effect was produced following infusion of 48 mg/kg over 2 weeks. The increase in lipid peroxidation was significantly dependent on dose and did not vary significantly with brain region similar to the effects on OGG1. However, post-hoc t-tests revealed that lipid peroxidation was significantly higher in CB than in MB following a dose of 12 mg/kg ($p<0.05$). Similarly, lipid peroxidation was greater in CB than in the PONS following 24 mg/kg.

Effects of slow infusion of dieldrin on SOD:

Further evidence of oxidative stress was evidenced by a dose-dependent increase in total SOD activity following slow infusion of dieldrin **(Fig 9).** Unlike the curve for OGG1, the SOD dose-response curve assumed an inverted U-shape, with SOD activities increased at lower doses and decreased at the highest cumulative doses of dieldrin. Mitochondrial SOD (mSOD) was also increased at the lower doses and decreased at the highest dose. Like the total SOD response, the cumulative dose accounted for most of the total variance in mSOD activities with brain regions accounting for a small proportion of the total variance. When the effects of 24 mg/kg were plotted against brain region, it was clear that mSOD in MB and Thal/Hypot were significantly lower than in CB (**Fig 9**, panel on the right).

INSERT FIGURE 9

DISCUSSION

Dieldrin, whether administered acutely or infused slowly over 2 wks, had biphasic effects on striatal DA and metabolites. Both low and high single doses of dieldrin caused an initial depletion of DA (at 6 hrs) followed by a return to normal or greater than normal levels by 72 hrs. Turnover of striatal DA was initially increased but was significantly diminished by 72 hrs. When sub-acute infusions of dieldrin were delivered with an osmotic pump over 2 weeks, there was a significant increase in striatal DA steady-state levels. These results are not consistent with a cytotoxic effect on nigro-striatal DA neurons, but appear to reflect a reversible metabolic or pharmacologic effect. Dieldrin has previously been reported to interact with brain monoaminergic neurotransmission in several species, and the effects *in vivo* have never been linked in a neuropathological study to a permanent cytotoxic lesion of DA neurons. True cytotoxicity with cell death has only been reported in rat midbrain cultures of DA neurons (12). In mallard ducks, dietary exposure to dieldrin caused appreciable depletion of whole brain norepinephrine, serotonin and dopamine (10, 11). Dopamine was decreased to 30% of controls and this was attained with dieldrin concentrations in the feed of 10 to 30 ppm. Feeding ring doves with dieldrin also caused significant depletion of dopamine and norepinephrine in whole brain (8). Regional brain analysis of rats fed dieldrin chronically revealed decreases in levels of norepinephrine and serotonin, but not dopamine, in medulla and pons, midbrain and striatum (9). Behavioral effects noted after acute treatment included transient hypokinesia (in male rats only) and whole body tremors(9).

In the present study, dieldrin caused a transient, subtle tremor but no gross changes in motor behavior were noted the male ICR mice. Accelerometry measurements revealed that dieldrin caused a shift in the power spectrum of whole body tremor. The effects were transient and may be related to changes in striatal DA and metabolites. The tremor in PD is associated with DA depletion, but overactive nigro-striatal DA system can also result in tremor as observed following high doses of amphetamines.

The effects on striatal DA levels and the transient “sub-clinical” tremor can perhaps be understood in the context of a metabolic compromise caused by the toxicant. Dieldrin is known to interfere with mitochondrial respiration. Adult rats fed dieldrin for two for eight weeks

developed morphological changes in liver mitochondria (33). These changes included an increase in the number of cristae, a double outer membrane or portion of the outer membrane and mitochondrial "ring-like" formations. Dieldrin has also been reported to inhibit mitochondrial respiration in isolated rat liver mitochondria at a site before the dinitro-phenol-sensitive coupling site (13). According to Bergen, the inhibition of electron transport is localized to the *cytochrome b* site and terminal electron transport is not affected by dieldrin. Interference with electron transport is known to generate superoxide anion which interacts with macromolecules including lipids, proteins and DNA (16).

In the present study, dieldrin elicited a dose-dependent global oxidative stress evidenced by the relatively homogenous distribution of lipid peroxidation across all brain regions. The repair of oxidized DNA (OGG1 activity) was also stimulated in a dose-response pattern that paralleled the lipid peroxidation. However the distribution of SOD (and mSOD) across brain regions assumed an inverted U pattern, distinct from the OGG1 dose-response curve. SOD was initially increased across all brain regions, but at higher cumulative doses, SOD activity was suppressed. At certain cumulative doses, there appeared to be some regions with greater suppression of mSOD activity; mSOD activity was the lowest in MB after a cumulative dose of 24 mg/kg.

Although the DNA repair response to dieldrin was more homogenous than the anti-oxidant SOD response, there were differences across some brain regions. Following a single dose of dieldrin, OGG1 activity showed the greatest fold increase in MB, PM and CP, regions known to have high levels of monoaminergic activities (DA, serotonin, norepineprhine). With slow infusion of dieldrin, the marked increase in OGG1 activities also involved all brain regions, but only at the 24 mg/kg cumulative dose was there evidence of a differential distribution of OGG1, with the pons exhibiting highest levels of activity.

It is possible that a robust DNA repair response may have provided DA neurons of the SN and monoaminergic neurons of the brainstem resistance to the cytotoxic effects of pesticide. This response to dieldrin is unlike the DNA repair response to MPTP, a mitochondrial toxicant which does cause nigro-striatal DA neuron degeneration. MPTP was reported to elicit a significant up-regulation of OGG1 in all brain regions, but the s. nigra and striatum failed to maintain the increased repair activity (26) . By 72 hours, OGG1 activity declined below control levels and this failure in repair activity was associated with appearance of apoptotic profiles in the s. nigra

(26).

The effects of dieldrin more closely resemble those of the mitochondrial toxicant, ochratoxin-A (OTA) which also produced a global increase in oxidative stress across all brain regions and did not result in irreversible cytotoxicity (25). However, unlike the response to dieldrin, the DNA repair response to OTA was biphasic, with an initial inhibition of OGG1 activity followed by a trend towards recovery to normal levels after 3 days in all regions (25). Similar to the effects of dieldrin, the impact on behavior was negligible and there was no evidence of neuronal degeneration.

The relationship between OGG1 activity and extent of oxidative DNA damage, indicated by measures of 8-hydroxy-2'deoxyguanosine (oxo^8dG) has been previously studied (29,30). In the mouse, there is an age-dependent accumulation of oxo^8dG in brain regions involved in locomotor control, and these increased levels of oxo^8dG were associated with a decline in spontaneous locomotor activity and balance in the aged mice (29). There was a significant inverse correlation between OGG1 activity and oxo8dG levels in specific brain regions (30). Those regions with high OGG1 activity tend to have the lowest amount of oxidized DNA (oxo8dG). In the murine model of PD, MPTP treatment resulted in age-dependent damage to gene-specific nuclear and mitochondrial DNA in the nigro-striatal system (34). There was an increase in DNA damage to a 10 kb fragment of the mitochondrial genome from the caudate-putamen in "old" mice but there was no significant DNA damage in the nuclear DNA target, *β-polymerase*. MPTP treatment led to damage in both the mitochondrial DNA fragment and in nuclear *β-polymerase* of the SN. The increased oxidative DNA damage in the nigrostriatal system may be due to increased generation of oxyradical species in DA neurons and/or diminished capacity to scavenge oxyradical species. Repair of the oxidized DNA also plays a critical, though understudied, role in maintaining the integrity of DNA especially in transcriptionally active genes. Recent studies have identified a subpathway of nucleotide-excision repair in which transcriptionally active genes are more rapidly cleared of certain types of DNA lesions than are silent domains of the genome (35). In the realm of human pathology, oxo^8G levels have been shown to increase in the SN, basal ganglia and cortex of idiopathic PD cases compared to controls (36, 37).

Despite the identification of multiple genetic mutations that result in a clinical phenotype of Parkinson's Disease (PD), the vast majority of cases are sporadic and none have implicated a

DNA repair problem. There is ample evidence to support the hypothesis that environmental factors contribute to its cause (38, 39). The prevalence of PD has increased in industrialized countries compared with newly industrialized or non-industrialized nations (40). In addition, prevalence appears to be increasing for early onset PD (41, 42). Other studies have found an increased risk of PD with a history of rural residence especially for those persons with early onset PD (i.e., <50 year old), and many of these persons had histories of drinking well water in their youth (43). Case-control studies in China, Spain, and Canada have found a relationship between an increased risk of PD and pesticide and industrial chemical exposures (44-47). Many commonly used pesticides, such as the majority of the organophosphates, are not stored in the human body. However, the organochlorines, such as 2, 2-bis(p-chlorophenyl)-1, 1, 1, -trichloroethane (DDT), lindane and dieldrin which had wide use in the United States until 1972, can still be found in humans from environmental contamination, and can be measured in adipose-containing tissues Other organochlorines from both lifetime occupational and environmental exposures can be found in adipose tissues of humans throughout the world (1).

Despite the implication of dieldrin as a potential etiological agent for a PD-like syndrome, the present data does not support the hypothesis that it is a selective DA neurotoxin. Dieldrin triggers a robust anti-oxidative and DNA repair across the entire brain consistent with its known capacity to impact mitochondrial bioenergetics. However, the long term consequences of chronic dieldrin exposure remain to be studied, especially in light of the concept of “slow excitotoxicity” which postulates that even a mild bioenergetic compromise can over time result in the demise of neurons by sensitizing neurons to the endogenous excitatory neurotransmitters.

Acknowledgements
Supported by DAMD # 17-03-1-0501 and VA Merit Review to JSR

CITATIONS

1. Levine R. Recognized and Possible Effects of Pesticides in Humans. In: Hayes WJJ, Laws ERJ, eds. Handbook of Pesticide Toxicology. San Diego, New York, Boston, London, Sydney, Tokyo, Toronto: Academic Press, Inc., 1991: 275-360.
2. Yang CF, Sun YP. Partition distribution of insecticides as a critical factor affecting their rates of absorption from water and relative toxicities to fish. Archives of Environmental Contamination & Toxicology 1977;6(2-3):325-335.
3. Schuytema GS, Nebeker AV, Griffis WL, Wilson KN. Teratogenesis, toxicity, and bioconcentration in frogs exposed to dieldrin. Archives of Environmental Contamination & Toxicology 1991;21(3):332-350.
4. Geyer HJ, Scheunert I, Rapp K, Gebefugi I, Steinberg C, Kettrup A. The relevance of fat content in toxicity of lipophilic chemicals to terrestrial animals with special reference to dieldrin and 2,3,7,8-tetrachlorodibenzo-p-dioxin (TCDD). Ecotoxicology & Environmental Safety 1993;26(1):45-60.
5. Fleming L, Mann JB, Bean J, Briggle T, Sanchez-Ramos JR. Parkinson's disease and brain levels of organochlorine pesticides. Annals of Neurology 1994;36(1):100-103.
6. Corrigan FM, French M, Murray L. Organochlorine compounds in human brain. Human & Experimental Toxicology 1996;15(3):262-264.
7. Corrigan FM, Wienburg CL, Shore RF, Daniel SE, Mann D. Organochlorine insecticides in substantia nigra in Parkinson's disease. Journal of Toxicology & Environmental Health 2000;59(4):229-234.
8. Heinz GH, Hill EF, Contrera JF. Dopamine and norepinephrine depletion in ring doves fed DDE, dieldrin and aroclor 1254. Toxicol. and Applied Pharmacol. 1980;53:75-82.
9. Wagner SR, Greene FE. Dieldrin-induced alterations in biogenic amine content of rat brain. Toxicology & Applied Pharmacology 1978;43(1):45-55.
10. Sharma RP. Brain biogenic amines: depletion by chronic dieldrin exposure. Life Sciences 1973;13:1245-1251.
11. Sharma RP, Winn DS, Low JB. Toxic, neurochemical and behavioral effects of dieldrin exposure in mallard ducks. Archives of Environmental Contamination & Toxicology 1976;5(1):43-53.
12. Sanchez-Ramos J, Facca A, Basit A, Song S. Toxicity of dieldrin for dopaminergic neurons in mesencepahlic cultures. Exp Neurol 1998; 150:263-671.
13. Bergen WG. The in vitro effect of dieldrin on respiration of rat liver mitochondria. Proceedings of the Society for Experimental Biology & Medicine 1971;136(3):732-735.
14. Pardini RS, Heidker JC, Payne B. The effect of some cyclodiene pesticides, benzenehexachloride and toxaphene on mitochondrial electron transport. Bulletin of Environmental Contamination & Toxicology 1971;6(5):436-444.
15. Moffett GB, Yarbrough JD. The effects of DDT, toxaphene, and dieldrin on succinic dehydrogenase activity in insecticide-resistant and susceptible Gambusia affinis. Journal of Agricultural & Food Chemistry 1972;20(3):558-560.
16. Hasegawa E, Takeshige K, Oishi T, et al. MPP+ induces NADH-dependent superoxide formation and enhances NADH-dependent lipid peroxidation in bovine heart submitochondrial particles. Biochem Biophys Res Com 1990;170:1049-1055.
17. Ramsay RR, Singer TP. Relation of superoxide generation and lipid peroxidation to the inhibition of NADH-Q oxidoreductase by rotenone, piericidin A, and MPP+. Biochemical & Biophysical Research Communications 1992;189(1):47-52.

18. Betarbet R, Sherer TB, MacKenzie G, Garcia-Osuna M, Panov AV, Greenamyre T. Chronic systemic pesticide exposure reproduces features of Parkinson's disease. Nature Neuroscience 2000;3:1301-1306.
19. Vyas I, Heikkila RE, Nicklas WJ. Studies on the neurotoxicity of MPTP; inhibition of NAD-linked substrate oxidation by its metabolite, MPP+. J Neurochem 1986;46:1501-1507.
20. Parker WD, Boyson SJ, Parks JR. Abnormalities of the electron transport chain in idiopathic Parkinson's disease. Ann Neurol : 1989;26:719-723.
21. Mizuno Y, Ohta S, Tanaka M, Takamiya S, Suzuki K, Sato T, et al. Deficiencies in complex I subunits of the respiratory chain in Parkinson's disease. Biochem Biophys Res Commun 1989;163(3):1450-1455.
22. Schapira AHV, Cooper JM, Dexter D, et al. Mitochondrial complex I deficiency in Parkinson's disease. Lancet 1989;i:1269.
23. Beal MF. Does impairment of energy metabolism result in excitotoxic neuronal death in neurodegenerative illnesss? Ann Neurol 1992;31:119-130.
24. Greenamyre JT, MacKenzie G, Peng TI, Stephans SE. Mitochondrial dysfunction in Parkinson's disease. Biochem Soc Symp 1999;66:85-97.
25. Sava V, Reunova O, Velasquez A, Harbison R, Sanchez-Ramos J. Acute neurotoxic effects of the fungal metabolite ochratoxin-A. Neurotoxicology 2006;27(1):82-92.
26. Sava V, Reunova O, Velasquez A, Song S, Sanchez-Ramos J. Neuroanatomical mapping of DNA repair and antioxidative responses in mouse brain: Effects of a single dose of MPTP. NeuroToxicology 2006;27(6):1080-1093.
27. Robbins JH, Otsuka F, Tarone RE, et al. Parkinson's disease and Alzheimer's disease: hypersensitivity to X-rays in culture cell lines. J Neurol Neurosurg Psychiatry 1985;48:916-923.
28. Lovell MA, Xie C, Markesbery WR. Decreased base excision repair and increased helicase activity in Alzheimer's disease brain. Brain Research 2000;855(1):116-123.
29. Cardozo-Pelaez F, Song S, Parthasarathy A, Hazzi C, Naidu K, Sanchez-Ramos J. Oxidative DNA damage in the aging mouse brain. Movement Disorders 1999;14(6):972-980.
30. Cardozo-Pelaez F, Brooks PJ, Stedeford T, Song S, Sanchez-Ramos J. DNA damage, repair, and antioxidant systems in brain regions: a correlative study. Free Radical Biology & Medicine 2000;28(5):779-785.
31. Smith PK, Krohn RI, Hermanson GT, Mallia AK, Gartner FH, Provenzano MD, et al. Measurement of protein using bicinchoninic acid. Anal Biochem 1985;150(1):76-85.
32. Elstner EF, Heupel A. Inhibition of nitrite formation from hydroxyl-ammonium chloride: a simple assay for superoxide dismutase. Anal Biochem 1976;70:616-620.
33. Kimbrough RD, Gaines TB, Linder RE. The ultrastructure of livers of rats fed DDT and dieldrin. Archives of Environmental Health 1971;22(4):460-467.
34. Mandavilli BS, Ali SF, Van Houten B. DNA damage in brain mitochondria caused by aging and MPTP treatment. Brain Research 2000;885:45-52.
35. Hanawalt PC. Transcription-coupled repair and human disease: perspective. Science. 1994;266:1957-1958.
36. Alam ZI, Jenner A, Daniel SE, Lees AJ, Cairns N, Marsden CD, et al. Oxidative DNA Damage in the Parkinsonian Brain: An Apparent Selective Increase in 8-hydroxyguanine Levels in Substantia Nigra. Journal of Neurochemistry 1997;69:1196-1203.
37. Sanchez-Ramos J, Overvik E, Ames BN. A marker of oxyradical-mediated DNA damage (oxo8dG) is increased in Nigro-Striatum of Parkinson's Disease Brain. Neurodegeneration (incorporated into Exp. Neurology) 1994;3:197-204.
38. Schoenberg BS. Environmental risk factors for Parkinson's Disease: the epidemiologic evidence. Canadian Journal Neurological Science 1987;14:407-413.
39. Langston JW, Irwin I, Ricuarte GA. Neurotoxins, parkinsonism and Parkinson's disease. Pharmacol. Ther. 1987;32:19-49.

40. Tanner CM, Langston JW. Do enviornmental toxins cause Parkinson's disease? A critical review. Neurology 1990;40 (suppl):17-31.
41. Butterfield PG, Valanis BG, Spencer P. Environmental antecedents of young-onset Parkinson's disease. Neurology 1993;43:1150-1158.
42. Golbe LI. Risk factors in young-onset Parkinson's disease. Neurology 1993;43:1641-1643.
43. Rajput AH, Uitti RJ, Stern W, . ea. Geography, drinking water chemistry, pesticides and herbicides and the etiology of Parkinson's disease. Can J Neurol Sci 1987;14:414-418.
44. Hubble JP, Cao T, Hassanein RS, al. e. Risk factors for Parkinson's disease. Neurology 1993;3:1693-1697.
45. Rybicki BA, Johnson CC, Uman J, Gorell JM. Parkinons's Disease mortality and the industrial use of heavy metals in Michigan. Movement Disorders 1993;8:87-92.
46. Semchuck, K.M., E.J. L, Lee RG. Parkinson's disease: a test of the multifactorial etiologic hypothesis. Neurology 1993;43:1173-1180.
47. Tanner CM, Chen B, Wang WZ. Environmental factors in the etiology of Parkinson's disease. Can J Neurol Sci 1987(14):419-423.

FIGURE LEGENDS

Figure 1. Dieldrin (1,2,3,4,10,10-Hexachloro-6,7-Epoxy-1,4,4a,5,6,7,8,8a, octahydro-1,4,5,8-Dimethanonaphthalene)

Figure 2. Acute effects of dieldrin (6 mg/kg i.p.) on striatal dopamine and metabolites. A. Striatal DA was initially decreased at early time points and returned to levels above baseline at 72 hrs. B. Dieldrin had no effect on HVA at early time points and only was significantly increased at 72 hrs. C. Dieldrin decreased DOPAC levels significantly at 24 hrs but levels returned to baseline by 72 hours. D. DA turnover. One-way ANOVA showed that the DA, DOPAC and DA turnover means were significantly different ($p < 0.05$) and Dunnett's multiple comparison test showed significant differences in striatal DA, DOPAC and DA turnover at times indicated by asterisks.

Figure 3. Acute effects of dieldrin (30 mg/kg i.p.). A. Striatal DA was initially decreased at 6 hrs to half the baseline levels and then was elevated significantly above baseline at 24 and 72 hrs. B. Dieldrin had no effect on HVA at all time points. C. Dieldrin decreased DOPAC levels significantly at 6 and 24 hours. D. DA turnover was decreased significantly at 24 and 72 hrs. One-way ANOVA showed that the DA, DOPAC and DA turnover means were significantly different ($p < 0.05$) and Dunnett's multiple comparison test showed significant differences in striatal DA, DOPAC and DA turnover at times indicated by asterisks.

Figure 4. Effects of slow infusion of dieldrin on striatal DA and metabolites. Left panel: Striatal DA and metabolites following 2 wks of infusion of dieldrin by osmotic pump (cumulative dose 50 mg/kg). Right panel: Striatal DA turnover at 14 days compared to control turnover. Asterisks denote significant difference between values at baseline and 14 days (unpaired t-tests).

Figure 5. Effects of dieldrin on tremor. Whole body tremor was recorded with an accelerometer attached to the bottom of a plexiglass box in which individual animals were placed. Each point represents the mean value (± SEM) obtained from power spectra of 6 individual animals. The power spectra were derived from Fast Fourier transformation of the data, yielding the relative intensity against frequency of oscillations (Hz). Compared to control animals, cumulative infusion of 3 or 6 mg/kg of dieldrin resulted in a shift in the power spectrum to a greater intensity at the highest frequency (14 Hz) at 1 wk with a return to the control values at 2 wks (right panel). However, at 2 wks, animals receiving a cumulative dose of 3 mg/kg exhibited a small but significant shift in relative intensity at 9 and 10 Hz that was different than control values.

Figure 6. Acute effects of 30 mg/kg dieldrin i.p. Left panel: OGG1 activity plotted against brain region reveals a brain and time-dependent increase in OGG1 activity. Two-way ANOVA showed that time contributed 72% of total variance ($p < 0.0001$); brain regions accounted for 4% of total variance ($p< 0.01$) and the interaction with brain region accounted for 3% of total variance. Asterisks indicate significant differences from control values based on post-hoc t-tests with Bonferroni corrections for multiple comparisons. Right panel: Fold Increase of OGG1 activity (ratio of values at 72 hrs to control values) plotted against brain regions. The MB showed the greatest increase in DNA repair activity, followed by PM and CP. CB=cerebellum;

MB= midbrain; PONS=pons; MD=medulla; T/HT=thalamus/hypothalamus; HP=hippocampus; CP= caudate/putamen; CX= cerebral cortex.

Figure 7. Effects of 2 wk infusion of dieldrin on DNA repair (OGG1 activity) Left panel depicts OGG1 activity as a function of the cumulative dose of dieldrin. The increase in OGG1 activity was significantly dependent on the cumulative dose delivered but did not vary significantly as a function of brain region. Two-way ANOVA revealed that cumulative concentration of dieldrin accounted for 79% of total variance ($p < 0.0001$) and brain regions accounted for 1.84% of total variance ($p=0.61$). Post-hoc t-tests with Bonferroni corrections for multiple comparisons showed OGG1 activities in the pons were significantly higher than in the CP and CX following a cumulative dose of 24 mg/kg (right panel). CB=cerebellum; MB= midbrain; PONS=pons; MD=medulla; T/HT=thalamus/hypothalamus; HP=hippocampus; CP= caudate/putamen; CX= cerebral cortex.

Figure 8. Effects of 2 wk infusion of dieldrin (with pump) on lipid peroxidation (TBARS units). The increase in TBARS was significantly dependent on the cumulative dose delivered but did not vary significantly as a function of brain region. Two-way ANOVA revealed that cumulative concentration of dieldrin accounted for 76% of total variance ($p < 0.0001$) and brain regions accounted for 0.9 4% of total variance ($p=0.36$). * Post-hoc t-tests with Bonferroni corrections for multiple comparisons showed TBARS in the CB were significantly higher than in the MB ($p < 0.05$) following a cumulative dose of 12 mg/kg; TBARS in CB were also significantly higher than in the PONS ($p<0.05$) following 24 mg/kg.

Figure 9. Effects of 2 wk infusion of dieldrin on SOD (total SOD and mitochondrial SOD). Panel A illustrates changes in total SOD as a function of cumulative dose of dieldrin. Two-way ANOVA reveals that cumulative dose accounts for 23.9% of total variance ($p<0.001$) and brain region accounts for 2.2% of total variance ($p< 0.13$). * Post hoc t-tests with Bonferroni corrections for multiple comparisons indicate that total SOD activities in CB at 24 mg/kg are significantly greater than MD and CP ($p<0.05$).
Panel B illustrates effects of chronic OTA on mSOD across brain regions. Two-way ANOVA shows that cumulative dose contributes 11.46% of total variance of mSOD ($p < 0.0001$) and brain regions contribute 1.14% of total variance ($p=0.7$).
Panel C focuses on the effects of a cumulative dose of 24 mg/kg on mSOD plotted against brain regions. One-way ANOVA indicates that the means of mSOD activities in the distinct brain regions were significantly different ($p=0.03$). Dunnett's multiple comparison test indicates mSOD in CB was significantly higher than in MB and Thal/Hypot.($p<0.05$).

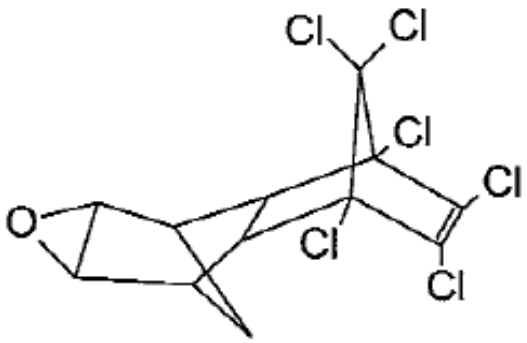

Figure 1. Dieldrin (1,2,3,4,10,10-Hexachloro-6,7-Epoxy-1,4,4a,5,6,7,8,8a, octahydro-1,4,5,8-Dimethanonaphthalene)

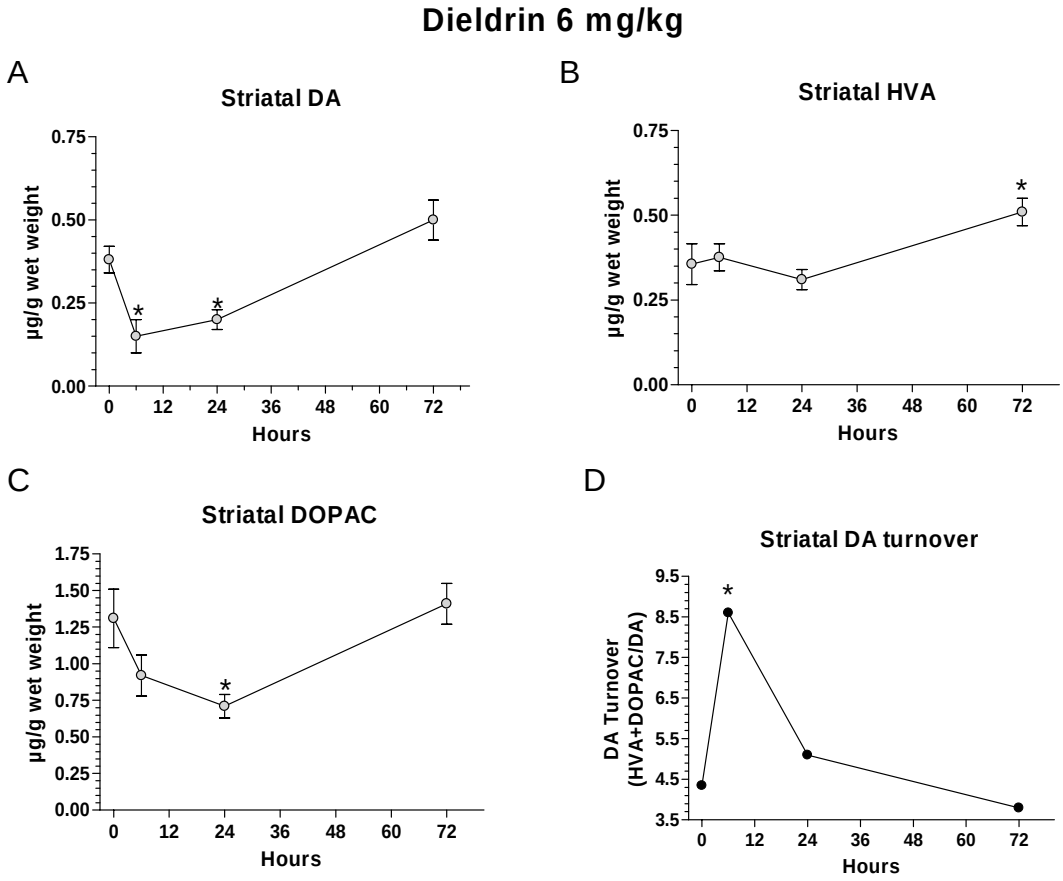

Figure 2. Acute effects of dieldrin (6 mg/kg i.p) on striatal dopamine and metabolites. A. Striatal DA was initially decreased at early time points and returned to levels above baseline at 72 hrs. B. Dieldrin had no effect on HVA at early time points and only was significantly increased at 72 hrs. C. Dieldrin decreased DOPAC levels significantly at 24 hrs but levels returned to baseline by 72 hours. D. DA turnover One-way ANOVA showed that the DA, DOPAC and DA turnover means were significantly different ($p < 0.05$) and Dunnett's multiple comparison test showed significant differences in striatal DA, DOPAC and DA turnover at times indicated by asterisks.

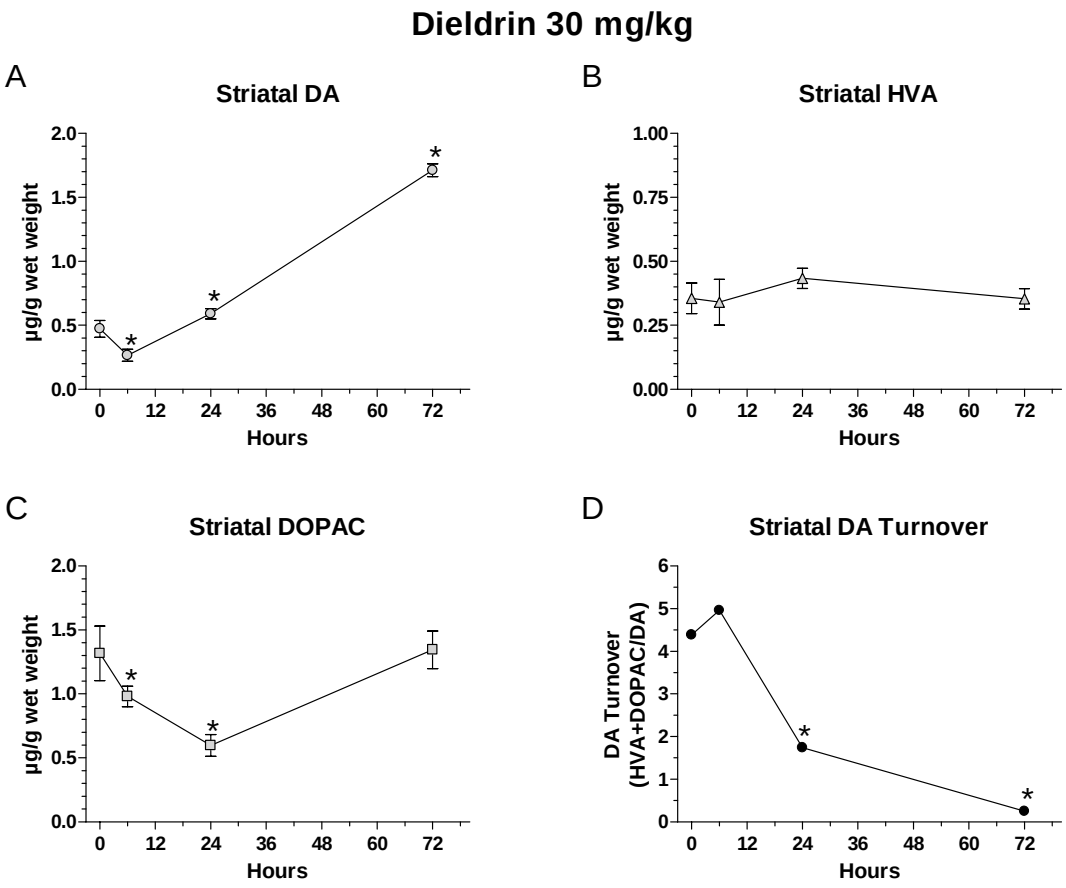

Figure 3. Acute effects of dieldrin (30 mg/kg i.p.). A. Striatal DA was initially decreased at 6 hrs to half the baseline levels and then was elevated significantly above baseline at 24 and 72 hrs. B. Dieldrin had no effect on HVA at all time points. C. Dieldrin decreased DOPAC levels significantly at 6 and 24 hours. D. DA turnover was decreased significantly at 24 and 72 hrs. One-way ANOVA showed that the DA, DOPAC and DA turnover means were significantly different ($p < 0.05$) and Dunnett's multiple comparison test showed significant differences in striatal DA, DOPAC and DA turnover at times indicated by asterisks.

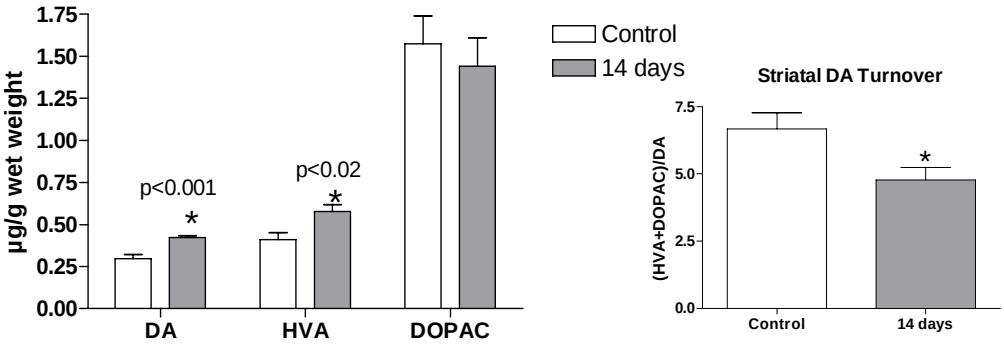

Figure 4. Effects of slow infusion of dieldrin on striatal DA and metabolites. Left panel: Striatal DA and metabolites following 2 wks of infusion of dieldrin by osmotic pump (cumulative dose 50 mg/kg). Right panel: Striatal DA turnover at 14 days compared to control turnover. Asterisks denote significant difference between values at baseline and 14 days (unpaired t-tests)

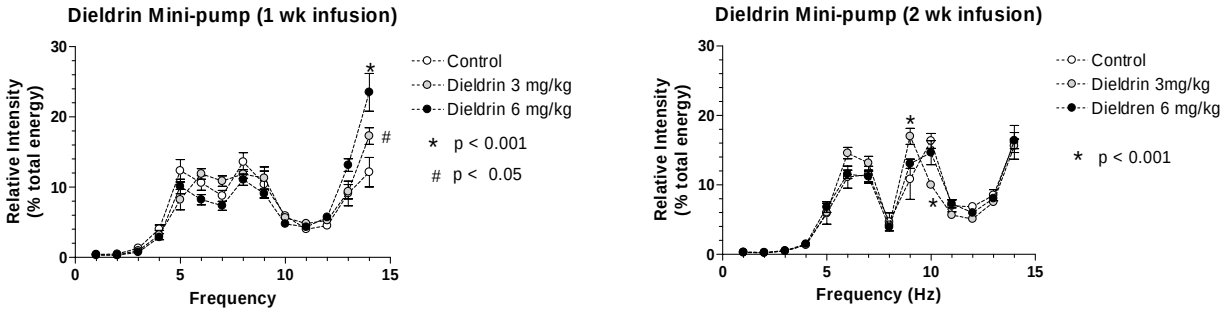

Figure 5. Effects of dieldrin on tremor. Whole body tremor was recorded with an accelerometer attached to the bottom of a polyethylene chamber in which individual animals were placed. Each point represents the mean value (± SEM) obtained from power spectra of 6 individual animals. The power spectra were derived from Fast Fourier transformation of the data, yielding the relative intensity against frequency of oscillations (Hz). Compared to control animals, cumulative infusion of 3 or 6 mg/kg of dieldrin resulted in a shift in the power spectrum to a greater intensity at the highest frequency (14 Hz) at 1 wk with a return to the control values at 2 wks (right panel). However, at 2 wks, animals receiving a cumulative dose of 3 mg/kg exhibited a small but significant shift in relative intensity at 9 and 10 Hz that was different than control values.

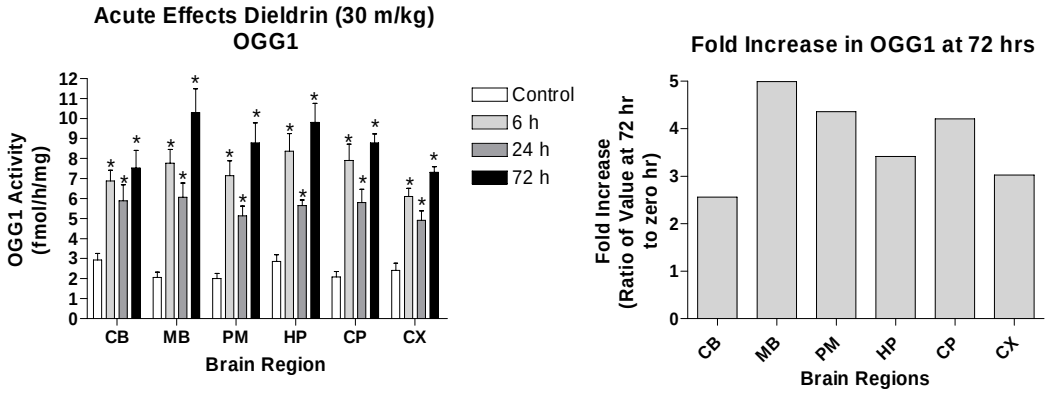

Figure 6. Acute effects of 30 mg/kg dieldrin i.p. Left panel: OGG1 activity plotted against brain region reveals a brain and time-dependent increase in OGG1 activity. Two-way ANOVA showed that time contributed 72% of total variance ($p < 0.0001$); brain regions accounted for 4% of total variance ($p< 0.01$) and the interaction with brain region accounted for 3% of total variance. Asterisks indicate significant differences from control values based on post-hoc t-tests with Bonferroni corrections for multiple comparisons. Right panel: Fold Increase of OGG1 activity (ratio of values at 72 hrs to control values) plotted against brain regions. The MB showed the greatest increase in DNA repair activity, followed by PM and CP. CB=cerebellum; MB= midbrain; PONS=pons; MD=medulla; T/HT=thalamus/hypothalamus; HP=hippocampus; CP= caudate/putamen; CX= cerebral cortex.

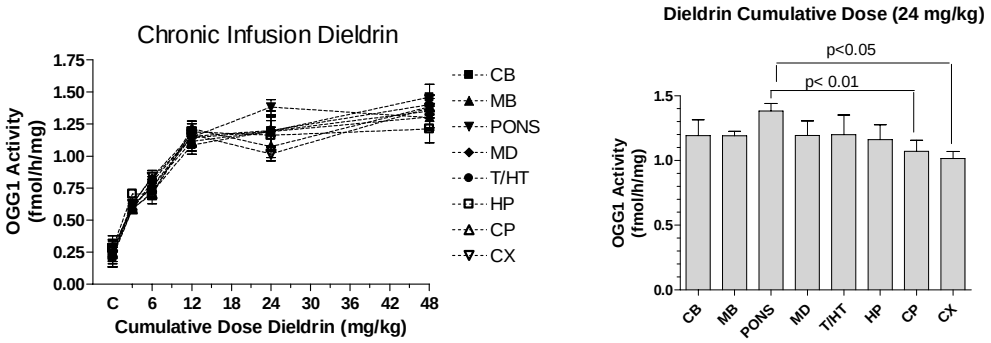

Figure 7. Effects of 2 wk infusion of dieldrin on DNA repair (OGG1 activity) Left panel depicts OGG1 activity as a function of the cumulative dose of dieldrin. The increase in OGG1 activity was significantly dependent on the cumulative dose delivered but did not vary significantly as a function of brain region. Two-way ANOVA revealed that cumulative concentration of dieldrin accounted for 79% of total variance ($p < 0.0001$) and brain regions accounted for 1.84% of total variance ($p=0.61$). Post-hoc t-tests with Bonferroni corrections for multiple comparisons showed OGG1 activities in the pons were significantly higher than in the CP and CX following a cumulative dose of 24 mg/kg (right panel). CB=cerebellum; MB= midbrain; PONS=pons; MD=medulla; T/HT=thalamus/hypothalamus; HP=hippocampus; CP= caudate/putamen; CX= cerebral cortex.

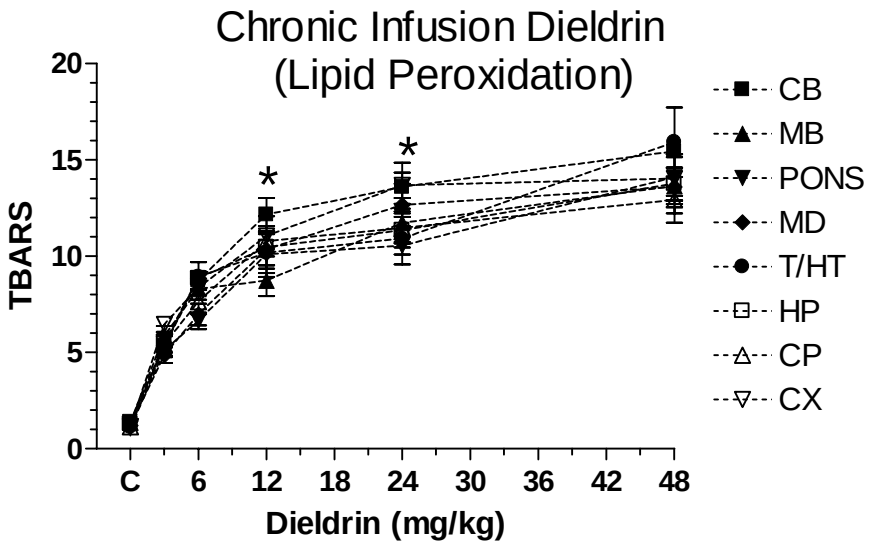

Figure 8. Effects of 2 wk infusion of dieldrin (with pump) on lipid peroxidation (TBARS units). The increase in TBARS was significantly dependent on the cumulative dose delivered but did not vary significantly as a function of brain region. Two-way ANOVA revealed that cumulative concentration of dieldrin accounted for 76% of total variance ($p < 0.0001$) and brain regions accounted for 0.9 4% of total variance ($p=0.36$). * Post-hoc t-tests with Bonferroni corrections for multiple comparisons showed TBARS in the CB were significantly higher than in the MB ($p < 0.05$) following a cumulative dose of 12 mg/kg; TBARS in CB were also significantly higher than in the PONS ($p<0.05$) following 24 mg/kg.

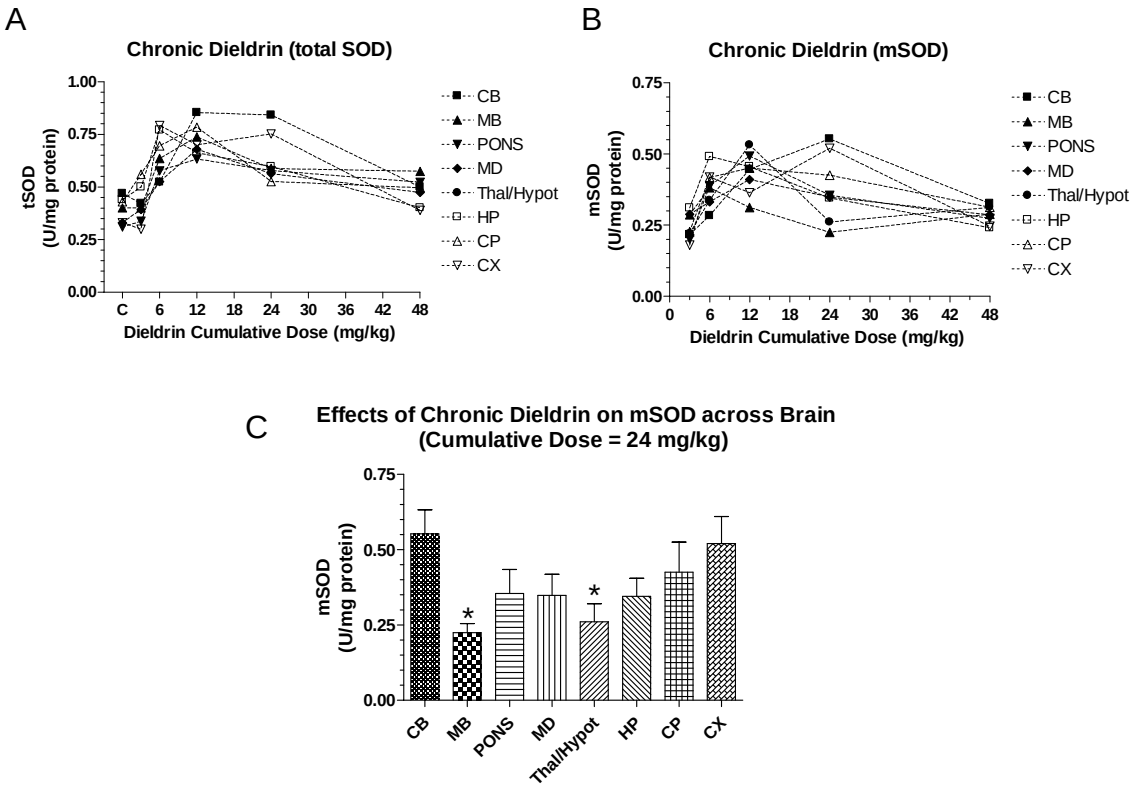

Figure 9. Effects of 2 wk infusion of dieldrin on SOD (total SOD and mitochondrial SOD). Panel A illustrates changes in total SOD as a function of cumulative dose of dieldrin. Two-way ANOVA reveals that cumulative dose accounts for 23.9% of total variance ($p<0.001$) and brain region accounts for 2.2% of total variance ($p< 0.13$). * Post hoc t-tests with Bonferroni corrections for multiple comparisons indicate that total SOD activities in CB at 24 mg/kg are significantly greater than MD and CP ($p<0.05$).
Panel B illustrates effects of chronic OTA on mSOD across brain regions. Two-way ANOVA shows that cumulative dose contributes 11.46% of total variance of mSOD ($p < 0.0001$) and brain regions contribute 1.14% of total variance ($p=0.7$).
Panel C focuses on the effects of a cumulative dose of 24 mg/kg on mSOD plotted against brain regions. One-way ANOVA indicates that the means of mSOD activities in the distinct brain regions were significantly different ($p=0.03$). Dunnett's multiple comparison test indicates mSOD in CB was significantly higher than in MB and Thal/Hypot.($p<0.05$).

Published Abstracts

Sava, V Reunova, O Velasquez, A Song, S Sanchez-Ramos, J
Mapping the brain's DNA repair response to an acute dose of MPTP
JOURNAL OF NEUROCHEMISTRY
AUG 2004, Vol 90 (Suppl. 1) p. 95

Sava, V Velasquez, A Song, S Sanchez-Ramos, J
The ubiquitous mycotoxin ochratoxin A causes dopamine depletion and alterations in oxidative DNA repair in striatum.
MOVEMENT DISORDERS
SEP 2004, Vol 19: p1120

Sanchez-Ramos, J., Sava, V.
Mycotoxins: Can low level, non-lethal exposure result in Parkinsonism? JOURNAL OF THE NEUROLOGICAL SCIENCES
NOV 15, 2005; Vol 238 (Suppl. 1): S8

Sava, V., Velazquez, A., Song, S., Sanchez-Ramos, J
Regulation of DNA repair in the MPTP mouse model of Parkinson's disease
MOVEMENT DISORDERS
SEP 2005, Vol 20, p1248